



## 9. INTERNAL PRESSURE

### 9.1. Phenomenon

The gas pressure within a fuel rod changes continuously during irradiation. Since fuel rod internal pressure is a design criterion, it is necessary to ensure that the COPERNIC internal gas pressure predictions are accurate.

### 9.2. Model

The gases within a fuel rod are considered to be ideal and the BOYLE-MARIOTTE law can therefore be applied:

$$P \cdot V_i = n_i \cdot R \cdot T_i \quad \text{Eq. 9-1}$$

where:

- P : fuel rod internal gas pressure,
- $V_i$  :  $i^{\text{th}}$  internal void volume,
- $n_i$  : number of moles in the  $V_i$  void volume,
- R : universal ideal gas constant, and
- $T_i$  : mean gas temperature in the  $V_i$  void volume.

The pressure P for n inter-connected volumes can be expressed as:

$$P = R \cdot \frac{\sum n_i}{\sum \frac{V_i}{T_i}} \quad \text{Eq. 9-2}$$

The  $\sum n_i$  term represents the total free gas inventory. The various internal volumes are:

[b.]



[b.]

Eq. 9-3

[b., d.]

**9.3. Experimental Validation and Uncertainties**

The void volume and internal pressure measured to predicted comparisons for  $\text{UO}_2$  are presented in Figures 9-1 and 9-2 respectively, for both the Zircaloy-4 and Alloy 5 claddings. This data is listed in Table 9-1. The application of the code internal pressure predictions to fuel rod design analyses, including fuel-clad lift-off, is described in Chapter 12.

**9.4. Adaptation to Mixed Fuels**

The calculations that are performed to predict the internal gas pressure of  $\text{UO}_2$  fuel rods are identical to MOX and gadolinia fuel rods.

The void volume and internal pressure measured to predicted comparisons are presented in Figures 9-3 and 9-4 (Table 9-2) for MOX fuel and Figures 9-5 and 9-6 (Table 9-3) for gadolinia fuel, respectively.

**9.5. Validity Range**

The validity range of this model corresponds to the code benchmarking ranges described in Chapter 1.



# COPERNIC

FCF Non Proprietary

Chapter 9

PAGE 9-3

## FIGURES

FRAMATOME COGEMA FUELS



COPERNIC

FCF Non Proprietary

Chapter 9

PAGE 9-4

**FIGURE 9-1 MEASURED AND PREDICTED  $\text{UO}_2$  FREE VOLUME  
COMPARISON**

[b.]





## FIGURE 9-2 MEASURED AND PREDICTED $UO_2$ INTERNAL PRESSURE COMPARISON

[b.]



**FIGURE 9-3 MEASURED AND PREDICTED MOX FREE VOLUME  
COMPARISON**

[b.]



## FIGURE 9-4 MEASURED AND PREDICTED MOX INTERNAL PRESSURE COMPARISON

[b.]



COPERNIC

FCF Non Proprietary

Chapter 9

PAGE 9-8

**FIGURE 9-5 MEASURED AND PREDICTED  $\text{UO}_2\text{-Gd}_2\text{O}_3$  FREE VOLUME  
COMPARISON**

[b.]



**FIGURE 9-6 MEASURED AND PREDICTED  $\text{UO}_2\text{-Gd}_2\text{O}_3$  INTERNAL  
PRESSURE COMPARISON**

[b.]



COPERNIC

FCF Non Proprietary

Chapter 9

PAGE 9-10

This page intentionally left blank.



# COPERNIC

FCF Non Proprietary

Chapter 9

PAGE 9-11

## TABLES

FRAMATOME COGEMA FUELS

TABLE 9-1 GLOBAL MEASURED/PREDICTED COMPARISON (UO<sub>2</sub>)


Fuel Rod Name	Prog.	Cladding Type	Fast Fluence (n/cm <sup>2</sup> )	Burnup (MWd/tU)	Pred. FGR (%)	Meas. FGR (%)	Pred. Void Vol. (cm <sup>3</sup> )	Meas. Void Vol. (cm <sup>3</sup> )	Pred. Int. Press. (bar)	Meas. Int. Press. (bar)	Pred. F. Rod $\Delta L/L$ (%)	Meas. F. Rod $\Delta L/L$ (%)	Pred. F. Col. $\Delta L/L$ (%)	Meas. F. Col. $\Delta L/L$ (%)
---------------	-------	---------------	-----------------------------------	-----------------	---------------	---------------	------------------------------------	------------------------------------	-------------------------	-------------------------	-------------------------------	-------------------------------	--------------------------------	--------------------------------

[b.]



Fuel Rod Name	Prog.	Cladding Type	Fast Fluence (n/cm <sup>2</sup> )	Burnup (MWd/tU)	Pred. FGR (%)	Meas. FGR (%)	Pred. Void Vol. (cm <sup>3</sup> )	Meas. Void Vol. (cm <sup>3</sup> )	Pred. Int. Press. (bar)	Meas. Int. Press. (bar)	Pred. F Rod $\Delta L/L$ (%)	Meas. F Rod $\Delta L/L$ (%)	Pred. F Col. $\Delta L/L$ (%)	Meas. F Col. $\Delta L/L$ (%)
---------------	-------	---------------	-----------------------------------	-----------------	---------------	---------------	------------------------------------	------------------------------------	-------------------------	-------------------------	------------------------------	------------------------------	-------------------------------	-------------------------------

[b.]


  
 COGEMA FUELS

Fuel Rod Name	Prog.	Cladding Type	Fast Fluence (n/cm <sup>2</sup> )	Burnup (MWd/tU)	Pred. FGR (%)	Meas. FGR (%)	Pred. Void Vol. (cm <sup>3</sup> )	Meas. Void Vol. (cm <sup>3</sup> )	Pred. Int. Press. (bar)	Meas. Int. Press. (bar)	Pred. F. Rod $\Delta L/L$ (%)	Meas. F. Rod $\Delta L/L$ (%)	Pred. F. Col. $\Delta L/L$ (%)	Meas. F. Col. $\Delta L/L$ (%)
---------------	-------	---------------	-----------------------------------	-----------------	---------------	---------------	------------------------------------	------------------------------------	-------------------------	-------------------------	-------------------------------	-------------------------------	--------------------------------	--------------------------------

[b.]

COGEMA

Fuel Rod Name	Prog	Cladding Type	Fast Fluence (n/cm <sup>2</sup> )	Burnup (MWd/tU)	Pred. FGR (%)	Meas. FGR (%)	Pred. Void Vol (cm <sup>3</sup> )	Meas. Void Vol (cm <sup>3</sup> )	Pred. Int. Press (bar)	Meas. Int. Press (bar)	Pred. F. Rod $\Delta L/L$ (%)	Meas. F. Rod $\Delta L/L$ (%)	Pred. F. Col. $\Delta L/L$ (%)	Meas. F. Col. $\Delta L/L$ (%)
---------------	------	---------------	-----------------------------------	-----------------	---------------	---------------	-----------------------------------	-----------------------------------	------------------------	------------------------	-------------------------------	-------------------------------	--------------------------------	--------------------------------

[b.]

  
COPERNIC

FRAMATOME COGEMA FUELS

Fuel Rod Name	Prog.	Cladding Type	Fast Fluence (n/cm <sup>2</sup> )	Burnup (MWd/tU)	Pred. FGR (%)	Meas. FGR (%)	Pred. Void Vol. (cm <sup>3</sup> )	Meas. Void Vol. (cm <sup>3</sup> )	Pred. Int. Press. (bar)	Meas. Int. Press. (bar)	Pred. F. Rod $\Delta L/L$ (%)	Meas. F. Rod $\Delta L/L$ (%)	Pred. F. Col. $\Delta L/L$ (%)	Meas. F. Col. $\Delta L/L$ (%)
---------------	-------	---------------	-----------------------------------	-----------------	---------------	---------------	------------------------------------	------------------------------------	-------------------------	-------------------------	-------------------------------	-------------------------------	--------------------------------	--------------------------------

[b.]



FRAMATOME  
COGEMA

FCF Non Proprietary

Chapter 9

PAGE 9-16

FRAMATOME COGEMA FUELS

Fuel Rod Name	Prog.	Clad- ding Type	Fast Fluence (n/cm <sup>2</sup> )	Burnup (MWd/ tU)	Pred. FGR (%)	Meas. FGR (%)	Pred. Void Vol. (cm <sup>3</sup> )	Meas. Void Vol. (cm <sup>3</sup> )	Pred. Int. Press. (bar)	Meas. Int. Press. (bar)	Pred. F. Rod $\Delta L/L$ (%)	Meas. F. Rod $\Delta L/L$ (%)	Pred. F. Col. $\Delta L/L$ (%)	Meas. F. Col. $\Delta L/L$ (%)
------------------	-------	-----------------------	---	------------------------	---------------------	---------------------	---	---	----------------------------------	----------------------------------	--	--	---	---

[b.]



COPERNIC

FCF Non Proprietary

Chapter 9

PAGE 9-17

FRAMATOME COGEMA FUELS

Fuel Rod Name	Prog.	Clad- ding Type	Fast Fluence (n/cm <sup>2</sup> )	Burnup (MWd/ tU)	Pred. FGR (%)	Meas. FGR (%)	Pred. Void Vol. (cm <sup>3</sup> )	Meas. Void Vol. (cm <sup>3</sup> )	Pred. Int. Press. (bar)	Meas. Int. Press. (bar)	Pred. F. Rod $\Delta L/L$ (%)	Meas. F. Rod $\Delta L/L$ (%)	Pred. F. Col. $\Delta L/L$ (%)	Meas. F. Col. $\Delta L/L$ (%)
---------------	-------	-----------------------	---	------------------------	---------------------	---------------------	---	---	----------------------------------	----------------------------------	--	--	---	---

[b.]

**CONFIDENTIAL**


FCF Non Proprietary

Chapter 9

PAGE 9-18

Fuel Rod Name	Prog	Cladding Type	Fast Fluence (n/cm <sup>2</sup> )	Burnup (MWd/tU)	Pred. FGR (%)	Meas. FGR (%)	Pred. Void Vol. (cm <sup>3</sup> )	Meas. Void Vol. (cm <sup>3</sup> )	Pred. Int. Press. (bar)	Meas. Int. Press. (bar)	Pred. F. Rod $\Delta L/L$ (%)	Meas. F. Rod $\Delta L/L$ (%)	Pred. F. Col. $\Delta L/L$ (%)	Meas. F. Col. $\Delta L/L$ (%)
---------------	------	---------------	-----------------------------------	-----------------	---------------	---------------	------------------------------------	------------------------------------	-------------------------	-------------------------	-------------------------------	-------------------------------	--------------------------------	--------------------------------

[b.]

  
COGEMA

Fuel Rod Name	Prog.	Clad- ding Type	Fast Fluence (n/cm <sup>2</sup> )	Burnup (MWd/ tU)	Pred. FGR (%)	Meas. FGR (%)	Pred. Void Vol. (cm <sup>3</sup> )	Meas. Void Vol. (cm <sup>3</sup> )	Pred. Int. Press. (bar)	Meas. Int. Press. (bar)	Pred. F. Rod $\Delta L/L$ (%)	Meas. F. Rod $\Delta L/L$ (%)	Pred. F. Col. $\Delta L/L$ (%)	Meas. F. Col. $\Delta L/L$ (%)
---------------	-------	-----------------------	---	------------------------	---------------------	---------------------	---	---	----------------------------------	----------------------------------	--	--	---	---

[b.]

COGEMA  
FRAMATOME



FRAMATOME COGEMA FUELS

Fuel Rod Name	Prog	Cladding Type	Fast Fluence (n/cm <sup>2</sup> )	Burnup (MWd/tU)	Pred. FGR (%)	Meas. FGR (%)	Pred. Void Vol. (cm <sup>3</sup> )	Meas. Void Vol. (cm <sup>3</sup> )	Pred. Int. Press. (bar)	Meas. Int. Press. (bar)	Pred. F. Rod ΔL/L (%)	Meas. F. Rod ΔL/L (%)	Pred. F. Col. ΔL/L (%)	Meas. F. Col. ΔL/L (%)
---------------	------	---------------	-----------------------------------	-----------------	---------------	---------------	------------------------------------	------------------------------------	-------------------------	-------------------------	-----------------------	-----------------------	------------------------	------------------------

[b.]

**COPELINTIC**

FCF Non Proprietary

Chapter 9 PAGE 9-21

Fuel Rod Name	Prog.	Clad- ding Type	Fast Fluence (n/cm <sup>2</sup> )	Burnup (MWd/ tU)	Pred. FGR (%)	Meas. FGR (%)	Pred. Void Vol. (cm <sup>3</sup> )	Meas. Void Vol. (cm <sup>3</sup> )	Pred. Int. Press. (bar)	Meas. Int. Press. (bar)	Pred. F. Rod $\Delta L/L$ (%)	Meas. F. Rod $\Delta L/L$ (%)	Pred. F. Col. $\Delta L/L$ (%)	Meas. F. Col. $\Delta L/L$ (%)
---------------	-------	-----------------------	---	------------------------	---------------------	---------------------	---	---	----------------------------------	----------------------------------	--	--	---	---

[b.]

FRAMATOME COGEMA FUELS

Fuel Rod Name	Prog.	Clad- ding Type	Fast Fluence (n/cm <sup>2</sup> )	Burnup (MWd/ tU)	Pred. FGR (%)	Meas. FGR (%)	Pred. Void Vol. (cm <sup>3</sup> )	Meas. Void Vol. (cm <sup>3</sup> )	Pred. Int. Press. (bar)	Meas. Int. Press. (bar)	Pred. F. Rod $\Delta L/L$ (%)	Meas. F. Rod $\Delta L/L$ (%)	Pred. F. Col. $\Delta L/L$ (%)	Meas. F. Col. $\Delta L/L$ (%)
------------------	-------	-----------------------	---	------------------------	---------------------	---------------------	---	---	----------------------------------	----------------------------------	--	--	---	---

[b.]

**COPIERNIC**


Fuel Rod Name	Prog.	Clad- ding Type	Fast Fluence (n/cm <sup>2</sup> )	Burnup (MWd/ tU)	Pred. FGR (%)	Meas. FGR (%)	Pred. Void Vol. (cm <sup>3</sup> )	Meas. Void Vol. (cm <sup>3</sup> )	Pred. Int. Press. (bar)	Meas. Int. Press. (bar)	Pred. F. Rod $\Delta L/L$ (%)	Meas. F. Rod $\Delta L/L$ (%)	Pred. F. Col. $\Delta L/L$ (%)	Meas. F. Col. $\Delta L/L$ (%)
---------------	-------	-----------------------	---	------------------------	---------------------	---------------------	---	---	----------------------------------	----------------------------------	--	--	---	---

[b.]

COGEMA

Fuel Rod Name	Prog.	Cladding Type	Fast Fluence (n/cm <sup>2</sup> )	Burnup (MWd/tU)	Pred. FGR (%)	Meas. FGR (%)	Pred. Void Vol. (cm <sup>3</sup> )	Meas. Void Vol. (cm <sup>3</sup> )	Pred. Int. Press. (bar)	Meas. Int. Press. (bar)	Pred. F. Rod $\Delta L/L$ (%)	Meas. F. Rod $\Delta L/L$ (%)	Pred. F. Col. $\Delta L/L$ (%)	Meas. F. Col. $\Delta L/L$ (%)
---------------	-------	---------------	-----------------------------------	-----------------	---------------	---------------	------------------------------------	------------------------------------	-------------------------	-------------------------	-------------------------------	-------------------------------	--------------------------------	--------------------------------

[b.]


  
**COPERNIC**

Fuel Rod Name	Prog.	Clad- ding Type	Fast Fluence (n/cm <sup>2</sup> )	Burnup (MWd/ tU)	Pred. FGR (%)	Meas. FGR (%)	Pred. Void Vol. (cm <sup>3</sup> )	Meas. Void Vol. (cm <sup>3</sup> )	Pred. Int. Press. (bar)	Meas. Int. Press. (bar)	Pred. F. Rod $\Delta L/L$ (%)	Meas. F. Rod $\Delta L/L$ (%)	Pred. F. Col. $\Delta L/L$ (%)	Meas. F. Col. $\Delta L/L$ (%)
---------------	-------	-----------------------	---	------------------------	---------------------	---------------------	---	---	----------------------------------	----------------------------------	--	--	---	---


[b.]



COGEMA

Fuel Rod Name	Prog.	Cladding Type	Fast Fluence (n/cm <sup>2</sup> )	Burnup (MWd/tU)	Pred. FGR (%)	Meas. FGR (%)	Pred. Void Vol. (cm <sup>3</sup> )	Meas. Void Vol. (cm <sup>3</sup> )	Pred. Int. Press (bar)	Meas. Int. Press (bar)	Pred. F. Rod $\Delta L/L$ (%)	Meas. F. Rod $\Delta L/L$ (%)	Pred. F. Col. $\Delta L/L$ (%)	Meas. F. Col. $\Delta L/L$ (%)
---------------	-------	---------------	-----------------------------------	-----------------	---------------	---------------	------------------------------------	------------------------------------	------------------------	------------------------	-------------------------------	-------------------------------	--------------------------------	--------------------------------

[b.]


  
**COPERNIC**

FRAMATOME COGEMA FUELS

Fuel Rod Name	Prog.	Cladding Type	Fast Fluence (n/cm <sup>2</sup> )	Burnup (MWd/tU)	Pred. FGR (%)	Meas. FGR (%)	Pred. Void Vol. (cm <sup>3</sup> )	Meas. Void Vol. (cm <sup>3</sup> )	Pred. Int. Press. (bar)	Meas. Int. Press. (bar)	Pred. F. Rod $\Delta L/L$ (%)	Meas. F. Rod $\Delta L/L$ (%)	Pred. F. Col. $\Delta L/L$ (%)	Meas. F. Col. $\Delta L/L$ (%)
---------------	-------	---------------	-----------------------------------	-----------------	---------------	---------------	------------------------------------	------------------------------------	-------------------------	-------------------------	-------------------------------	-------------------------------	--------------------------------	--------------------------------

[b.]														
------	--	--	--	--	--	--	--	--	--	--	--	--	--	--

FCF Non Proprietary



Fuel Rod Name	Prog.	Cladding Type	Fast Fluence (n/cm <sup>2</sup> )	Burnup (MWd/tU)	Pred. FGR (%)	Meas. FGR (%)	Pred. Void Vol. (cm <sup>3</sup> )	Meas. Void Vol. (cm <sup>3</sup> )	Pred. Int. Press. (bar)	Meas. Int. Press. (bar)	Pred. F. Rod $\Delta L/L$ (%)	Meas. F. Rod $\Delta L/L$ (%)	Pred. F. Col. $\Delta L/L$ (%)	Meas. F. Col. $\Delta L/L$ (%)
---------------	-------	---------------	-----------------------------------	-----------------	---------------	---------------	------------------------------------	------------------------------------	-------------------------	-------------------------	-------------------------------	-------------------------------	--------------------------------	--------------------------------

[b.]

**COFERNIO**

FCF Non Proprietary

Chapter 9

PAGE 9-29

Fuel Rod Name	Prog.	Cladding Type	Fast Fluence (n/cm <sup>2</sup> )	Burnup (MWd/tU)	Pred. FGR (%)	Meas. FGR (%)	Pred. Void Vol. (cm <sup>3</sup> )	Meas. Void Vol. (cm <sup>3</sup> )	Pred. Int. Press. (bar)	Meas. Int. Press. (bar)	Pred. F. Rod $\Delta L/L$ (%)	Meas. F. Rod $\Delta L/L$ (%)	Pred. F. Col. $\Delta L/L$ (%)	Meas. F. Col. $\Delta L/L$ (%)
---------------	-------	---------------	-----------------------------------	-----------------	---------------	---------------	------------------------------------	------------------------------------	-------------------------	-------------------------	-------------------------------	-------------------------------	--------------------------------	--------------------------------


[b.]



COGEMA

Fuel Rod Name	Prog	Cladding Type	Fast Fluence (n/cm <sup>2</sup> )	Burnup (MWd/tU)	Pred. FGR (%)	Meas. FGR (%)	Pred. Void Vol. (cm <sup>3</sup> )	Meas. Void Vol. (cm <sup>3</sup> )	Pred. Int. Press. (bar)	Meas. Int. Press. (bar)	Pred. F. Rod $\Delta L/L$ (%)	Meas. F. Rod $\Delta L/L$ (%)	Pred. F. Col. $\Delta L/L$ (%)	Meas. F. Col. $\Delta L/L$ (%)
---------------	------	---------------	-----------------------------------	-----------------	---------------	---------------	------------------------------------	------------------------------------	-------------------------	-------------------------	-------------------------------	-------------------------------	--------------------------------	--------------------------------

[b.]

  
COPERNIC

FRAMATOME COGEMA FUELS

Fuel Rod Name	Prog.	Cladding Type	Fast Fluence (n/cm <sup>2</sup> )	Burnup (MWd/tU)	Pred. FGR (%)	Meas. FGR (%)	Pred. Void Vol. (cm <sup>3</sup> )	Meas. Void Vol. (cm <sup>3</sup> )	Pred. Int. Press. (bar)	Meas. Int. Press. (bar)	Pred. F. Rod $\Delta L/L$ (%)	Meas. F. Rod $\Delta L/L$ (%)	Pred. F. Col. $\Delta L/L$ (%)	Meas. F. Col. $\Delta L/L$ (%)
---------------	-------	---------------	-----------------------------------	-----------------	---------------	---------------	------------------------------------	------------------------------------	-------------------------	-------------------------	-------------------------------	-------------------------------	--------------------------------	--------------------------------

[b.]



CONFIDENTIAL

FCF Non Proprietary


Chapter 9

PAGE 9-32

TABLE 9-2 GLOBAL MEASURED/PREDICTED COMPARISON (MOX)

Fuel Rod Name	Prog.	Fast Fluence (n/cm <sup>2</sup> )	Burnup (MWd/tM)	Pred. FGR (%)	Meas. FGR (%)	Pred. Void Vol. (cm <sup>3</sup> )	Meas. Void Vol. (cm <sup>3</sup> )	Pred. Int. Press. (bar)	Meas. Int. Press. (bar)	Pred. F. Rod $\Delta L/L$ (%)	Meas. F. Rod $\Delta L/L$ (%)	Pred. F. Col. $\Delta L/L$ (%)	Meas. F. Col. $\Delta L/L$ (%)
---------------	-------	--------------------------------------	--------------------	------------------	------------------	---------------------------------------	---------------------------------------	----------------------------	----------------------------	----------------------------------	----------------------------------	-----------------------------------	-----------------------------------

[b.]


  
**COOPERNICO**

FRAMATOME COGEMA FUELS

Fuel Rod Name	Prog.	Fast Fluence (n/cm <sup>2</sup> )	Burnup (MWd/ tM)	Pred. FGR (%)	Meas. FGR (%)	Pred. Void Vol. (cm <sup>3</sup> )	Meas. Void Vol. (cm <sup>3</sup> )	Pred. Int. Press. (bar)	Meas. Int. Press. (bar)	Pred. F. Rod $\Delta L/L$ (%)	Meas. F. Rod $\Delta L/L$ (%)	Pred. F. Col. $\Delta L/L$ (%)	Meas. F. Col. $\Delta L/L$ (%)
---------------	-------	---	------------------------	---------------------	---------------------	---	---	----------------------------------	----------------------------------	--	--	---	---

[b.]



FRAMATOME  
COGEMA


FCF Non Proprietary

Chapter 9

PAGE 9-34

Fuel Rod Name	Prog.	Fast Fluence (n/cm <sup>2</sup> )	Burnup (MWd/tM)	Pred. FGR (%)	Meas. FGR (%)	Pred. Void Vol (cm <sup>3</sup> )	Meas. Void Vol (cm <sup>3</sup> )	Pred. Int. Press. (bar)	Meas. Int. Press. (bar)	Pred. F Rod $\Delta L/L$ (%)	Meas. F Rod $\Delta L/L$ (%)	Pred. F. Col. $\Delta L/L$ (%)	Meas. F. Col. $\Delta L/L$ (%)
---------------	-------	--------------------------------------	--------------------	------------------	------------------	--------------------------------------	--------------------------------------	----------------------------	----------------------------	------------------------------------	------------------------------------	--------------------------------------	--------------------------------------

[b.]


  
**COPERNIC**

FRAMATOME COGEMA FUELS

Fuel Rod Name	Prog.	Fast Fluence (n/cm <sup>2</sup> )	Burnup (MWd/ tM)	Pred. FGR (%)	Meas. FGR (%)	Pred. Void Vol. (cm <sup>3</sup> )	Meas. Void Vol. (cm <sup>3</sup> )	Pred. Int. Press. (bar)	Meas. Int. Press. (bar)	Pred. E. Rod $\Delta L/L$ (%)	Meas. E. Rod $\Delta L/L$ (%)	Pred. F. Col. $\Delta L/L$ (%)	Meas. F. Col. $\Delta L/L$ (%)
---------------	-------	---	------------------------	---------------------	---------------------	---	---	----------------------------------	----------------------------------	--	--	---	---

[b.]



COGEMA

FCF Non Proprietary

Chapter 9

PAGE 9-36



# FRAMATOME COGEMA FUELS

Fuel Rod Name	Prog	Fast Fluence (n/cm <sup>2</sup> )	Burnup (MWd/tM)	Pred. FGR (%)	Meas. FGR (%)	Pred. Void Vol (cm <sup>3</sup> )	Meas. Void Vol (cm <sup>3</sup> )	Pred. Int. Press. (bar)	Meas. Int. Press. (bar)	Pred. F-Rod ΔL/L (%)	Meas. F-Rod ΔL/L (%)	Pred. F-Col ΔL/L (%)	Meas. F-Col ΔL/L (%)
---------------	------	-----------------------------------	-----------------	---------------	---------------	-----------------------------------	-----------------------------------	-------------------------	-------------------------	----------------------	----------------------	----------------------	----------------------

[b.]

**COPIERNO**

Chapter 9

PAGE 9-37

FCF Non Proprietary

FRAMATOME COGEMA FUELS

Fuel Rod Name	Prog.	Fast Fluence (n/cm <sup>2</sup> )	Burnup (MWd/ tM)	Pred. FGR (%)	Meas. FGR (%)	Pred. Void Vol. (cm <sup>3</sup> )	Meas. Void Vol. (cm <sup>3</sup> )	Pred. Int. Press. (bar)	Meas. Int. Press. (bar)	Pred. F. Rod $\Delta L/L$ (%)	Meas. F. Rod $\Delta L/L$ (%)	Pred. F. Col. $\Delta L/L$ (%)	Meas. F. Col. $\Delta L/L$ (%)
---------------	-------	---	------------------------	---------------------	---------------------	---	---	----------------------------------	----------------------------------	--	--	---	---


[b.]



CONFIDENTIAL

TABLE 9-3 GLOBAL MEASURED/PREDICTED COMPARISON ( $\text{UO}_2\text{-Gd}_2\text{O}_3$ )

Fuel Rod Name	Prog.	Fast Fluence (n/cm <sup>2</sup> )	Burnup (MWd/ tM)	Pred. FGR (%)	Meas. FGR (%)	Pred. Void Vol. (cm <sup>3</sup> )	Meas. Void Vol. (cm <sup>3</sup> )	Pred. Int. Press. (bar)	Meas. Int. Press. (bar)	Pred. F Rod $\Delta\text{L/L}$ (%)	Meas. F Rod $\Delta\text{L/L}$ (%)	Pred. F Col. $\Delta\text{L/L}$ (%)	Meas. F Col. $\Delta\text{L/L}$ (%)
---------------	-------	---	------------------------	---------------------	---------------------	---	---	----------------------------------	----------------------------------	---	---	--	--


  
 COPERNIC

FRAMATOME COGEMA FUELS

Fuel Rod Name	Prog.	Fast Fluence (n/cm <sup>2</sup> )	Burnup (MWd/ tM)	Pred. FGR (%)	Meas. FGR (%)	Pred. Void Vol. (cm <sup>3</sup> )	Meas. Void Vol. (cm <sup>3</sup> )	Pred. Int. Press. (bar)	Meas. Int. Press. (bar)	Pred. F. Rod $\Delta L/L$ (%)	Meas. F. Rod $\Delta L/L$ (%)	Pred. F. Col. $\Delta L/L$ (%)	Meas. F. Col. $\Delta L/L$ (%)



COGEMA  
FRAMATOME

FCF Non Proprietary

Chapter 9 PAGE 9-40

## 10. MATERIAL PROPERTIES

### 10.1. Density

#### 10.1.1. Notations and Units

- $\rho$  : density ( $\text{g.cm}^{-3}$  - material 100% dense)  
 $M_i$  : atomic masses ( $\text{g.mol}^{-1}$ )  
 $N$  : Avogadro number =  $6.022 \cdot 10^{23}$  (atomes.mol $^{-1}$ )  
 $a_i$  : lattice parameter (cm)  
 $\text{enr}_{\text{Pu}}$  : plutonium weight fraction  
 $\text{pgado}$  :  $\text{Gd}_2\text{O}_3$  weight fraction  
 $x$  : deviation from stoichiometry = (oxygen/uranium) - 2.000  
 $y_i$  : mole fractions (U235, Pu, Gd)

#### 10.1.2. Zircaloy

$$\rho = 6.54 \quad \text{Eq. 10-1}$$

#### 10.1.3. Advanced Alloy 5 Cladding

$$\rho = 6.50 \quad \text{Eq. 10-2}$$

#### 10.1.4. $\text{UO}_2$

$$\rho_{\text{UO}_2} = \frac{4 \cdot ((1 - y_{\text{U235}}) \cdot M_{\text{U238}} + y_{\text{U235}} \cdot M_{\text{U235}}) + 8 \cdot (1 + \frac{x}{2}) \cdot M_{\text{O}}}{a_{\text{UO}_2}^3 \cdot N} \quad \text{Eq. 10-3}$$

where

$$a_{\text{UO}_2} = (5.4704 + 0.25|x|) \cdot 10^{-8} \quad \text{Eq. 10-4}$$

#### 10.1.5. MOX

$$\rho_{(\text{U,Pu})\text{O}_2} = \frac{4 \cdot ((1 - y_{\text{U235}} - y_{\text{Pu}}) \cdot M_{\text{U238}} + y_{\text{U235}} \cdot M_{\text{U235}} + y_{\text{Pu}} \cdot M_{\text{Pu}}) + 8 \cdot (1 + \frac{x}{2}) \cdot M_{\text{O}}}{a_{(\text{U,Pu})\text{O}_2}^3 \cdot N} \quad \text{Eq. 10-5}$$

where

[b., c., d.]

Eq. 10-6

### 10.1.6. $\text{UO}_2\text{-Gd}_2\text{O}_3$

$$P_{\text{UO}_2 - \text{Gd}_2\text{O}_3} = \frac{4 \cdot \left( (1 - y_{\text{U235}} - y_{\text{gado}}) \cdot M_{\text{U238}} + y_{\text{U235}} \cdot M_{\text{U235}} + y_{\text{gado}} \cdot M_{\text{gado}} \right) + 8 \cdot \left( 1 + \frac{x}{2} \right) \cdot M_{\text{O}}}{^3\text{UO}_2 - \text{Gd}_2\text{O}_3 \cdot N}$$

Eq. 10-7

where

[b., c., d.]

Eq. 10-8

## 10.2. Melting Point

### 10.2.1. Notations and Units

$T_{fc}$	:	melting temperature in °C
$T_{f0}$	:	MOX melting temperature in °C at zero burnup
Bu	:	burnup in MWd/tU
$Bu_M$	:	burnup in MWd/tM
y	:	plutonium content in weight fraction

### 10.2.2. Zircaloy

$$T_{fc} = 1850$$

Eq. 10-9

### 10.2.3. Advanced Alloy 5 Cladding

$$T_{fc} = 1855$$

Eq. 10-10

#### 10.2.4. $\text{UO}_2$ , $\text{UO}_2\text{-Gd}_2\text{O}_3$

The melting point is given by:

$$[b., c., d.]$$

Eq. 10-11

#### 10.2.5. MOX

The melting point is given by the following equations:

$$[b., c., d.]$$

Eq. 10-12

$$[b., c., d.]$$

Eq. 10-13

### 10.3. Thermal Expansion

#### 10.3.1. Notations and Units

$\Delta x/x$  : thermal expansion (fractional)

$D_0$  : diameter at [e.]

$L_0$  : length at [e.]

$T_c$  : temperature in  $^{\circ}\text{C}$

$T_k$  : temperature in K

$e_0$  : thickness at [e.]

#### 10.3.2. Zircaloy

The thermal expansion values (from 20 to 800  $^{\circ}\text{C}$ ) for stress-relieved Zircaloy-4 cladding are:

$$\frac{\Delta e}{e_0}(\text{radial}) = 9.62 \cdot 10^{-6} \cdot (T_c - 20) \quad \text{Eq. 10-14}$$

$$\frac{\Delta D}{D_0}(\text{circumferential}) = 7.40 \cdot 10^{-6} \cdot (T_c - 20) \quad \text{Eq. 10-15}$$

$$\frac{\Delta L}{L_0}(\text{axial}) = 5.49 \cdot 10^{-6} \cdot (T_c - 20) \quad \text{Eq. 10-16}$$

### 10.3.3. Advanced Alloy 5 Cladding

The thermal expansion expressions (in %) for the advanced Alloy 5 cladding are:

Eq. 10-17

Eq. 10-18

Eq. 10-19

Eq. 10-20

Eq. 10-21

Eq. 10-22

[b., c., d.]

Eq. 10-23

Eq. 10-24

Eq. 10-25



### 10.3.4. $\text{UO}_2$ , MOX, $\text{UO}_2\text{-Gd}_2\text{O}_3$

The thermal expansion (from 273 K to 3120 K) of uranium dioxide is:

$$\frac{\Delta L}{L} = -0.00328 + 1.179 \cdot 10^{-5} \cdot T_k - 2.429 \cdot 10^{-9} \cdot T_k^2 + 1.219 \cdot 10^{-12} \cdot T_k^3 \quad \text{Eq. 10-26}$$

The thermal expansion is the same for  $\text{UO}_2$ , MOX and  $\text{UO}_2\text{-Gd}_2\text{O}_3$  fuels.

## 10.4. Thermal Conductivity

### 10.4.1. Notations and Units

$\lambda$	:	thermal conductivity ( $\text{W} \cdot \text{m}^{-1} \cdot \text{K}^{-1}$ )
Bu	:	burnup (MWd/t)
$T_c$	:	temperature ( $^{\circ}\text{C}$ )
$T_k$	:	temperature (K)
$k_B$	:	Boltzmann constant = $8.6144 \cdot 10^{-5} \text{ eV} \cdot \text{K}^{-1}$
S	:	Zirconia thickness (m)
p	:	porosity (fraction)
x	:	deviation from stoichiometry
y	:	plutonium content (weight fraction)
z	:	gadolinia content (weight %)

### 10.4.2. Zircaloy

The thermal conductivity for stress-relieved Zircaloy-4 cladding is:

$$0 \leq T_c \leq 455 \quad \lambda(T_c) = 12.291 + 0.0108 \cdot T_c \quad \text{Eq. 10-27}$$

$$455 \leq T_c \leq 1049 \quad \lambda(T_c) = 9.925 + 0.0160 \cdot T_c \quad \text{Eq. 10-28}$$

$$1049 \leq T_c \leq 1500 \quad \lambda(T_c) = -7.067 + 0.0322 \cdot T_c \quad \text{Eq. 10-29}$$



### 10.4.3. Advanced Alloy 5 Cladding

The thermal conductivity for the advanced Alloy 5 cladding is:

$$[b., c., d.]$$

Eq. 10-30

### 10.4.4. Zirconia

Under PWR operating conditions, the thermal conductivity of zirconia ( $ZrO_2$ ) is:

$$[b., c., d.]$$

Eq. 10-31

$$[b., c., d.]$$

Eq. 10-32

$$[b., c., d.]$$

Eq. 10-33

### 10.4.5. $UO_2$

The thermal conductivity for 100% dense  $UO_2$  between 273 K and 3120 K is:

$$[b., c., d.]$$

Eq. 10-34

The following correction for porosity is used (Ref. 10-1):

$$\lambda_p = \lambda_{100} \cdot (1 - \alpha p) \quad \text{where } \alpha = 2.58 - 5.8 \cdot 10^{-4} \cdot T_c$$

Eq. 10-35

### 10.4.6. MOX

Eq. 10-36

[b., c., d.]

### 10.4.7. $\text{UO}_2\text{-Gd}_2\text{O}_3$

[b., c., d.]

Eq. 10-37

[b., c., d.]

Eq. 10-38

## 10.5. Specific Heat

### 10.5.1. Notations and Units

$\theta$	:	constant = 535.85 K
$E_D$	:	constant = $157.7707 \cdot 10^3 \text{ J.mol}^{-1}$
$K_1$	:	constant = $80.1314 \text{ J.mol}^{-1}.\text{K}^{-1}$
$K_2$	:	constant = $32.845 \cdot 10^{-4} \text{ J.mol}^{-1}.\text{K}^{-2}$
$K_3$	:	constant = $23.62183 \cdot 10^6 \text{ J.mol}^{-1}$
$R$	:	ideal gas constant = $8.314 \text{ J.mol}^{-1}.\text{K}^{-1}$
$T_c$	:	temperature ( $^{\circ}\text{C}$ )



- $T_k$  : temperature (K)  
 $c_m$  : specific heat ( $J \cdot mol^{-1} \cdot K^{-1}$ )  
 $c_{pc}$  : specific heat ( $J \cdot g^{-1} \cdot ^\circ C^{-1}$ )  
 $c_{pk}$  : specific heat ( $J \cdot g^{-1} \cdot K^{-1}$ )

### 10.5.2. Zircaloy

The specific heat values for Zircaloy-4 cladding are:

$$0 \leq T_c \leq 570 \quad c_{pc} = 0.28796 + 8.67486 \cdot 10^{-5} \cdot T_c \quad \text{Eq. 10-39}$$

$$570 \leq T_c \leq 825 \quad c_{pc} = 0.3632 \quad \text{Eq. 10-40}$$

$$825 \leq T_c \leq 957 \quad c_{pc} = 0.6970 \quad \text{Eq. 10-41}$$

$$957 \leq T_c \leq 1500 \quad c_{pc} = 0.3597 \quad \text{Eq. 10-42}$$

### 10.5.3. Advanced Alloy 5 Cladding

The specific heat values for the advanced alloy 5 cladding are:

Eq. 10-43

Eq. 10-44

[b., c., d.]

Eq. 10-45

Eq. 10-46

### 10.5.4. $UO_2$ , MOX, $UO_2$ - $Gd_2O_3$

The specific heat of uranium dioxide is:

$$298 \leq T_k \leq 3120 \quad c_m = \frac{K_1 \cdot \Theta^2 \cdot \exp\left(\frac{\Theta}{T_k}\right)}{T_k^2 \cdot \left(\exp\left(\frac{\Theta}{T_k}\right) - 1\right)^2} + 2K_2 \cdot T_k + \frac{K_3 \cdot E_D}{R \cdot T_k^2} \cdot \exp\left(\frac{-E_D}{R \cdot T_k}\right) \quad \text{Eq. 10-47}$$

The specific heat is the same for  $UO_2$ , MOX and  $UO_2$ - $Gd_2O_3$ .



## 10.6. Emissivity

### 10.6.1. Notations and Units

$\epsilon$	:	emissivity
$T_k$	:	temperature (K)
$T_c$	:	temperature (°C)

### 10.6.2. Zircaloy

The emissivity for stress-relieved or recrystallized Zircaloy-4 cladding is:

$$\epsilon = 0.808 \quad \text{Eq. 10-48}$$

### 10.6.3. Advanced Alloy 5 Cladding

The emissivity for advanced Alloy 5 cladding is:

$$[b., c., d.] \quad \text{Eq. 10-49}$$

### 10.6.4. $\text{UO}_2$ , MOX, $\text{UO}_2\text{-Gd}_2\text{O}_3$

The uranium dioxide emissivity (Ref. 10-2) is:

$$T_k \leq 1000 \quad \epsilon = 0.8707 \quad \text{Eq. 10-50}$$

$$1000 \leq T_k \leq 2050 \quad \epsilon = 1.311 - 4.404 \cdot 10^{-4} \cdot T_k \quad \text{Eq. 10-51}$$

$$T_k \geq 2050 \quad \epsilon = 0.4083 \quad \text{Eq. 10-52}$$

The emissivity is the same for  $\text{UO}_2$ , MOX and  $\text{UO}_2\text{-Gd}_2\text{O}_3$  fuels.

### 10.7. Young's Modulus

#### 10.7.1. Notations and Units

$E$	:	Young's modulus (GPa)
$E_p$	:	Young's modulus (GPa) at a given porosity $p$
$T_k$	:	temperature (K)
$T_c$	:	temperature ( $^{\circ}\text{C}$ )
$p$	:	porosity (fraction)

#### 10.7.2. Zircaloy

Young's modulus for Zircaloy-4 cladding ([b., c., d.]) is:

$$[b., c., d.] \quad \text{Eq. 10-53}$$

#### 10.7.3. Advanced Alloy 5 Cladding

Young's modulus for the advanced Alloy 5 cladding ([b., c., d.]) is:

$$[b., c., d.] \quad \text{Eq. 10-54}$$

#### 10.7.4. $\text{UO}_2$ , MOX, $\text{UO}_2\text{-Gd}_2\text{O}_3$

The adiabatic Young's modulus of stoichiometric uranium dioxide at 100% theoretical density ( $E_{100}$  in GPa), is given by the relationships:

$$0 \leq T_c \leq 2337 \quad E_{100} = 222.46 - 1.8749 \cdot 10^{-2} \cdot T_c - 9.746 \cdot 10^{-6} \cdot T_c^2 \quad \text{Eq. 10-55}$$

$$2337 \leq T_c \leq 2656 \quad E_{100} = -1146.24 + 115.258 \cdot 10^{-2} \cdot T_c - 260.352 \cdot 10^{-6} \cdot T_c^2 \quad \text{Eq. 10-56}$$

Porosity effects are taken into account with:

$$E_p = E_{100} \cdot (1 - 2.5 \cdot p) \quad \text{Eq. 10-57}$$

Young's modulus is the same for  $\text{UO}_2$ , MOX and  $\text{UO}_2\text{-Gd}_2\text{O}_3$  fuels.

## 10.8. Poisson's Ratio

### 10.8.1. Notations and Units

$\nu$	:	Poisson's ratio
$E$	:	Young's modulus (GPa)
$G$	:	Coulomb's modulus (GPa)
$G_p$	:	Coulomb's modulus (GPa) at a given porosity $p$
$T$	:	temperature ( $^{\circ}\text{C}$ )
$p$	:	porosity (fraction)

### 10.8.2. Zircaloy

Poisson's ratio for stress-relieved or recrystallized Zircaloy-4 cladding between [b., c., d.] is:

$$[\text{b., c., d.}] \quad \text{Eq. 10-58}$$

### 10.8.3. Advanced Alloy 5 Cladding

Poisson's ratio for the advanced Alloy 5 cladding between [b., c., d.] is:

$$[\text{b., c., d.}] \quad \text{Eq. 10-59}$$

### 10.8.4. $\text{UO}_2$ , MOX, $\text{UO}_2\text{-Gd}_2\text{O}_3$

Poisson's ratio for uranium dioxide is:

$$\nu = \frac{E}{2 \cdot G} - 1 \quad \text{Eq. 10-60}$$

Coulomb's modulus of stoichiometric uranium dioxide at 100% of theoretical density ( $G_{100}$  in GPa), is:

$$0 \leq T \leq 2337 \quad G_{100} = 84.14 - 0.7203 \cdot 10^{-2} \cdot T - 3.747 \cdot 10^{-6} \cdot T^2 \quad \text{Eq. 10-61}$$

$$2337 \leq T \leq 2656 \quad G_{100} = -446.68 + 44.7076 \cdot 10^{-2} \cdot T - 100.939 \cdot 10^{-6} \cdot T^2 \quad \text{Eq. 10-62}$$

Porosity effects are taken into account with:

$$G_p = G_{100} \cdot (1 - 2.25 \cdot p) \quad \text{Eq. 10-63}$$

Poisson's ratio is the same for  $\text{UO}_2$ , MOX and  $\text{UO}_2\text{-Gd}_2\text{O}_3$  fuels.

### 10.9. 0.2% Yield Strength

#### 10.9.1. Notations and Units

$\Phi$  : fluence ( $10^{21}$  n/cm<sup>2</sup>)  
 $R_{P0.2}$  : 0.2% yield strength (MPa)  
 $T$  : temperature (°C)

#### 10.9.2. Cold Worked Stress Relieved Zircaloy

[b., c., d.] Eq. 10-64

[b., c., d.] Eq. 10-65

[b., c., d.]

[b., c., d.] Eq. 10-66

#### 10.9.3. Advanced Alloy 5 Cladding

[b., c., d.] Eq. 10-67

[b., c., d.] Eq. 10-68

[b., c., d.]

[b., c., d.] Eq. 10-69

### 10.10. Ultimate Tensile Strength

#### 10.10.1. Notations and Units

$\Phi$  : fluence ( $10^{21}$  n/cm<sup>2</sup>)  
 $\sigma_R$  : ultimate tensile strength (MPa)  
 $T$  : temperature (°C)



### 10.10.2. Cold Worked Stress Relieved Zircaloy

[b., c., d.] Eq. 10-70

[b., c., d.] Eq. 10-71

[b., c., d.]

[b., c., d.] Eq. 10-72

### 10.10.3. Advanced Alloy 5 Cladding

[b., c., d.] Eq. 10-73

[b., c., d.] Eq. 10-74

[b., c., d.]

[b., c., d.] Eq. 10-75

## 10.11. Uniform Elongation

### 10.11.1. Notations and Units

$\Phi$  : fluence ( $10^{21}$  n/cm<sup>2</sup>)

$\delta$  : uniform elongation (fraction)

T : temperature (°C)

### 10.11.2. Cold Worked Stress Relieved Zircaloy

[b., c., d.] Eq. 10-76



## 10.11.3. Advanced Alloy 5 Cladding

[b., c., d.]

Eq. 10-77

[b., c., d.]

Eq. 10-78

[b., c., d.]

[b., c., d.]

Eq. 10-79

**REFERENCES**

Ref. 10-1 J.C. VAN CRAEYNEST, J. P. STORA, *Effet de la porosité sur la variation de la conductibilité thermique du bioxyde d'uranium en fonction de la température*, JNM 37 (1970), pp 153-158.

Ref. 10-2 R.E. MASON, *Matpro-Version 11 (Rev.2), A Handbook of Material Properties for Use in the Analysis of Light Water Reactor Fuel Rod Behavior*, NUREG/CR0497, TREE-1280, Rev.2, US NRC (Aug. 1981).



COFERNIC

FCF Non Proprietary

Chapter 10

PAGE 10-16

This page intentionally left blank.

## 11. USER'S GUIDE

### 11.1. General

[b., d.]



## 11.2. Input Description

[b., d.]

**11.3. Output Description****11.3.1. Files**

[b., d.]

**11.3.2. Code Error Messages**

[b., d.]

**11.3.3. Code Performance**

[b., d.]

Eq. 11-1



COGEMA

FCF Non Proprietary

Chapter 11

PAGE 11-4

This page intentionally left blank.



**FIGURES**



COPERNIC

FCF Non Proprietary

Chapter 11

PAGE 11-6

## FIGURE 11-1 PROCEDURE TO RUN COPERNIC

[b.]



## FIGURE 11-2 SAMPLE INPUT DECK

[b.]



CORPENTIC

FCF Non Proprietary

Chapter 11

PAGE 11-8

FRAMATOME COGEMA FUELS

[b.]

FRAMATOME COGEMA FUELS

[b.]



**FIGURE 11-3 SAMPLE OUTPUT**

[b.]



# COPERNIC

FCF Non Proprietary

Chapter 11

PAGE 11-11

[b.]

FRAMATOME COGEMA FUELS



COFERMO

FCF Non Proprietary

Chapter 11

PAGE 11-12

[b.]

FRAMATOME COGEMA FUELS





# COPERNIC

FCF Non Proprietary

Chapter 11

PAGE 11-13

FRAMATOME COGEMA FUELS

[b.]



COPERNIC

FCF Non Proprietary

Chapter 11

PAGE 11-14

[b.]



COPERNIC

FCF Non Proprietary

Chapter 11

PAGE 11-15

[b.]

FRAMATOME COGEMA FUELS



COGEMA

FCF Non Proprietary

Chapter 11

PAGE 11-16

[b.]

FRAMATOME COGEMA FUELS



# COPERNIC

FCF Non Proprietary

Chapter 11

PAGE 11-17

[b.]

FRAMATOME COGEMA FUELS



COPERNIC

FCF Non Proprietary

Chapter 11

PAGE 11-18

[b.]



# COPERNIC

FCF Non Proprietary

Chapter 11

PAGE 11-19

FRAMATOME COGEMA FUELS

[b.]



COPERNIC

FCF Non Proprietary

Chapter 11

PAGE 11-20

[b.]

FRAMATOME COGEMA FUELS





# COPERNIC

FCF Non Proprietary

Chapter 11

PAGE 11-21

[b.]

FRAMATOME COGEMA FUELS



COPIER

FCF Non Proprietary

Chapter 11

PAGE 11-22

[b.]



COPERNIC

FCF Non Proprietary

Chapter 11

PAGE 11-23

[b.]

FRAMATOME COGEMA FUELS



COPIED

FCF Non Proprietary

Chapter 11

PAGE 11-24

This page intentionally left blank.



**COPERNIC**

FCF Non Proprietary

Chapter 11

PAGE 11-25

**TABLES**

FRAMATOME COGEMA FUELS

TABLE 11-1 INPUT VARIABLE DESCRIPTION

COPERNIC List of input variables

Name	Group	Dim.	Description	Default	Unit
[b.]					



COPERNIC

FCF Non Proprietary

Chapter 11

PAGE 11-26

COPERNIC List of input variables

Name	Group	Dim	Description	Default	Unit
[b.]					



COPERNIC

FCF Non Proprietary

Chapter 11 PAGE 11-27

## COPERNIC List of input variables

Name	Group	Dim.	Description	Default	Unit
[b.]					

COPERNIC

FCF Non Proprietary

Chapter 11 PAGE 11-28



## COPERNIC List of input variables

Name	Group	Dim	Description	Default	Unit
[b.]					



COPERNIC

FCF Non Proprietary

Chapter 11

PAGE 11-29

## COPERNIC List of input variables

Name	Group	Dim.	Description	Default	Unit
[b.]					

COPERNIC

FCF Non Proprietary

Chapter 11 PAGE 11-30

COPERNIC List of input variables

Name	Group	Dim	Description	Default	Unit
[b.]					

**COPERNIC**

FCF Non Proprietary

Chapter 11      PAGE 11-31

## COPERNIC List of input variables

Name	Group	Dim.	Description	Default	Unit
[b.]					

COPERNIC

FCF Non Proprietary

Chapter 11 PAGE 11-32

## COPERNIC List of input variables

Name	Group	Dim	Description	Default	Unit
[b.]					



COPERNIC

FCF Non Proprietary

Chapter 11

PAGE 11-33

## COPERNIC List of input variables

Name	Group	Dim.	Description	Default	Unit
[b.]					



COPERNIC

FCF Non Proprietary

Chapter 11 PAGE 11-34

## COPERNIC List of input variables

Name	Group	Dim.	Description	Default	Unit
[b.]					

COPERNIC

FCF Non Proprietary

Chapter 11 PAGE 11-35

## COPERNIC List of input variables

Name	Group	Dim.	Description	Default	Unit
[b.]					



COPERNIC

FCF Non Proprietary


Chapter 11

PAGE 11-36



## COPERNIC List of input variables

Name	Group	Dim	Description	Default	Unit
[b.]					

  
COPERNIC

FCF Non Proprietary

Chapter 11      PAGE 11-37

## COPERNIC List of input variables

Name	Group	Dim.	Description	Default	Unit
[b.]					

COPERNIC

FCF Non Proprietary

Chapter 11

PAGE 11-38

## COPERNIC List of input variables

Name	Group	Dim.	Description	Default	Unit
------	-------	------	-------------	---------	------

[b.]



COPERNIC

FCF Non Proprietary

Chapter 11

PAGE 11-39

## COPERNIC List of input variables

Name	Group	Dim.	Description	Default	Unit
[b.]					



COPERNIC

FCF Non Proprietary

Chapter 11

PAGE 11-40

COPERNIC List of input variables

Name	Group	Dlm.	Description	Default	Unit
[b.]					



COPERNIC

FCF Non Proprietary

Chapter 11

PAGE 11-41

COPERNIC List of input variables

Name	Group	Dim.	Description	Default	Unit
[b.]					



COPERNIC

FCF Non Proprietary

Chapter 11

PAGE 11-42



## 12. APPLICATION METHODOLOGY (UNITED STATES)

Fuel performance codes are used in a wide variety of disciplines: thermal, mechanical, nuclear and material. The COPERNIC code is no exception. It will be used primarily as a design tool for light water reactor fuel rods. The following design criteria will be used with the COPERNIC code to verify fuel rod designs.

**Fuel Rod Internal Gas Pressure:** the internal gas pressure of the peak fuel rod in the reactor will be limited to a value below that which would cause (1) the fuel-cladding gap to increase due to outward cladding creep during steady-state operation and (2) extensive DNB propagation to occur.

**LOCA Initialization:** LOCA initialization predictions will be input into LOCA evaluation models that are used to verify two principal LOCA criteria: (1) fuel rod fragmentation must not occur as a direct result of the blowdown loads, and (2) the 10 CFR Part 50 temperature and oxidation limits must not be exceeded.

**Fuel Melting:** fuel melting during normal operation and anticipated operational occurrences is precluded.

**Cladding Strain:** the maximum uniform hoop strain (elastic plus plastic) shall not exceed 1%; steady-state creep-down and irradiation growth are excluded.

**Creep Collapse Initialization:** cladding collapse is precluded during the fuel rod design life.

**Cladding Peak Oxide Thickness:** the cladding peak oxide thickness shall not exceed a best-estimate predicted value of 100 microns.

These design criteria satisfy the fuel cycle review recommendations defined in Reg. Guide 1.70 (4.4.1) and the licensing requirements defined in 10 CFR 50.46 and SRP 4.2.

The COPERNIC code will also be used to provide data for analyses that have no explicit basis in the regulations. These include best-estimate fuel temperatures for nuclear analysis codes such as NEMO (Ref. 12-1) and initialization data for core thermal-hydraulic codes such as LYNXT (Ref. 12-2). The COPERNIC code will also provide best-estimate fuel performance predictions for other similar analyses as appropriate.

The manner in which the COPERNIC code will be applied to the fuel rod design criteria is discussed below. These analyses are applicable to uranium dioxide and uranium-gadolinia fuel with low tin Zircaloy-4 and advanced alloy M5 cladding.

### 12.1. Fuel Rod Internal Gas Pressure

#### 12.1.1. Fuel Rod Internal Gas Pressure Methodology

The COPERNIC code will be used to predict fuel rod internal gas pressures that are used to verify the fuel rod internal gas pressure design criteria are met. The following analysis method will be used.



Bounding steady-state internal gas pressures will be determined from COPERNIC internal gas pressure predictions. These bounding pressures will be used with an approved fuel rod gas pressure criterion to determine the limiting internal gas pressure that will result in the onset of fuel-clad lift-off. The Fuel Rod Gas Pressure Criterion (Ref. 12-3) was approved for Zircaloy-4 cladding July 1995 and extended to advanced alloy M5 cladding November 1999 (Ref. 12-4). The bounding pressure used in this analysis is composed, at any given time-in-life, of a COPERNIC best-estimate predicted pressure plus a pressure uncertainty allowance. The pressure uncertainty allowance is composed of a COPERNIC code uncertainty allowance and allowances due to fuel rod manufacturing variations.

[b.]

Steady state and transient power history effects will be evaluated with COPERNIC. The treatment of code uncertainties, manufacturing variations, power histories, and transients is described in detail below.

Code Uncertainties: The COPERNIC code contains

[b.]

Nominal fuel rod design characteristics and thermal-hydraulic conditions will be used in these evaluations that are similar to those listed in Tables 12-1 through 12-6 and Tables 12-7 through 12-10, respectively.

Manufacturing Variations: The effects of fuel rod manufacturing variations will be included in the pressure uncertainty allowance. COPERNIC best-estimate cases will be run with nominal fuel rod design characteristics

[b.]

The COPERNIC cases used to generate the pressure allowances described above will contain cladding oxide formation and the additional following characteristics.

Power History: The rod average power history selected for the COPERNIC internal gas pressure analyses will vary according to the stage of the fuel design process the analysis is supporting.





Fuel rod design analyses, for example, will be performed with

[b.]

Applications analyses performed to support fuel reload operations will

[b.]

The power histories used in the COPERNIC internal gas pressure analyses will contain transient effects which are defined below.

Transients: The power histories discussed above will include both Condition-I and Condition-II transients. A transient is defined as a temporary change in the local power level of a fuel rod.

A Condition-I transient may occur during normal operation or the maneuvering of a plant. Condition-I design transients will be used in the fuel rod internal gas pressure analyses. A Condition-I design transient bounds all transients that are expected to occur during normal operation. [b.] Condition-I design transients will be included in the COPERNIC power histories. [b.]

In addition, if the power history contains regions of low power operation (such as reactor coast-down), the Condition-I design transients will be placed at those times in life that are at or near full power operation.

[b.]

This method of defining the Condition-I transients for the fuel rod internal gas pressure analyses will be applied to both uranium-dioxide and urania-gadolinia fuel rods.

[b.]

A Condition-II transient or Anticipated Operational Occurrence (AOO) is an event of moderate frequency. These events may result in a reactor trip but the plant will be capable of returning to operation. These events, by definition, will not propagate to cause a more serious event such as a Condition-III or IV event and are not expected to compromise the fuel rod integrity or cause an over-pressurization of the reactor coolant or secondary systems. The limiting power distributions that could occur during those Condition-II transients that would result in a fuel rod internal gas pressure increase [b.]



[b.]

This method of defining the Condition-II transients for the fuel rod internal gas pressure analyses will be applied to both uranium-dioxide and uranium-gadolinia rods.

### 12.1.2. Fuel Rod Internal Gas Pressure Examples

Six typical fuel rod designs will be used for all examples presented in this section. These fuel rod designs were selected from two uranium-dioxide and two uranium-gadolinia typical fuel cycle designs.

Mark-B,	Uranium-Dioxide [b.],
Mark-B,	Uranium-Gadolinia, [b.],
Mark-B,	Uranium-Gadolinia, [b.],
Mark-BW17,	Uranium-Dioxide [b.],
Mark-BW17,	Uranium-Gadolinia, [b.], and
Mark-BW17,	Uranium-Gadolinia, [b.].

Mark-B and Mark-BW17 are fuel rods designed for the Babcock & Wilcox (15 x 15) and Westinghouse (17 x 17) plants, respectively. The fuel rod characteristics and thermal hydraulic conditions for typical examples of these fuel rods are listed in Tables 12-1 through 12-6 and Tables 12-7 through 12-10, respectively. Note that these tables contain [b.]

[b.] shown in Figures 12-1 through 12-6 were selected for the fuel rod internal gas pressure methodology examples. These figures also contain [b.]

that are predicted to have the greatest end-of-life internal gas pressures. The transients [b.]

that are applied to the power histories are presented in Tables 12-11 through 12-16. These tables contain the following information for each transient: the [b.]

were determined to be necessary for these

examples based upon the manufacturing variations criteria presented above: [b.]

The bounding fuel rod internal gas pressures that were predicted using the methodology defined above are shown in Figures 12-7 through 12-12. The best-estimate internal gas pressure predictions which were generated [b.] (Figures 12-1 through 12-6) are also shown in Figures 12-7 through 12-12. The best-estimate cases were run with nominal fuel rod characteristics (Tables 12-1 through 12-6) and thermal-hydraulic conditions (Tables 12-7 through 12-10) and without the additional transients (Tables 12-11 through 12-16) and manufacturing variations (Tables 12-1 through 12-6) that are necessary for the bounding analysis. Figures 12-7 through 12-12 illustrate the internal gas pressure differences that may be expected to exist between best-estimate and bounding COPERNIC cases.

## 12.2. LOCA Initialization

### 12.2.1. LOCA Initialization Methodology

The COPERNIC code will be used to generate LOCA initialization predictions. These predictions will be used for LOCA evaluation models such as BWNT LOCA EM (Ref. 12-5) for B&W plants and RSG LOCA EM (Ref. 12-6) for Westinghouse plants.

[b.]

Eq. 12-1

[b.]

The following method will be used to generate the LOCA initialization predictions.

Nominal fuel rod characteristics and thermal-hydraulic conditions will be used that are similar to those listed in Tables 12-1 through 12-6 and Tables 12-7 through 12-10, respectively. The COPERNIC predictions will include cladding oxide formation. The rods will be analyzed with

[b.]



[b.]

## 12.2.2. LOCA Initialization Examples

Examples of the [b.] , obtained using the LOCA initialization methodology described above are presented for six typical fuel rod designs in Figures 12-21 through 12-26. Note that the power levels of the urania-gadolinia rods are initially restrained by the presence of the unburned gadolinia. [b.]

were used for these examples.

## 12.3. Fuel Melt

### 12.3.1. Fuel Melt Methodology

The COPERNIC code will be used to predict the linear heat rates where the onset of fuel centerline melting occurs. Fuel melting is not permitted during normal operation or anticipated operational occurrences.

Centerline fuel melt analyses will be performed with COPERNIC best-estimate predictions and nominal fuel rod design parameters. [b.]

The best-estimate fuel melt temperature relationship from Chapter 4 is:

[b.]

Eq. 12-2

where:

$T_m$  = best-estimate centerline fuel melt temperature, °C, and

Bu = pellet burnup, GWd/tU.

[b.]



[b.]

Eq. 12-3

The following fuel melt analysis method will be used.

Nominal fuel rod characteristics and thermal-hydraulic conditions will be used that are similar to those listed in Tables 12-1 through 12-6 and Tables 12-7 through 12-10, respectively. The COPERNIC predictions will include cladding oxide formation. The COPERNIC cases will be run [b.]

### 12.3.2. Fuel Melt Examples

Examples of the local linear heat rate predictions obtained [b.] are presented for the six typical fuel rod designs in Figures 12-28 through 12-33. [b.]

were used for these examples.

## 12.4. Cladding Strain

### 12.4.1. Cladding Strain Methodology

The COPERNIC code will be used to predict the local linear heat rates at which the cladding uniform hoop strains equal 1%. Cladding uniform hoop strain is limited to 1% during normal operation or anticipated operational occurrences. Cladding strain analyses will be performed with COPERNIC best-estimate predictions and nominal fuel rod characteristics across the range of operational burnups.

The cladding uniform hoop strains [b.]

The induced strain, therefore, is defined as:

[b.]

Eq. 12-4



where:

$\epsilon_{\text{hoop}}$  = cladding uniform hoop strain,

[b.]

Cladding strain analyses will be performed in the following manner. Nominal fuel rod characteristics and thermal-hydraulic conditions will be used that are similar to those listed in Tables 12-1 through 12-6 and Tables 12-7 through 12-10, respectively. The COPERNIC predictions will include cladding oxide formation. The COPERNIC cases will be run

[b.]

#### 12.4.2. Cladding Strain Examples

Examples of the linear heat rates obtained where the cladding uniform hoop strain is 1% are presented for the six typical fuel rod designs in Figures 12-28 through 12-33.

[b.]

### 12.5. Creep Collapse Initialization

#### 12.5.1. Creep Collapse Initialization Methodology

The COPERNIC code will be used to generate cladding creep collapse initialization predictions. These predictions will be input into cladding creep collapse codes such as CROV (Ref. 12-7). Cladding collapse is not permitted during the fuel rod design life.

Cladding creep collapse predictions will be generated. Conservatism will be incorporated in these analyses [b.]



The following method will be used for generating the creep collapse predictions.

Nominal fuel rod characteristics and thermal-hydraulic conditions will be used that are similar to those listed in Tables 12-1 through 12-6 and Tables 12-7 through 12-10, respectively. The COPERNIC predictions will include cladding oxide formation and these cases will be run [b.].

Creep collapse evaluations will be performed during the fuel rod design process. The power history envelopes selected for these evaluations would be expected to bound the operating power levels of all future fuel cycle designs without introducing excessive conservatism into the design process. The validity of these envelopes will be verified as part of the reload design analysis.

## 12.5.2. Creep Collapse Initialization Examples

Examples of the fuel rod internal gas pressures obtained with the creep collapse initialization methodology defined above are presented in Figures 12-34 and 12-35. The pressure differences between the uranium-dioxide and urania-gadolinia fuel rod designs shown in these figures illustrate the effect that the power histories have on the predicted creep collapse initialization internal gas pressures. [b.] that were used for these examples are shown in Figures 12-36 to 12-41.

## 12.6. Cladding Peak Oxide Thickness

### 12.6.1. Cladding Peak Oxide Thickness Methodology

The COPERNIC code will be used to generate cladding peak oxide thickness predictions. The peak cladding oxide thickness will not be allowed to exceed a best-estimate predicted value of 100 microns.

The following method will be used to generate the cladding peak oxide thickness predictions.

Best-estimate values will be used for all predictions. Nominal fuel rod characteristics and thermal-hydraulic conditions will be used, similar to those listed in Tables 12-1 through 12-6 and Tables 12-7 through 12-10, respectively. [b.]

A sub-batch is defined as fuel assemblies within a given fuel batch that have the same make-up (fuel rod designs, number and placement of urania-gadolinia rods, etc.) and that are inserted and discharged from the core at the same time so that the fuel assembly residence times are identical.

[b.]



[b.]

The COPERNIC cladding oxide model was developed from European PWR data. The fuel rod designs for these reactors are generally similar to those used by FCF. The fuel cycle designs and cycle lengths of European reactors, however, often differ significantly from United States reactors.

[b.]

to ensure that the model provides best-estimate predictions at the 100 micron level.

#### 12.6.2. Cladding Peak Oxide Thickness Examples

Examples of the COPERNIC cladding peak oxide predictions obtained are presented in Figures 12-42 through 12-47. These examples contain the predictions for both low-tin Zircaloy-4 and M5 advanced alloy claddings, and illustrate the cladding oxide thickness margin gains obtained with the M5 advanced alloy cladding. [b.] used for these examples are shown in Figures 12-36 through 12-41.





## REFERENCES

- Ref. 12-1 BAW-10180-A, Rev. 1, *NEMO - Nodal Expansion Method Optimized*, March 1993.
- Ref. 12-2 BAW-10156-A, Rev. 1, *LYNXT - Core Transient Thermal-Hydraulic Program*, August 1993.
- Ref. 12-3 BAW-10183-A, *Fuel Rod Gas Pressure Criterion (FRGPC)*, July 1995.
- Ref. 12-4 BAW-10227P-A, *Evaluation of Advanced Cladding and Structural Material (M5) in PWR Reactor Fuel*, November 1999.
- Ref. 12-5 BAW-10192P, *BWNT Loss-Of-Coolant-Accident Evaluation Model for Once-Through Steam Generator Plants*, February 1994.
- Ref. 12-6 BAW-10168P-A, Rev. 3, *B&W Loss-Of-Coolant-Accident Evaluation Model for Recirculating Steam Generator Plants*, December 1996.
- Ref. 12-7 BAW-10084P-A, Rev. 3, *Program to Determine In-Reactor Performance of BWFC Fuel Cladding Creep Collapse*, July 1995.



This page intentionally left blank.



# COPERNIC

FCF Non Proprietary

Chapter 12

PAGE 12-13

## FIGURES

FRAMATOME COGEMA FUELS



COGEMA

FCF Non Proprietary

Chapter 12

PAGE 12-14

# **FIGURE 12-1 Typical Mark-B Uranium-Dioxide Cycle**

[b.]

[b.]



## FIGURE 12-2 Typical Mark-B Urania-Gadolinia Cycle

[b.]

[b.]



COPERNIC

FCF Non Proprietary

Chapter 12 . PAGE 12-16

### FIGURE 12-3 Typical Mark-B Urania-Gadolinia Cycle

[b.]

[b.]



**COPERNIC**

FCF Non Proprietary

Chapter 12

PAGE 12-17

**FIGURE 12-4 Typical Mark-BW17 Uranium-Dioxide Cycle**

[b.]

[b.]



COGEMA

FCF Non Proprietary

Chapter 12

PAGE 12-18

**FIGURE 12-5 Typical Mark-BW17 Urania-Gadolinia Cycle**

[b.]

[b.]





## FIGURE 12-6 Typical Mark-BW17 Urania-Gadolinia Cycle

[b.]

[b.]



**COGEMA**

FCF Non Proprietary

Chapter 12

PAGE 12-20

## FIGURE 12-7 Typical Mark-B Uranium-Dioxide Cycle

[b.]

[b.]



## FIGURE 12-8 Typical Mark-B Urania-Gadolinia Cycle

[b.]

[b.]



**FIGURE 12-9 Typical Mark-B Urania-Gadolinia Cycle**

[b.]

[b.]



## FIGURE 12-10 Typical Mark-BW17 Uranium-Dioxide Cycle

[b.]

[b.]



COGEMA

FCF Non Proprietary

Chapter 12

PAGE 12-24

**FIGURE 12-11 Typical Mark-BW17 Urania-Gadolinia Cycle**

[b.]

[b.]



## FIGURE 12-12 Typical Mark-BW17 Urania-Gadolinia Cycle

[b.]

[b.]



**FIGURE 12-13 Typical Mark-B Uranium-Dioxide Cycle**

[b.]

[b.]





## FIGURE 12-14 Typical Mark-B Urania-Gadolinia Cycle

[b.]

[b.]



COGEMA

FCF Non Proprietary

Chapter 12

PAGE 12-28

**FIGURE 12-15 Typical Mark-B Urania-Gadolinia Cycle**

[b.]

[b.]



## FIGURE 12-16 Typical Mark-BW17 Uranium-Dioxide Cycle

[b.]

[b.]



COGEMA

FCF Non Proprietary

Chapter 12

PAGE 12-30

# FIGURE 12-17 Typical Mark-BW17 Urania-Gadolinia Cycle

[b.]

[b.]



## FIGURE 12-18 Typical Mark-BW17 Urania-Gadolinia Cycle

[b.]

[b.]



**FIGURE 12-19 Typical Mark-B Fuel Cycles**

[b.]

[b.]



## FIGURE 12-20 Typical Mark-BW17 Fuel Cycles

[b.]

[b.]



COPIED

FCF Non Proprietary

Chapter 12

PAGE 12-34

# FIGURE 12-21 Typical Mark-B Uranium-Dioxide Cycle

[b.]

[b.]





**FIGURE 12-22 Typical Mark-B Urania-Gadolinia Cycle**

[b.]

[b.]



COGEMA

FCF Non Proprietary

Chapter 12

PAGE 12-36

# **FIGURE 12-23 Typical Mark-B Urania-Gadolinia Cycle**

[b.]

[b.]



## FIGURE 12-24 Typical Mark-BW17 Uranium-Dioxide Cycle

[b.]

[b.]



CONFIDENTIAL

FCF Non Proprietary

Chapter 12

PAGE 12-38

**FIGURE 12-25 Typical Mark-BW17 Urania-Gadolinia Cycle**

[b.]

[b.]



## FIGURE 12-26 Typical Mark-BW17 Urania-Gadolinia Cycle

[b.]

[b.]



OPERA

FCF Non Proprietary

Chapter 12

PAGE 12-40

**FIGURE 12-27 Typical Mark-B and Mark-BW17 Fuel Cycles**

[b.]

[b.]



## FIGURE 12-28 Typical Mark-B Uranium-Dioxide Cycle

[b.]

[b.]



COPERNIC

FCF Non Proprietary

Chapter 12

PAGE 12-42

**FIGURE 12-29 Typical Mark-B Urania-Gadolinia Cycle**

[b.]

[b.]





**FIGURE 12-30 Typical Mark-B Urania-Gadolinia Cycle**

[b.]

[b.]



COPIERNIC

FCF Non Proprietary

Chapter 12

PAGE 12-44

**FIGURE 12-31 Typical Mark-BW17 Uranium-Dioxide Cycle**

[b.]

[b.]



## FIGURE 12-32 Typical Mark-BW17 Urania-Gadolinia Cycle

[b.]

[b.]



COGEMA

FCF Non Proprietary

Chapter 12

PAGE 12-46

**FIGURE 12-33 Typical Mark-BW17 Urania-Gadolinia Cycle**

[b.]

[b.]



FIGURE 12-34 Typical Mark-B Fuel Cycles

[b.]

[b.]



COGEMA

FCF Non Proprietary

Chapter 12

PAGE 12-48

**FIGURE 12-35 Typical Mark-BW17 Fuel Cycles**

[b.]

[b.]



## FIGURE 12-36 Typical Mark-B Uranium-Dioxide Cycle

[b.]

[b.]



COGEMA

FCF Non Proprietary

Chapter 12

PAGE 12-50

**FIGURE 12-37 Typical Mark-B Urania-Gadolinia Cycle**

[b.]

[b.]





## FIGURE 12-38 Typical Mark-B Urania-Gadolinia Cycle

[b.]

[b.]



CERN

FCF Non Proprietary

Chapter 12

PAGE 12-52

**FIGURE 12-39 Typical Mark-BW17 Uranium-Dioxide Cycle**

[b.]

[b.]



## FIGURE 12-40 Typical Mark-BW17 Urania-Gadolinia Cycle

[b.]

[b.]



**FIGURE 12-41 Typical Mark-BW17 Urania-Gadolinia Cycle**

[b.]

[b.]



## FIGURE 12-42 Typical Mark-B Uranium-Dioxide Cycle

[b.]

[b.]



COPERNIC

FCF Non Proprietary

Chapter 12

PAGE 12-56

**FIGURE 12-43 Typical Mark-B Urania-Gadolinia Cycle**

[b.]

[b.]



## FIGURE 12-44 Typical Mark-B Urania-Gadolinia Cycle

[b.]

[b.]



**FIGURE 12-45 Typical Mark-BW17 Uranium-Dioxide Cycle**

[b.]

[b.]





## FIGURE 12-46 Typical Mark-BW17 Urania-Gadolinia Cycle

[b.]

[b.]



COPERNIC

FCF Non Proprietary

Chapter 12

PAGE 12-60

**FIGURE 12-47 Typical Mark-BW17 Urania-Gadolinia Cycle**

[b.]

[b.]



COPERNIC

FCF Non Proprietary

Chapter 12

PAGE 12-61

TABLES

FRAMATOME COGEMA FUELS



**TABLE 12-1 Typical Mark-B Uranium-Dioxide Fuel Cycle  
Fuel Rod Characteristics**

[b.]



**TABLE 12-2 Typical Mark-B Urania-Gadolinia Fuel Cycle  
Fuel Rod Characteristics**

[b.]



COGEMA

FCF Non Proprietary

Chapter 12

PAGE 12-64

**TABLE 12-3 Typical Mark-B Urania-Gadolinia Fuel Cycle**

**Fuel Rod Characteristics**

[b.]



**TABLE 12-4 Typical Mark-BW17 Uranium-Dioxide Fuel Cycle  
Fuel Rod Characteristics**

[b.]



COPIED

FCF Non Proprietary

Chapter 12

PAGE 12-66

**TABLE 12-5 Typical Mark-BW17 Urania-Gadolinia Fuel Cycle  
Fuel Rod Characteristics**

[b.]





**TABLE 12-6 Typical Mark-BW17 Urania-Gadolinia Fuel Cycle**  
**Fuel Rod Characteristics**

[b.]



COGEMA

FCF Non Proprietary

Chapter 12

PAGE 12-68

**TABLE 12-7 Typical Mark-B Uranium-Dioxide Fuel Cycle  
Thermal-Hydraulic Conditions**

[b.]



**TABLE 12-8 Typical Mark-B Urania-Gadolinia Fuel Cycle**  
**Thermal-Hydraulic Conditions**

[b.]



COPERNIC

FCF Non Proprietary

Chapter 12

PAGE 12-70

**TABLE 12-9 Typical Mark-BW17 Uranium-Dioxide Fuel Cycle  
Thermal-Hydraulic Conditions**

[b.]



**TABLE 12-10 Typical Mark-BW17 Urania-Gadolinia Fuel Cycle**  
**Thermal-Hydraulic Conditions**

[b.]



COGEMA

FCF Non Proprietary

Chapter 12

PAGE 12-72

**TABLE 12-11 Typical Mark-B Uranium-Dioxide Cycle**

[b.]

[b.]

**TABLE 12-12 Typical Mark-B Urania-Gadolinia Cycle**

[b.]

[b.]



CONFIDENTIAL

FCF Non Proprietary

Chapter 12

PAGE 12-74

**TABLE 12-13 Typical Mark-B Urania-Gadolinia Cycle**

[b.]

[b.]





## TABLE 12-14 Typical Mark-BW17 Uranium-Dioxide Cycle

[b.]

[b.]



CONFIDENTIAL

FCF Non Proprietary

Chapter 12

PAGE 12-76

**TABLE 12-15 Typical Mark-BW17 Urania-Gadolinia Cycle**

[b.]

[b.]



**TABLE 12-16 Typical Mark-BW17 Urania-Gadolinia Cycle**

[b.]

[b.]



This page intentionally left blank.



### 13. MOX APPLICATION METHODOLOGY (UNITED STATES)

The U.S. Department of Energy (DOE) has recommended that a significant portion of the nation's surplus weapons-grade (WG) plutonium be disposed of by reconstituting the plutonium into mixed-oxide ( $\text{UO}_2\text{-PuO}_2$ , MOX) fuel rods and irradiating them in commercial light water reactors. The COPENIC code, developed utilizing the extensive European experience with reactor-grade (RG) MOX fuels, will be used to perform fuel performance analyses for MOX fuel with weapons-grade plutonium in support of this Material Disposition Program.

The MOX fuel produced from weapons-grade material will be virtually identical to the fuel produced from reactor-grade material in terms of physical characteristics and performance. The manufacturing processes, plutonium isotopics, impurities, and pellet microstructure will be controlled to ensure this equivalence. The fabrication process will use the COGEMA/BELGONUCLEAIRE-developed Micronized MASTER blend (MIMAS) process currently supplying MOX fuel to 32 reactors in Europe. The use of WG plutonium will significantly reduce the  $\text{PuO}_2$  content of MOX fuel relative to RG material. The WG material is about 95% fissile, whereas the RG material contains significant amounts of absorber isotopes ( $\text{Pu-240}$ ,  $\text{Pu-242}$ ). Thus, MOX fuel from WG material will require Pu contents of 4% to 5% instead of the 8% to 9% for RG MOX. Gallium and other impurities will be effectively eliminated through the use of an aqueous polishing process step added to the manufacturing process being used to produce the WG MOX fuel. Due to the different isotopics, the WG material will have a fissile plutonium content about 50% greater than that of the RG plutonium. However, the master mix of  $\text{UO}_2$  and  $\text{PuO}_2$  will be adjusted from the 70/30 ratio typical of RG material, to 80/20 for the WG material to ensure that the fissile content of the plutonium-rich particles remains the same as the reactor grade material. Since the fission density and thus, the fission product concentration and distribution, will be comparable to the RG fuel, the WG fuel behavior will be consistent with that of the European experience base.

The COPENIC fuel performance code will be used primarily as a design tool for light water reactor fuel rods – both low enriched uranium (LEU) as discussed in Chapter 12 and mixed oxide as discussed in this chapter. This chapter prescribes the application methodology and presents example calculational results of the COPENIC code applied to MOX fuel. The same design criteria applied to LEU fuel in Chapter 12 will be used with the COPENIC code to verify the acceptable performance of MOX fuel rod designs, namely:

**Fuel Rod Internal Gas Pressure:** the internal gas pressure of the maximum pressure fuel rod in the reactor will be limited to a value below that which would cause (1) the fuel-cladding gap to increase due to outward cladding creep during steady-state operation and (2) extensive DNB propagation to occur.

**LOCA Initialization:** LOCA initialization predictions will be input into LOCA evaluation models that are used to verify two principal LOCA criteria: (1) fuel rod fragmentation must not occur as a direct result of the blowdown loads, and (2) the 10 CFR Part 50 temperature and oxidation limits must not be exceeded.

**Fuel Melting:** fuel melting during normal operation and anticipated operational



occurrences is precluded.

**Cladding Strain:** the maximum uniform hoop strain (elastic plus plastic) shall not exceed 1%; the impact of steady-state creep-down and irradiation growth is excluded.

**Creep Collapse Initialization:** cladding collapse is precluded during the fuel rod design life.

**Cladding Peak Oxide Thickness:** the cladding peak oxide thickness shall not exceed a best-estimate predicted value of 100 microns.

These design criteria satisfy the fuel cycle review recommendations defined in Reg. Guide 1.70 (4.4.1) and the licensing requirements defined in 10 CFR 50.46 and SRP 4.2.

The COPERNIC code will also be used to provide data for analyses that have no explicit basis in the regulations. These include best-estimate fuel temperatures for nuclear analysis codes such as NEMO (Ref. 13-1) and initialization data for core thermal-hydraulic codes such as LYNXT (Ref. 13-2). The COPERNIC code will also provide best-estimate fuel performance predictions for other similar analyses.

The manner in which the COPERNIC code will be applied to the fuel rod design criteria is discussed below.

## **13.1. Fuel Rod Internal Gas Pressure**

### **13.1.1. Fuel Rod Internal Gas Pressure Methodology**

The COPERNIC code will be used to predict fuel rod internal gas pressures that are used to verify that the fuel rod internal gas pressure design criteria are met. The following analysis method which is consistent with that described in Chapter 12 for  $\text{UO}_2$  fuel will be used.

Bounding steady-state internal gas pressures will be determined from COPERNIC internal gas pressure predictions. These bounding pressures will be used with an approved fuel rod gas pressure criterion to determine the limiting internal gas pressure that will result in the onset of fuel-clad lift-off. The Fuel Rod Gas Pressure Criterion (Ref. 13-3) was approved for Zircaloy-4 cladding in July 1995 and extended to advanced alloy M5 cladding in November 1999 (Ref. 13-4). The bounding pressure used in this analysis is composed, at any given time-in-life, of a COPERNIC best-estimate predicted pressure plus a pressure uncertainty allowance. The pressure uncertainty allowance is composed of a COPERNIC code uncertainty allowance and allowances for fuel rod manufacturing variations.

[b.]

Steady state and transient power history effects will be evaluated with COPERNIC. The treatment of code uncertainties, manufacturing variations, power histories, and transients is described in detail below.



Code Uncertainties: The COPERNIC code contains [b.]

Nominal fuel rod design characteristics and thermal-hydraulic conditions that are similar to those listed in Tables 13-1 and 13-2, respectively, will be used in these evaluations.

Manufacturing Variations: The effects of fuel rod manufacturing variations will be included in the pressure uncertainty allowance. COPERNIC best-estimate cases will be run with nominal fuel rod design characteristics

[b.]

The COPERNIC cases used to generate the pressure allowances described above will contain cladding oxide formation and the additional following characteristics.

Power History: The rod average power history selected for the COPERNIC internal gas pressure analyses will vary according to the stage of the fuel cycle design process the analysis is supporting.

Fuel rod design analyses, for example, will be performed with

[b.]

Applications analyses performed to support fuel reload operations will

[b.]

The power histories used in the COPERNIC internal gas pressure analyses will contain transient effects which are defined below.



**Transients:** The power histories discussed above will include both Condition-I and Condition-II transients. A transient is defined as a temporary change in the local power level of a fuel rod.

A Condition-I transient may occur during normal operation or the maneuvering of a plant. Condition-I design transients will be used in the fuel rod internal gas pressure analyses. A Condition-I design transient bounds all transients that are expected to occur during normal operation. [b.] Condition-I design transients will be included in the COPERNIC power histories. [b.]

In addition, if the power history contains regions of low power operation (such as reactor coast-down), the Condition-I design transients will be placed at those times in life that are at or near full power operation. [b.]

This method of defining the Condition-I transients for the fuel rod internal gas pressure analyses will be applied to both  $\text{UO}_2$  and MOX fuel rods.

[b.]

A Condition-II transient or Anticipated Operational Occurrence (AOO) is an event of moderate frequency. These events may result in a reactor trip but the plant will be capable of returning to operation. These events, by definition, will not propagate to cause a more serious event such as a Condition-III or IV event and are not expected to compromise the fuel rod integrity or cause an over-pressurization of the reactor coolant or secondary systems. The limiting power distributions that could occur during those Condition-II transients that would result in a fuel rod internal gas pressure increase

[b.]

This method of defining the Condition-II transients for the fuel rod internal gas pressure analyses will be applied to both  $\text{UO}_2$  and mixed oxide fuel rods.

### 13.1.2. Fuel Rod Internal Gas Pressure Example

One typical fuel rod design is used for the example presented in this section. This fuel rod design, the Mark-BW/MOX1 (non-axial blanket) design, is representative of the planned design to be





employed in the partial-MOX core fuel cycles and is an adaptation of the Advanced Mk-BW fuel rod design. Partial-MOX fuel cycles utilize both LEU and MOX fuel assemblies in the reactor core.

The Mark-BW/MOX1 is a fuel rod designed for Westinghouse (17 x 17)-type plants. The fuel rod characteristics and thermal hydraulic conditions for this example are listed in Tables 13-1 and 13-2, respectively. Note that these tables contain [b.]

[b.] shown in Figure 13-1 was selected for the fuel rod internal gas pressure methodology example. [b.]

The transients [b.]

that are applied to the power history envelope are presented in Table 13-3. These tables contain the following information for each transient: the [b.]

were determined for this example based upon the manufacturing variations criteria presented above: [b.]

The bounding fuel rod internal gas pressure that was predicted using the methodology defined above is shown in Figure 13-2.

## **13.2. LOCA Initialization**

### **13.2.1. LOCA Initialization Methodology**

The COPERNIC code will be used to generate LOCA initialization predictions. These predictions will be used for LOCA evaluation models such as the RSG LOCA EM (Ref. 13-5) for Westinghouse-type plants and the LOCA EM Topical Addendum for MOX fuel (to be submitted). [b.]

[b.]

Eq. 13-1

The following method will be used to generate the LOCA initialization predictions.



Nominal fuel rod characteristics and thermal-hydraulic conditions will be used that are similar to those listed in Tables 13-1 and 13-2, respectively. The COPERNIC predictions will include cladding oxide formation. The rods will be analyzed with

[b.]

### 13.2.2. LOCA Initialization Example

An example of the [b.] obtained using the LOCA initialization methodology described above is presented for a typical MOX fuel rod design in Figure 13-4. [b.]

were used for this example.

### 13.3. Fuel Melt

#### 13.3.1. Fuel Melt Methodology

The COPERNIC code will be used to predict the linear heat rates where the onset of fuel centerline melting occurs. Fuel melting is not permitted during normal operation or anticipated operational occurrences.

Centerline fuel melt analyses will be performed with COPERNIC best-estimate predictions and nominal fuel rod design parameters. [b.]

The best-estimate fuel melt temperature relationship for MOX fuel from Chapter 10 is:

[b.]

Eq. 13-2

where:

$T_m$  = best-estimate centerline fuel melt temperature, °C,



$y$  = plutonium content weight fraction, and

Bu = pellet burnup, GWd/tM.

[b.]

[b.]

Eq. 13-3

The following fuel melt analysis method will be used.

Nominal fuel rod characteristics and thermal-hydraulic conditions will be used that are similar to those listed in Tables 13-1 and 13-2, respectively. The COPERNIC predictions will include cladding oxide formation. The COPERNIC cases will be run

[b.]

### 13.3.2. Fuel Melt Example

An example of the local linear heat rate predictions obtained [b.]  
is presented for the typical MOX fuel rod design in Figure 13-6. [b.]

were used for this example.

## 13.4. Cladding Strain

### 13.4.1. Cladding Strain Methodology

The COPERNIC code will be used to predict the local linear heat rates at which the cladding uniform hoop strains equal 1%. Cladding uniform hoop strain is limited to 1% during normal operation or anticipated operational occurrences. Cladding strain analyses will be performed with COPERNIC best-estimate predictions and nominal fuel rod characteristics across the range of operational burnups.

The cladding uniform hoop strains [b.]



The induced strain, therefore, is defined as:

[b.]

Eq. 13-4

where:

$\epsilon_{\text{hoop}}$  = cladding uniform hoop strain,

[b.]

Cladding strain analyses will be performed in the following manner.

Nominal fuel rod characteristics and thermal-hydraulic conditions will be used that are similar to those listed in Tables 13-1 and 13-2, respectively. The COPERNIC predictions will include cladding oxide formation. The COPERNIC cases will be run [b.]

### 13.4.2. Cladding Strain Example

An example of the linear heat rates obtained where the cladding uniform hoop strain is 1% is presented for the typical MOX fuel rod design in Figure 13-6. [b.]

## 13.5. Creep Collapse Initialization

### 13.5.1. Creep Collapse Initialization Methodology

The COPERNIC code will be used to generate cladding creep collapse initialization predictions. These predictions will be input into cladding creep collapse analysis codes such as CROV (Ref. 13-6). Cladding collapse is not permitted during the fuel rod design life.



Cladding creep collapse predictions will incorporate conservatism [b.]

The following method will be used for generating the creep collapse predictions.

Nominal fuel rod characteristics and thermal-hydraulic conditions will be used that are similar to those listed in Tables 13-1 and 13-2, respectively. The COPERNIC predictions will include cladding oxide formation and these cases will be run [b.]

Creep collapse evaluations will be performed during the fuel rod design process. The power history envelopes selected for these evaluations would be expected to bound the operating power levels of all future fuel cycle designs without introducing excessive conservatism into the design process. The validity of these envelopes will be verified as part of the reload design analysis.

### 13.5.2. Creep Collapse Initialization Example

An example of the fuel rod internal gas pressures obtained with the creep collapse initialization methodology defined above is presented in Figure 13-7. [b.] that was used for this example is shown in Figure 13-1.

## 13.6. Cladding Peak Oxide Thickness

### 13.6.1. Cladding Peak Oxide Thickness Methodology

The COPERNIC code will be used to generate cladding peak oxide thickness predictions. The peak cladding oxide thickness will not be allowed to exceed a best-estimate predicted value of 100 microns.

The following method will be used to generate the cladding peak oxide thickness predictions.

Best-estimate values will be used for all predictions. Nominal fuel rod characteristics and thermal-hydraulic conditions will be used, similar to those listed in Tables 13-1 and 13-2, respectively. [b.]

A sub-batch is defined as fuel assemblies within a given fuel batch that have the same make-up (fuel rod designs, plutonium content, etc.) and that are inserted and discharged from the core at the same time so that the fuel assembly residence times are identical. [b.]



The COPERNIC cladding oxide model was developed from European PWR data. The fuel rod designs for these reactors are generally similar to those used by FCF. The fuel cycle designs and cycle lengths of European reactors, however, often differ significantly from United States reactors. [b.]

that the model provides best-estimate predictions at the 100 micron level. to ensure

### 13.6.2. Cladding Peak Oxide Thickness Example

An example of the COPERNIC cladding peak oxide predictions obtained is presented in Figure 13-8. This example contains the predictions for both low-tin Zircaloy-4 and M5 advanced alloy claddings, and illustrates the cladding oxide thickness margin gains obtained with the M5 advanced alloy cladding. [b.] used for this example is shown in Figure 13-1.



## REFERENCES

- Ref. 13-1 BAW-10180-A, Rev. 1, *NEMO - Nodal Expansion Method Optimized*, March 1993.
- Ref. 13-2 BAW-10156-A, Rev. 1, *LYNXT - Core Transient Thermal-Hydraulic Program*, August 1993.
- Ref. 13-3 BAW-10183-A, *Fuel Rod Gas Pressure Criterion (FRGPC)*, July 1995.
- Ref. 13-4 BAW-10227P-A, *Evaluation of Advanced Cladding and Structural Material (M5) in PWR Reactor Fuel*, November 1999.
- Ref. 13-5 BAW-10168P-A, Rev. 3, *B&W Loss-Of-Coolant-Accident Evaluation Model for Recirculating Steam Generator Plants*, December 1996.
- Ref. 13-6 BAW-10084P-A, Rev. 3, *Program to Determine In-Reactor Performance of BWFC Fuel Cladding Creep Collapse*, July 1995.

This page intentionally left blank.





# COPERNIC

FCF Non Proprietary

Chapter 13

PAGE 13-13

## FIGURES

FRAMATOME COGEMA FUELS



## FIGURE 13-1 Typical Mark-BW/MOX1 Partial-MOX Fuel Cycle

[b.]

[b.]



## FIGURE 13-2 Typical Mark-BW/MOX1 Partial-MOX Fuel Cycle

[b.]

[b.]



## FIGURE 13-3 Typical Mark-BW/MOX1 Partial-MOX Fuel Cycle

[b.]

[b.]



## FIGURE 13-4 Typical Mark-BW/MOX1 Partial-MOX Fuel Cycle

[b.]

[b.]



## FIGURE 13-5 Typical Mark-BW/MOX1 Partial-MOX Fuel Cycle

[b.]

[b.]



## FIGURE 13-6 Typical Mark-BW/MOX1 Partial-MOX Fuel Cycle

[b.]

[b.]



## FIGURE 13-7 Typical Mark-BW/MOX1 Partial-MOX Fuel Cycle

[b.]

[b.]





## FIGURE 13-8 Typical Mark-BW/MOX1 Partial-MOX Fuel Cycle

[b.]

[b.]



# COPERNIC

FCF Non Proprietary

Chapter 13

PAGE 13-22

This page intentionally left blank.



# COPERNIC

FCF Non Proprietary

Chapter 13

PAGE 13-23

## TABLES

FRAMATOME COGEMA FUELS



**TABLE 13-1 Typical Mark-BW/MOX1 Partial-MOX Fuel Cycle  
Fuel Rod Characteristics**

[b.]



## TABLE 13-2 Typical Mark-BW/MOX1 Partial-MOX Fuel Cycle

### Thermal-Hydraulic Conditions

[b.]



**TABLE 13-3 Typical Mark-BW/MOX1 Partial-MOX Fuel Cycle**

[b.]

[b.]



**COPERNIC**

BAW-10231(NP)-A

June, 2002

## **APPENDIX A**

**Correspondence with the NRC, including  
Requests for Additional Information and Responses**

FRAMATOME ANP

# FRAMATOME COGEMA FUELS

September 16, 1999  
GR99-191.doc

*File*

U. S. Nuclear Regulatory Commission  
ATTN: Document Control Desk  
Washington, DC 20555

Subject: Topical Report BAW-10231P, "COPERNIC Fuel Rod Design  
Computer Code."

References: 1. T. A. Coleman to NRC Document Control Desk,  
GR074.doc, January 22, 1998.

2. T. A. Coleman to NRC Document Control Desk,  
GR506.doc, July 14, 1998.

Gentlemen:

Enclosed are fifteen copies of topical report BAW-10231P, COPERNIC Fuel Rod Design Computer Code dated September, 1999. Also enclosed are 12 copies of the revised BAW-10231 which is the non-proprietary version of BAW-10231P. This report describes the COPERNIC fuel rod design computer code and its application to fuel designed and licensed by Framatome Cogema Fuels (FCF).

COPERNIC is applicable to natural, slightly enriched, reprocessed, and re-blended highly enriched uranium dioxide fuels as well as urania-gadolinia, and mixed oxide fuels. FCF requests that approval of BAW-10231P be limited to application to uranium dioxide and urania-gadolinia fuels. An addendum to BAW-10231P to support application to mixed oxide fuel will be submitted in August 2000.

COPERNIC will be used in the fuel rod design and analysis of the fuel that uses FCF's advanced cladding material. NRC review of the advanced cladding topical report is near completion and now is an appropriate time to update BAW-10231P to reflect the methodology that will be used for that material. FCF also found that a revision of the COPERNIC thermal model is required with this submittal. Incorporating these changes has impact throughout BAW-10231P. Therefore the report is being resubmitted in its entirety rather than being issued as change pages.

Reference 1 was the original transmittal of the COPERNIC computer code topical report to the NRC. The same report was resubmitted to the NRC in reference 2 to clarify the proprietary classification of some of the material. FCF hereby requests that



Framatome Cogema Fuels  
3315 Old Forest Road, P.O. Box 10935, Lynchburg, VA 24506-0935  
Telephone: 804-832-3000 Fax: 804-832-3663



these two submittals of BAW-10231P dated January 1998 and July 1998 respectively, be destroyed and replaced with the updated version of the report.

The applications portion of BAW-10231P is still in preparation. The applications will be completed and documented to the NRC as chapter 12 of BAW-10231P. Chapter 12 will be submitted in December 1999.

In accordance with 10CFR2.790, it is requested that this report be considered proprietary. An affidavit supporting this request, is attached. In order to complete the engineering activities associated with implementation of advanced cladding and other new product designs, NRC approval of COPERNIC for uranium dioxide and urania-gadolinia fuels is needed by December 31, 2000.

Very truly yours,



T. A. Coleman, Vice President  
Government Relations

cc: J. S. Wermiel, NRC  
S. L. Wu, NRC  
R. Caruso, NRC  
S. N. Bailey, NRC  
C. E. Beyer, PNL  
M. A. Schoppman  
R. N. Edwards

# FRAMATOME COGEMA FUELS

December 2, 1999  
GR99-234.doc

U. S. Nuclear Regulatory Commission  
ATTN: Document Control Desk  
Washington, DC 20555

Subject: Topical Report BAW-10231P, "COPERNIC Fuel Rod Design  
Computer Code."

Reference: T. A. Coleman to NRC Document Control Desk,  
GR99-191.doc, September 16, 1999.

Gentlemen:

The reference letter transmitted the updated version of the COPERNIC topical report, BAW-10231P. As was noted in the letter, the applications portion of BAW-10231P was still in preparation and was not included with the submittal. The letter also stated that the applications portion would be submitted in December 1999. The Applications Methodology (chapter 12) is enclosed with this letter. Fifteen copies of the proprietary version and twelve copies of the non-proprietary version are attached.

Please replace pages xvii and xviii and add pages xix and xx to the Table of Contents in BAW-10231P. Place the remaining pages (chapter 12) at the very end of the report

In accordance with 10CFR2.790, it is requested that this report be considered proprietary. An affidavit supporting this request, is attached. In order to complete the engineering activities associated with implementation of advanced cladding and other new product designs, NRC approval of COPERNIC for uranium dioxide and urania-gadolinia fuels is needed by December 31, 2000.

Very truly yours,

*T. A. Coleman*

T. A. Coleman, Vice President  
Government Relations

cc: J. S. Wermiel, NRC  
S. L. Wu, NRC  
R. Caruso, NRC  
S. N. Bailey, NRC  
C. E. Beyer, PNL  
M. A. Schoppman  
R. N. Edwards

  
**FRAMATOME**  
TECHNOLOGIES

Framatome Cogema Fuels  
3315 Old Forest Road, P.O. Box 10935, Lynchburg, VA 24506-0935  
Telephone: 804-832-3000 Fax: 804-832-3683

AFFIDAVIT OF THOMAS A. COLEMAN

- A. My name is Thomas A. Coleman. I am Vice President of Government Relations for Framatome Cogema Fuels (FCF). Therefore, I am authorized to execute this Affidavit.
- B. I am familiar with the criteria applied by FCF to determine whether certain information of FCF is proprietary and I am familiar with the procedures established within FCF to ensure the proper application of these criteria.
- C. In determining whether an FCF document is to be classified as proprietary information, an initial determination is made by the Unit Manager, who is responsible for originating the document, as to whether it falls within the criteria set forth in Paragraph D hereof. If the information falls within any one of these criteria, it is classified as proprietary by the originating Unit Manager. This initial determination is reviewed by the cognizant Section Manager. If the document is designated as proprietary, it is reviewed again by personnel and other management within FCF as designated by the Vice President of Government Relations to assure that the regulatory requirements of 10 CFR Section 2.790 are met.
- D. The following information is provided to demonstrate that the provisions of 10 CFR Section 2.790 of the Commission's regulations have been considered:
- (i) The information has been held in confidence by FCF. Copies of the document are clearly identified as proprietary. In addition, whenever FCF transmits the information to a customer, customer's agent, potential customer or regulatory agency, the transmittal requests the recipient to hold the information as proprietary. Also, in order to strictly limit any potential or actual customer's use of proprietary information, the substance of the following provision is included in all agreements entered into by FCF, and an equivalent version of the proprietary provision is included in all of FCF's proposals:

AFFIDAVIT OF THOMAS A. COLEMAN (Cont'd.)

"Any proprietary information concerning Company's or its Supplier's products or manufacturing processes which is so designated by Company or its Suppliers and disclosed to Purchaser incident to the performance of such contract shall remain the property of Company or its Suppliers and is disclosed in confidence, and Purchaser shall not publish or otherwise disclose it to others without the written approval of Company, and no rights, implied or otherwise, are granted to produce or have produced any products or to practice or cause to be practiced any manufacturing processes covered thereby.

Notwithstanding the above, Purchaser may provide the NRC or any other regulatory agency with any such proprietary information as the NRC or such other agency may require; provided, however, that Purchaser shall first give Company written notice of such proposed disclosure and Company shall have the right to amend such proprietary information so as to make it non-proprietary. In the event that Company cannot amend such proprietary information, Purchaser shall, prior to disclosing such information, use its best efforts to obtain a commitment from NRC or such other agency to have such information withheld from public inspection.

Company shall be given the right to participate in pursuit of such confidential treatment."

AFFIDAVIT OF THOMAS A. COLEMAN (Cont'd.)

(ii) The following criteria are customarily applied by FCF in a rational decision process to determine whether the information should be classified as proprietary. Information may be classified as proprietary if one or more of the following criteria are met:

- a. Information reveals cost or price information, commercial strategies, production capabilities, or budget levels of FCF, its customers or suppliers.
- b. The information reveals data or material concerning FCF research or development plans or programs of present or potential competitive advantage to FCF.
- c. The use of the information by a competitor would decrease his expenditures, in time or resources, in designing, producing or marketing a similar product.
- d. The information consists of test data or other similar data concerning a process, method or component, the application of which results in a competitive advantage to FCF.
- e. The information reveals special aspects of a process, method, component or the like, the exclusive use of which results in a competitive advantage to FCF.
- f. The information contains ideas for which patent protection may be sought.

AFFIDAVIT OF THOMAS A. COLEMAN (Cont'd.)

The document(s) listed on Exhibit "A", which is attached hereto and made a part hereof, has been evaluated in accordance with normal FCF procedures with respect to classification and has been found to contain information which falls within one or more of the criteria enumerated above. Exhibit "B", which is attached hereto and made a part hereof, specifically identifies the criteria applicable to the document(s) listed in Exhibit "A".

- (iii) The document(s) listed in Exhibit "A", which has been made available to the United States Nuclear Regulatory Commission was made available in confidence with a request that the document(s) and the information contained therein be withheld from public disclosure.
- (iv) The information is not available in the open literature and to the best of our knowledge is not known by Combustion Engineering, Siemens, General Electric, Westinghouse or other current or potential domestic or foreign competitors of Framatome Cogema Fuels.
- (v) Specific information with regard to whether public disclosure of the information is likely to cause harm to the competitive position of FCF, taking into account the value of the information to FCF; the amount of effort or money expended by FCF developing the information; and the ease or difficulty with which the information could be properly duplicated by others is given in Exhibit "B".

I have personally reviewed the document(s) listed on Exhibit "A" and have found that it is considered proprietary by FCF because it contains information which falls within one or more of the criteria enumerated in Paragraph D, and it is information which is customarily held in confidence and protected as proprietary information by FCF. This report comprises information utilized by FCF in its business which afford FCF an

AFFIDAVIT OF THOMAS A. COLEMAN (Cont'd.)

opportunity to obtain a competitive advantage over those who may wish to know or use the information contained in the document(s).

*TH Coleman*  
THOMAS A. COLEMAN

State of Virginia) ) SS. Lynchburg  
City of Lynchburg)

Thomas A. Coleman, being duly sworn, on his oath deposes and says that he is the person who subscribed his name to the foregoing statement, and that the matters and facts set forth in the statement are true.

*TH Coleman*  
THOMAS A. COLEMAN

Subscribed and sworn before me  
this 6<sup>th</sup> day of December, 1999.

*Skanda L. Skade*  
Notary Public in and for the City  
of Lynchburg, State of Virginia.

My Commission Expires 8/31/01.

**EXHIBITS A & B**

**EXHIBIT A**

Applications Methodology - Chapter 12 of  
Topical Report BAW-10231P, "COPERNIC Fuel Rod Design Computer Code"

**EXHIBIT B**

The above listed document contains information which is considered Proprietary in  
Accordance with Criteria b,c,d, and e of the attached affidavit.





UNITED STATES  
NUCLEAR REGULATORY COMMISSION

WASHINGTON, D.C. 20555-0001

August 11, 2000

RECEIVED  
AUG 18 2000

Mr. T. A. Coleman, Vice President  
Government Relations  
Framatome Cogema Fuels  
3315 Old Forest Road  
P. O. Box 10935  
Lynchburg, Virginia 24506-0935

SUBJECT: REQUEST FOR ADDITIONAL INFORMATION - FRAMATOME TOPICAL  
REPORT BAW-10231P (TAC NO. MA6792)

*File one  
copy  
tie one  
for  
Sept. 11th*

Dear Mr. Coleman:

By letter dated September 16, 1999, Framatome Cogema Fuels requested a review of Topical Report BAW-10231P, "COPERNIC Fuel Rod Design Code." The staff has determined that additional information is needed in order to complete its review.

The enclosed questions have been discussed with Mr. F. McPhatter of your staff. Please provide a response to these questions within 30 days of receipt of this letter. If you have any questions concerning our review, please contact me at (301) 415-1321.

Sincerely,

Stewart Bailey, Project Manager, Section 2  
Project Directorate III  
Division of Licensing Project Management  
Office of Nuclear Reactor Regulation

Project No. 693

Enclosure: Request for Additional Information

cc w/enc: See next page

Mr. T. A. Coleman

Project No. 693

cc:  
Mr. F. McPhatter, Manager  
Framatome Cogema Fuels  
3315 Old Forest Road  
P.O. Box 10935  
Lynchburg, VA 24506-0935

Mr. Michael Schoppman  
Licensing Manager  
Framatome Technologies, Inc.  
1700 Rockville Pike, Suite 525  
Rockville, MD 20852-1631

## REQUEST FOR ADDITIONAL INFORMATION

### TOPICAL REPORT BAW-10231

#### "COPERNIC FUEL ROD DESIGN CODE"

1. Section 2.4 mentions iterations/convergence on gap conductance or contact pressure and also on axial interaction forces but does not mention an iteration on fissions gas released (FGR and # of moles), however, Figure 2-4 indicates that the code may iterate on number of moles released. Please discuss which is correct. If the code does not iterate on number of moles please discuss why this is satisfactory for code applications including transients.
2. Please compare the COPERNIC fuel thermal conductivity predictions to out-of-reactor  $\text{UO}_2$  thermal diffusivity data from References 1 and 2 and any other high burnup diffusivity data that are applicable. The  $\text{UO}_2$  diffusivity data can be converted to thermal conductivity for these comparisons using the COPERNIC equations for specific heat. In order to fully understand the rim model thermal conductivity as applied to Halden temperature predictions, please provide a one axial node calculation of temperature profile for IFA 562 at burnups of 60, 80 and 90 GWd/MTU with and without the rim model. Please provide the radial burnup profiles used for this calculation.
3. The temperature uncertainties for LOCA and fuel melt analyses should ideally be based on data at linear heat generator rates (LHGRs)  $\geq 30$  kW/m because these analyses are performed at high LHGRs. The problem with determining temperature uncertainties for burnups greater than 30 GWd/MTU is that there is very little measured centerline temperature data with LHGRs  $\geq 30$  kW/m. Please provide the COPERNIC comparisons to data by plotting predicted minus measured temperatures versus burnup for LHGRs  $\geq 30$  kW/m to determine whether there is a change in thermal uncertainty with increasing burnup, and provide the uncertainties from this data comparison. Also, provide the COPERNIC predicted minus measured centerline temperature data versus burnup for LHGRs  $\geq 15$  kW/m, and the uncertainties from this data comparison. These comparisons will help to verify that the uncertainties for the data that includes the lower LHGRs are applicable to the higher LHGRs where LOCA and fuel melting analyses are performed.
4. Please provide LHGRs and design information for the EXTRAFORT test rod.
5. The comparison to IFA 432-1 inlet thermocouple only extends to a burnup of 9 GWd/MTU, but the NUREG/CR-4717 report provides data up to a burnup of 27 GWd/MTU at the inlet thermocouple. Please provide the COPERNIC comparison up to the limit of the data or a justification why this comparison is not valid.
6. Is Framatome a member of Halden? If so, Halden has refabricated two high (~ 59 GWd/MTU) burnup rods (one with a functional thermocouple) and placed them first in IFA-597.2 (HWR-442) and subsequently in IFA- 597.3 (HWR-543) with measured centerline temperatures. Please compare COPERNIC code predictions to this data and include this data in the response to Question 3 above.

7. The athermal fission gas release model (Section 5.2.2) is dependent on open porosity but no values are provided for what is used for Framatome fuel. What values are used for open porosity? If more than one value is used, please provide the value for each fabrication process.
8. The Section 5.2.3.5 explanation is not very clear about how the fission gas release model applies to varying conditions of power and temperature. It would help to have several examples for conditions of both increasing temperature and decreasing temperature. Also, examples of fast and slow rate of change in fuel temperature are warranted. It appears that the resolution thickness is not used in the final equations in COPENIC for computing fission gas release. Is this interpretation correct?
9. A comparison of the COPENIC upperbound fission gas release predictions to measured data (with > 7 percent measured release) from  $\text{UO}_2$  -  $\text{Gd}_2\text{O}_3$  fuel rods with steady-state power operation (from Table 5-3) demonstrates that the code underpredicts 2 out of 6 rods (it is noted that one of the rods is only slightly underpredicted). A comparison of COPENIC upperbound predictions to the transient measured data with >5 percent release from  $\text{UO}_2$  -  $\text{Gd}_2\text{O}_3$  rods (from Table 5-4) demonstrates the code underpredicts 5 out of 25 rods. This indicates that the code's upperbound fission gas release model for  $\text{UO}_2$  -  $\text{Gd}_2\text{O}_3$  bounds much less than 95 percent of the data that are within the range of application for the rod pressure analysis. Also, the code does not appear to have been compared to the B&W segmented rodlets steady-state irradiated in ANO-1 and power ramped in the Sturesvik R2 reactor. If not, why was this comparison not made and presented because these rods are representative of U.S. designs?
10. The standard deviation of the gaseous swelling model is on the order of the inferred gas porosity from the measured porosity distributions. In fact there are only 3 data points out of 14 that have inferred gaseous swelling greater than 0.6, i.e., significantly greater than the standard deviation. Of these 3 data points only one of these is predicted well by the gaseous swelling model while the other two data points are significantly underpredicted by factors of 1.6 and 2.9. Therefore, the validity and the accuracy of the gaseous swelling model appears questionable. What is the impact of the gaseous swelling model on rod pressure, melting and strain predictions? Does the gaseous swelling model use local burnup or pellet average burnup. The COPENIC steady-state gaseous swelling model (Equations 6-13 to 6-15) has been programmed into FRAPCON-3 with calculational results of 0.007 inches of displacement at a pellet average burnup of 62 GWd/MTU with a centerline temperature of 1200°C. Is this predicted displacement with this model reasonable for these conditions? If not, further discussions are necessary to understand the gaseous swelling model.
11. Figure 6-8 (from September 1999 version) predicted versus measured densification data is significantly different from Figure 6-5 of the July 1998 version of COPENIC; however, the densification and swelling models appear to be the same. Please explain why the data in the two figures are not the same.
12. The fuel column growth data in Figure 6-9 (September 1999 version) appears to contain significantly less growth data than the same figure (Figure 6-6) in the July 1998 version of COPENIC. Please discuss why there is less data in the current version of

COPERNIC. Does the column growth data in Figure 6-11 include both ADU and AUC processed fuel or is it just AUC fuel?

13. Equation 7-1 for creep is a function of the shear stress component ( $\sigma_\theta - \sigma_r$ ). Please provide a derivation of how this shear stress is determined to be the only active determinant of creep from Hills or Von Mises equations because these are not the only shear stress or stress components in these equations.
14. Will the FRAGEMA AFA 2G cladding that is fabricated in Europe be used in U. S. plants? Sections 7.1.2.2.1 and 7.1.2.3.1 refer to a number of cladding tube (AFA 2G) irradiation tests in the SILOE test reactor. Please provide further information on the manufacturing differences between the cladding from these tests and those manufactured commercially for U. S. plants, e.g., FCF Base Zr-4 and AFA 2G. Also, were the hoop stresses quoted in Table 7-1 positive or negative? (The creep model needs to be validated against the current U.S. fabricated FCF Zr-4 cladding. See question 15.)
15. Section 7.1.2.3.2 and Figures 7-20, 21 and 22 all refer to creep data from fuel rods irradiated in the CAP test reactor. Pacific Northwest National Laboratory (PNNL) nor NRC is familiar with this test reactor. Please provide the test reactor or loop conditions that are pertinent to in-reactor creep such as coolant inlet-outlet temperatures, fast flux, system pressure, etc. Also, provide predicted versus measured creep for the FCF Zr-4 cladding used in the U.S. and the background information on this data.
16. Section 7.1.2.3.3 notes that creep data from one rod was excluded from the uncertainty determination because it was next to gadolinia rods. Does this mean that the creep model uncertainty does not apply to fuel rods near gadolinia rods? Also, Figure 7-20 shows a considerable amount of measured-to-predicted data that are outside of the uncertainty bounds proposed. Please discuss why it is ok to discard this data from the uncertainty determination for creep and those data in Figure 7-20 that are not within the proposed bounding creep uncertainty. Please identify those analyses where overprediction of creep is conservative and those analyses where underprediction is conservative.
17. Section 7.1.3.2.1 discusses the development of the M5 creep model from tube irradiations but no comparison to this data is provided, and the stress and temperature parameters of this data are also not provided. Please provide this data and comparisons to the M5 creep model. It is also stated that the secondary thermal creep rate is independent of alloy type, but no data is presented to corroborate this statement. Please provide this data.
18. Does COPERNIC consider the effects of cladding growth (Section 7.3.2) in the diametral direction or is this implicit in the creep data? Also, the upperbound model underpredicts a significant amount of growth data in Figure 7-50. Please explain why this is acceptable. The alloy 5 growth model, Equation 7-27, is not linearly dependent but has a decreasing slope with fluence while the majority of Zircaloy growth data show a linear dependence with fluence. In addition, an initial examination of Figure 7-54 appears to show that a linear dependent model would provide as good or better

prediction of the alloy 5 growth data compared to the model proposed. Please provide further information on why Equation 7-27 is more appropriate for predicting alloy 5 growth even though a linear model would be more conservative and provide as good a fit to the growth data.

19. Section 8.1 discusses the COPENIC corrosion model and comparisons to data. The coolant inlet temperatures are provided for some of the reactors from which corrosion data was taken but coolant outlet temperatures and LHGR are also important parameters. What were the outlet temperatures and average LHGR/cycle for both the Zr-4 and alloy 5 data (including the adjustment rod data) and identify high duty, medium duty and low duty plants (see 20 below)? Section 8.1.3.2 states that the alloy 5 data is based on the maximum average azimuthal oxide thickness over the span height. Please discuss how this is determined from actual measurements, e.g., is it an average over a given length and how many azimuthal orientations are measured?
20. Also, oxide predictions and comparisons to data from Zr-4 are provided for all axial rod locations; however, NRC is most concerned with rod locations that experience maximum oxide thicknesses and corrosion from high duty plants. The axial locations with maximum oxide thicknesses are typically in the next to last span or the next to last two spans from the top of the assembly depending on the number of spacer grids per assembly. Please provide predicted minus measured oxide thickness versus both burnup and measured oxide thickness only for those axial spans with maximum measured oxide thickness for each rod, and identify high duty, medium duty and low duty plants along with a discussion of the differences between the operating parameters of these different plants.
21. From examination of Figure 8-11, the COPENIC code appears to significantly underpredict a large amount of measured oxide data from U. S. plants with Zr-4 cladding. Please provide predicted minus maximum measured oxide thickness versus burnup and maximum measured oxide thickness only from rods from U. S. plants using both the COPENIC and COROSO2 corrosion models. Please provide predictions of this same U. S. data using the COPENIC upper bound corrosion model. PNNL's comparison of COROSO2 and COPENIC corrosion models at various temperatures for both Zr-4 and alloy 5 has demonstrated that COROSO2 predicts the greater oxide thicknesses. Please discuss why this is acceptable.
22. What is the basis for the oxide layer thermal conductivity functions provided at the bottom of page 8-3? It appears that the oxide conductivity is determined based on the oxide surface temperature. Is this interpretation correct?
23. Please provide the average LHGR/cycle for the hydrogen pickup data provided in Figure 8-22. The applicability of using only 5 cycle data to estimate the hydrogen pickup fraction is questionable because there may be other factors (such as heat flux) in the 3 and 4 cycle data that results in the 5 cycle data giving the lowest hydrogen pickup fractions.
24. Please provide the background data for the fuel melting temperature relationship used by COPENIC (Equations 10-11 and 12-2).

25. Section 12.0 notes that COPENIC is used for initialization of core thermal-hydraulic codes. Please list those calculated COPENIC parameters used for initialization and the specific applications of the thermal-hydraulic codes.
26. In Section 12.1.1 (page 12-2) under discussion on code uncertainties, it is noted that the code has an option that conservatively bounds the fissions gas release data and that this option is used to bound the fission gas release for the rod pressure predictions. However, there is a concern that this option will not bound the  $\text{UO}_2$  -  $\text{Gd}_2\text{O}_3$  data within the fission gas release range that is important to the rod pressure analysis for  $\text{UO}_2$  -  $\text{Gd}_2\text{O}_3$  rods (see Question 9 above) at the stated level of conservatism. Please discuss this issue further, particularly in relation to Question 9 above.
27. In Section 12.1.1 (page 12-3) under the discussion on transients, it is noted that plant specific operating data may be used to establish simulated transients. Please explain further by what is meant by sufficient plant operating data and provide an example.
28. There is a concern that the uncertainty factor provided in Equation 12-1 may be too small at the predicted operating temperatures (stored energy) calculated for LOCA initialization. Please discuss this issue further, particularly in relation to Question 3 above.
29. Are any of the example calculations provided in Section 12 for fuel cores with two 24 month cycles? It appears that there are no 24-month cycle results presented for the Mark BW-17 design. If so, please explain because it is anticipated that a large number of plants will be switching to 24-month cycles in the next few years.
30. The axial power distributions for the transients were found for the example licensing analyses, but the power distribution for the steady-state power operation were not found in the topical report. Please provide these axial power distributions. If there are more than 20 axial power profiles it would be helpful to condense the number down to 20 or less. Also, the steady-state power histories are only provided as plots versus burnup. Please provide these in tabular form to support the NRC audit calculation of these calculational examples?
31. Section 12.4.1 states that the cladding strain analyses will be run with .....and the gaseous swelling option turned off. Performing these analyses without gaseous swelling ..... produces more accurate predictions ..... at the very high local power levels that accompany these analyses. This appears to be contradictory to the comparisons to data in Figures 6-17, 6-18, and 6-19 that demonstrate that COPENIC with gaseous swelling option turned on provides an adequate prediction of diametral strains. Please provide data and information that supports the conclusion that the exclusion of gaseous swelling in COPENIC produces more accurate strain predictions.
32. Section 12.5 states that COPENIC will be used to generate cladding creep collapse initial conditions and example rod pressure results are provided in Figures 12-34 and 12-35. Are there any other initial conditions provided by COPENIC for the creep collapse analysis, e.g., cladding temperatures? If so, please provide predictions of these initial conditions.

References

1. Kinoshita, M. et al. 2000, "High Burnup Rim Project (II): Irradiation And Examination to Investigate Rim-Structured Fuel," *Proceedings of the ANS International Topical Meeting on LWR Fuel Performance, Park City, UT, April 10-13, 2000.*
2. J. Nakamura, et al. 1997, "Thermal Diffusivity Measurements of a High-Burnup  $\text{UO}_2$  Pellet," in *Proceedings of the ANS International Topical Meeting on LWR Fuel Performance, Portland OR, March 2-6 1997.*



# FRAMATOME COGEMA FUELS

September 29, 2000  
GR00-142.doc

U. S. Nuclear Regulatory Commission  
ATTN: Document Control Desk  
Washington, D. C. 20555

Reference: Stewart Bailey, NRC, to. T. A. Coleman, Framatome Cogema Fuels,  
Request for Additional Information - Framatome Topical Report BAW-  
10231P (TAC NO. MA6792), August 11, 2000.

Gentlemen:

The reference letter transmitted thirty-two questions on FCF Topical Report BAW - 10231P, "COPERNIC Fuel Rod Design Code." These questions are very comprehensive in nature and will require a significant effort by FCF. Many of the questions will require input from Framatome in France. Some of the questions require comparisons of code predictions to data and some are direct requests for data. It will not be possible to provide adequate responses to the RAI in the thirty day time frame requested by the NRC. The current schedule is for submittal of responses to all questions by January 31, 2001. If there are any questions or problems with this schedule please contact C. F. McPhatter at (804) 832-2401.

Very truly yours,

*W. J. Ali Cornia for T. A. Coleman*

T. A. Coleman, Vice President  
Government Relations

cc: J. S. Wermeil, NRC  
S. N. Bailey, NRC  
R. Caruso, NRC  
S. L. Wu, NRC  
C. E. Beyer, PNNL  
M. S. Schoppman  
R. N. Edwards  
20A13 File/Records Management



Framatome Cogema Fuels  
P.O. Box 11648, Lynchburg, VA 24506-1648  
Telephone: 804-832-5000 Fax: 804-832-5167



February 5, 2001  
GR01-021.doc

U. S. Nuclear Regulatory Commission  
ATTN: Document Control Desk  
Washington, D. C. 20555

- Reference: 1. Stewart Bailey, NRC, to T. A. Coleman, Framatome Cogema Fuels, Request for Additional Information – Framatome Topical Report BAW-10231P (TAC NO. MA6792), August 11, 2000.
2. T. A. Coleman, Framatome Cogema Fuels, to U. S. Nuclear Regulatory Commission, GR00-142.doc, September 29, 2000.

Gentlemen:

Reference 1 provided a request for additional information (RAI) on Framatome Cogema Fuels (FCF) topical report BAW-10231P, "COPERNIC Fuel Rod Design Code." In reference 2, FCF agreed to provide responses to the RAI by January 31, 2001. The responses are enclosed. The responses are being submitted with the prefix 14 on each page. When the final NRC-approved version of BAW-10231P is issued, the responses will comprise chapter 14.

In accordance with the provisions of 10 CFR 2.790, Framatome ANP requests that these responses be considered proprietary and withheld from public disclosure. Attachment 1 is an affidavit supporting this request. Attachment 2 is the proprietary version of the responses and Attachment 3 is the non-proprietary version.

The approval of the COPERNIC code at this time is requested for the advanced alloy M5<sup>TM</sup> cladding only. Framatome ANP will continue to use the NRC approved code TACO for applications with Zircaloy cladding. Responses for the Zircaloy portions of the RAI (Questions 14, 15, 16, 19, 20, 21, and 23) will be provided at such time that approval for COPERNIC application to Zircaloy cladding is requested by our customers.

Very truly yours,

A handwritten signature in cursive script, appearing to read 'T. A. Coleman'.

T. A. Coleman, Vice President  
Government Relations

cc: J. S. Wermell, NRC  
S. N. Bailey, NRC  
R. Caruso, NRC  
S. L. Wu, NRC  
C. E. Beyer, PNNL  
M. S. Schoppman  
20A13 File/Records Management

AFFIDAVIT OF THOMAS A. COLEMAN

- A. My name is Thomas A. Coleman. I am Vice President of Government Relations for Framatome ANP. Therefore, I am authorized to execute this Affidavit.
- B. I am familiar with the criteria applied by Framatome ANP to determine whether certain information of Framatome ANP is proprietary and I am familiar with the procedures established within Framatome ANP to ensure the proper application of these criteria.
- C. In determining whether an Framatome ANP document is to be classified as proprietary information, an initial determination is made by the cognizant manager, who is responsible for originating the document, as to whether it falls within the criteria set forth in Paragraph D hereof. If the information falls within any one of these criteria, it is classified as proprietary by the originating cognizant manager. This initial determination is reviewed by the cognizant Section Manager. If the document is designated as proprietary, it is reviewed again by personnel and other management within Framatome ANP as designated by the Vice President of Government Relations to assure that the regulatory requirements of 10 CFR Section 2.790 are met.
- D. The following information is provided to demonstrate that the provisions of 10 CFR Section 2.790 of the Commission's regulations have been considered:
  - (i) The information has been held in confidence by Framatome ANP. Copies of the document are clearly identified as proprietary. In addition, whenever Framatome-ANP transmits the information to a customer, customer's agent, potential customer or regulatory agency, the transmittal requests the recipient to hold the information as proprietary. Also, in order to strictly limit any potential or actual customer's use of proprietary information, the substance of the following provision is included in all agreements entered into by Framatome ANP, and an equivalent version of the proprietary provision is included in all of Framatome ANP's proposals:

AFFIDAVIT OF THOMAS A. COLEMAN (Cont'd.)

"Any proprietary information concerning Company's or its Supplier's products or manufacturing processes which is so designated by Company or its Suppliers and disclosed to Purchaser incident to the performance of such contract shall remain the property of Company or its Suppliers and is disclosed in confidence, and Purchaser shall not publish or otherwise disclose it to others without the written approval of Company, and no rights, implied or otherwise, are granted to produce or have produced any products or to practice or cause to be practiced any manufacturing processes covered thereby.

Notwithstanding the above, Purchaser may provide the NRC or any other regulatory agency with any such proprietary information as the NRC or such other agency may require; provided, however, that Purchaser shall first give Company written notice of such proposed disclosure and Company shall have the right to amend such proprietary information so as to make it non-proprietary. In the event that Company cannot amend such proprietary information, Purchaser shall, prior to disclosing such information, use its best efforts to obtain a commitment from NRC or such other agency to have such information withheld from public inspection.

Company shall be given the right to participate in pursuit of such confidential treatment."

AFFIDAVIT OF THOMAS A. COLEMAN (Cont'd.)

(ii) The following criteria are customarily applied by Framatome ANP in a rational decision process to determine whether the information should be classified as proprietary. Information may be classified as proprietary if one or more of the following criteria are met:

- a. Information reveals cost or price information, commercial strategies, production capabilities, or budget levels of Framatome ANP, its customers or suppliers.
- b. The information reveals data or material concerning Framatome ANP research or development plans or programs of present or potential competitive advantage to Framatome ANP.
- c. The use of the information by a competitor would decrease his expenditures, in time or resources, in designing, producing or marketing a similar product.
- d. The information consists of test data or other similar data concerning a process, method or component, the application of which results in a competitive advantage to Framatome ANP.
- e. The information reveals special aspects of a process, method, component or the like, the exclusive use of which results in a competitive advantage to Framatome ANP.
- f. The information contains ideas for which patent protection may be sought.

AFFIDAVIT OF THOMAS A. COLEMAN (Cont'd.)

The document(s) listed on Exhibit "A", which is attached hereto and made a part hereof, has been evaluated in accordance with normal Framatome ANP procedures with respect to classification and has been found to contain information which falls within one or more of the criteria enumerated above. Exhibit "B", which is attached hereto and made a part hereof, specifically identifies the criteria applicable to the document(s) listed in Exhibit "A".

- (iii) The document(s) listed in Exhibit "A", which has been made available to the United States Nuclear Regulatory Commission was made available in confidence with a request that the document(s) and the information contained therein be withheld from public disclosure.
- (iv) The information is not available in the open literature and to the best of our knowledge is not known by Combustion Engineering, Siemens, General Electric, Westinghouse or other current or potential domestic or foreign competitors of Framatome ANP.
- (v) Specific information with regard to whether public disclosure of the information is likely to cause harm to the competitive position of Framatome ANP, taking into account the value of the information to Framatome ANP; the amount of effort or money expended by Framatome ANP developing the information; and the ease or difficulty with which the information could be properly duplicated by others is given in Exhibit "B".

E. I have personally reviewed the document(s) listed on Exhibit "A" and have found that it is considered proprietary by Framatome ANP because it contains information which falls within one or more of the criteria enumerated in Paragraph D, and it is information which is customarily held in confidence and protected as proprietary information by Framatome ANP. This report comprises information utilized by Framatome ANP in its business which afford

AFFIDAVIT OF THOMAS A. COLEMAN (Cont'd.)

Framatome ANP an opportunity to obtain a competitive advantage over those who may wish to know or use the information contained in the document(s).

TH Coleman

THOMAS A. COLEMAN

State of Virginia)

) SS. Lynchburg

City of Lynchburg)

Thomas A. Coleman, being duly sworn, on his oath deposes and says that he is the person who subscribed his name to the foregoing statement, and that the matters and facts set forth in the statement are true.

TH Coleman

THOMAS A. COLEMAN

Subscribed and sworn before me  
this 5<sup>th</sup> day of February 2001.

Wanda L. Wade

Notary Public in and for the City  
of Lynchburg, State of Virginia.

My Commission Expires 8/31/01



**EXHIBITS A & B**

**EXHIBIT A**

Documented Responses to NRC Request for Additional  
Information On BAW-10231P Dated August 11, 2000

**EXHIBIT B**

The above listed document contains information which is considered Proprietary in  
accordance with Criteria b, c, d, and e of the attached affidavit.

Table of Contents

Question 1 .....	14-1
Question 2 .....	14-4
Question 3 .....	14-9
Question 4 .....	14-12
Question 5 .....	14-20
Question 6 .....	14-22
Question 7 .....	14-24
Question 8 .....	14-25
Question 9 .....	14-32
Question 10 .....	14-34
Question 11 .....	14-39
Question 12 .....	14-40
Question 13 .....	14-42
Question 14 .....	14-44
Question 15 .....	14-45
Question 16 .....	14-46
Question 17 .....	14-47
Question 18 .....	14-53
Question 19 .....	14-54
Question 20 .....	14-56
Question 21 .....	14-57
Question 22 .....	14-58
Question 23 .....	14-60
Question 24 .....	14-61
Question 25 .....	14-63
Question 26 .....	14-64
Question 27 .....	14-65
Question 28 .....	14-67
Question 29 .....	14-68
Question 30 .....	14-69
Question 31 .....	14-222
Question 32 .....	14-223

List of Figures

Figure 14-1: LHGR vs. Macro- and Micro-Time Steps [d] .....	14-2
Figure 14-2: Bounding Fission Gas Release Predictions vs. Macro- and Micro-Time-Steps [d] .....	14-3
Figure 14-3: COPERNIC and NFIR-III Thermal Conductivity Comparison - 100% Theoretically Dense Fuel - 60 GWd/tU Burnup .....	14-5
Figure 14-4: COPERNIC and JAERI Thermal Conductivity Comparison - Sample No.2 - 100% Theoretically Dense Fuel - 63 GWd/tU Burnup, 83-89% Initial Density Range .....	14-5
Figure 14-5: COPERNIC and JAERI Thermal Conductivity Comparison - Sample No.3 - 100% Theoretically Dense Fuel - 63 GWd/tU Burnup, 92-96% Initial Density Range .....	14-6
Figure 14-6: Rim Effect at 60 GWd/tU - IFA 562 .....	14-6
Figure 14-7: Rim Effect at 80 GWd/tU - IFA 562 .....	14-7
Figure 14-8: Rim Effect at 90 GWd/tU - IFA 562 .....	14-7
Figure 14-9: Radial Burnup Profiles - IFA 562 .....	14-8
Figure 14-10: Predicted Minus Measured Centerline Temperature Differences vs. Burnup .....	14-10
Figure 14-11: Predicted Minus Measured Centerline Temperature Differences vs. Burnup .....	14-11
Figure 14-12: Measured and Predicted Fuel Temperatures vs. Burnup .....	14-21
Figure 14-13: Fuel Centerline Temperature Measurements and Predictions vs. Burnup, IFA-597.2 .....	14-23
Figure 14-14: Fuel Centerline Temperature Measurements and Predictions vs. Burnup, IFA-597.3 .....	14-23
Figure 14-15: FGR Transition Algorithm: Small Power Change .....	14-26
Figure 14-16: FGR Transition Algorithm: Significant Power Increase .....	14-27
Figure 14-17: FGR Transition Algorithm: Significant Power Decrease .....	14-28
Figure 14-18: Rapid Change in Fuel Temperature [d] .....	14-29
Figure 14-19: Slower Change in Fuel Temperature [d] .....	14-30
Figure 14-20: Local Gas Concentration with Decreasing Temperatures ([d]) .....	14-31
Figure 14-21: Upper-bound Predicted vs. Measured Steady-state Fission Gas Release for $UO_2$ - $Gd_2O_3$ Fuel .....	14-33
Figure 14-22: Upper-bound Predicted vs. Measured Transient Fission Gas Release for $UO_2$ , MOX and $UO_2$ - $Gd_2O_3$ Fuels .....	14-33
Figure 14-23: Bounding Internal Gas Pressure With and Without COPERNIC Gaseous Swelling Model Effects - Typical Mark-BW17 Urania-Gadolinia Cycle, $UO_2$ Rods .....	14-35
Figure 14-24: Fuel Melt With and Without COPERNIC Gaseous Swelling Model Effects - Typical Mark-BW17 Urania-Gadolinia Cycle, $UO_2$ Rods .....	14-35
Figure 14-25: 1% Cladding Strain With and Without COPERNIC Gaseous Swelling Model Effects - Typical Mark-BW17 Urania-Gadolinia Cycle, $UO_2$ Rods .....	14-36
Figure 14-26: Measured and Predicted Cladding Diameter Variations .....	14-37
Figure 14-27: Measured and Predicted Cladding Diameter Variations .....	14-38
Figure 14-28: Measured and Predicted Fuel Column Growth ( $UO_2$ ) [d] .....	14-41
Figure 14-29: Advanced Alloy M5 Creep Tests of Unirradiated Tubes at [b] .....	14-49
Figure 14-30: Advanced Alloy M5 Creep Tests of Unirradiated Tubes at [b] .....	14-50
Figure 14-31: Advanced Alloy M5 Secondary Thermal Creep Rate vs. Fluence [b] .....	14-51
Figure 14-32: Combined Data Set of Creep Strain vs. Fluence [b] .....	14-52
Figure 14-33: Oxide Thermal Conductivity vs. Temperature and Oxide Layer Thickness .....	14-59
Figure 14-34: Typical Mark-B Urania-Gadolinia Cycle Predictions [b] .....	14-66
Figure 14-35: Typical Mark-B Fuel Cycles - Creep Collapse Analyses [d] .....	14-224
Figure 14-36: Typical Mark-BW17 Fuel Cycles - Creep Collapse Analyses [d] .....	14-224
Figure 14-37: Typical Mark-B Fuel Cycles - Creep Collapse Analyses [d] .....	14-225
Figure 14-38: Typical Mark-BW17 Fuel Cycles - Creep Collapse Analyses [d] .....	14-225
Figure 14-39: Typical Mark-B Fuel Cycles - Creep Collapse Analyses [d] .....	14-226
Figure 14-40: Typical Mark-BW17 Fuel Cycles - Creep Collapse Analyses [d] .....	14-226
Figure 14-41: Typical Mark-B Fuel Cycles - Creep Collapse Analyses [d] .....	14-227
Figure 14-42: Typical Mark-BW17 Fuel Cycles - Creep Collapse Analyses [d] .....	14-227

List of Tables

Table 14-1: Design Information for the EXTRAFORT Mother Rod.....	14-12
Table 14-2: Thermal-Hydraulic Conditions for the EXTRAFORT Mother Rod .....	14-13
Table 14-3: EXTRAFORT Mother Rod Conditions History.....	14-14
Table 14-4: EXTRAFORT Mother Rod Power Shapes.....	14-16
Table 14-5: Design Information for the EXTRAFORT Re-fabricated Test Rodlets .....	14-18
Table 14-6: Thermal-Hydraulic Conditions for the EXTRAFORT Re-fabricated Test Rodlets .....	14-18
Table 14-7: Conditions History for the EXTRAFORT Re-fabricated Rod .....	14-19
Table 14-8: Calibration Database for Creep Hardening Effects .....	14-48
Table 14-9: Plant and Fuel Rod Data .....	14-55
Table 14-10: Unirradiated $\text{UO}_2$ Melt Temperature .....	14-61
Table 14-11: Unirradiated $(\text{U,Gd})\text{O}_2$ Melt Temperature.....	14-62
Table 14-12: Axial Power Distribution Data Sets.....	14-70

Note: Tables 14-13 through 14-59 are listed in Table 14-12.

Question 1

Section 2.4 mentions iterations/convergence on gap conductance or contact pressure and also on axial interaction forces but does not mention an iteration on fissions gas released (FGR and # of moles), however, Figure 2-4 indicates that the code may iterate on number of moles released. Please discuss which is correct. If the code does not iterate on number of moles please discuss why this is satisfactory for code applications including transients.

Response

Figure 2-4 [d]. There is no concern, however, that [d]. Micro-time-steps are generated at subdivisions between the user-selected macro-time-steps. A micro-time-step is [d]. [b, c]. This is illustrated in Figures 14-1 and 14-2 where the macro- and micro-time-steps are defined with the larger diamond and smaller cylindrical shaped symbols, respectively. These illustrations were developed from the [e] example of [e]. A total of [d] and [d] micro-time-steps were generated for the [d, e] macro-time-step transient and [d] macro-time-step entire internal gas pressure case, respectively. These figures illustrate the [d] additional time steps that are generated due to the micro-time-step feature. The [d] micro-time-steps [d].

**Figure 14-1: LHGR vs. Macro- and Micro-Time Steps**  
**[e]**

**[d]**

**Figure 14-2: Bounding Fission Gas Release Predictions vs. Macro- and Micro-Time-Steps [d]**

[d]

Question 2

Please compare the COPERNIC fuel thermal conductivity predictions to out-of-reactor  $\text{UO}_2$  thermal diffusivity data from References 1 and 2 and any other high burnup diffusivity data that are applicable. The  $\text{UO}_2$  diffusivity data can be converted to thermal conductivity for these comparisons using the COPERNIC equations for specific heat. In order to fully understand the rim model thermal conductivity as applied to Halden temperature predictions, please provide a one axial node calculation of temperature profile for IFA 562 at burnups of 60, 80, and 90 GWd/MTU with and without the rim model. Please provide the radial burnup profiles used for this calculation.

Response

COPERNIC fuel thermal conductivity predictions are compared in Figures 14-3 through 14-5 with fuel thermal conductivities that were obtained from three sets <sup>(2-4)</sup> of fuel thermal diffusivity measurements. These figures show that the COPERNIC thermal conductivities [b, d] with the Nuclear Fuels Research Program (NFIR) data <sup>(3,4)</sup> and somewhat [b,d] the Japan Atomic Energy Research Institute (JAERI) data <sup>(2)</sup>. There are no end-of-life density or porosity measurements presented with the Kinoshita <sup>(1)</sup>, et al, data that are needed to calculate the rim thermal conductivities. This fact is illustrated in the following statements<sup>(1)</sup>:

"It must be noted that the data in Figure 6<sup>(1)</sup> are just measured TD values and the effect of porosity of individual specimens were not considered. As the effect of coarsened pores, typical for the rim structure, on thermal resistance is not clear, the comparison<sup>(1)</sup> was made without corrections. Therefore, this presentation must be considered still preliminary and the evaluation of thermal conductivity should be discussed only after detailed analyses."

[c].

The COPERNIC predicted radial fuel temperature predictions with and without the COPERNIC rim model are shown in Figures 14-6 through 14-8, at burnups of 60, 80, and 90 GWd/tU, respectively. [b, d]. Although these differences are relatively small, Kinoshita<sup>(1)</sup>, et al, implies that these differences are very small or should not exist at all. Note, however, that the Kinoshita<sup>(1)</sup>, et al, data is preliminary and was obtained without stress inducing fuel restraints. Une<sup>(5)</sup>, et al, suggests that fuel restraint may play an important role in suppressing bubble growth within the rim and, therefore, in reducing thermal conductivity. If future work indicates that the Kinoshita<sup>(1)</sup>, et al, preliminary conclusions are correct, [b, d]. [b, d].

The radial power distributions at burnups of 60, 80, and 90 GWd/tU, that were used in the COPERNIC temperature predictions of the IFA 562 rods, are shown in Figure 14-9. These radial power distributions [b, d].



**Figure 14-3: COPERNIC and NFIR-III Thermal Conductivity Comparison  
60 GWd/tU Burnup - [c]**

[b, c, d]

**Figure 14-4: COPERNIC and JAERI Thermal Conductivity Comparison - Sample No.2  
63 GWd/tU Burnup, 83-89% Density Range, [c]**

[b, c, d]

**Figure 14-5: COPERNIC and JAERI Thermal Conductivity Comparison - Sample No.3  
63 GWd/tU Burnup, 92-96% Density Range, [c]**

[b, c, d]

**Figure 14-6: Rim Effect at 60 GWd/tU  
IFA 562**

[b, c, d]

**Figure 14-7: Rim Effect at 80 GWd/tU  
IFA 562**

[b, c, d]

**Figure 14-8: Rim Effect at 90 GWd/tU  
IFA 562**

[b, c, d]

**Figure 14-9: Radial Burnup Profiles  
IFA 562**

[b, c, d]

Question 3

The temperature uncertainties for LOCA and fuel melt analyses should ideally be based on data at linear heat generator rates (LHGRs)  $\geq 30$  kW/m because these analyses are performed at high LHGRs. The problem with determining temperature uncertainties for burnups greater than 30 GWd/MTU is that there is very little measured centerline temperature data with LHGRs  $\geq 30$  kW/m. Please provide the COPERNIC comparisons to data by plotting predicted minus measured temperatures versus burnup for LHGRs  $\geq 30$  kW/m to determine whether there is a change in thermal uncertainty with increasing burnup, and provide the uncertainties from this data comparison. Also, provide the COPERNIC predicted minus measured centerline temperature data versus burnup for LHGRs  $\geq 15$  kW/m, and the uncertainties from this data comparison. These comparisons will help to verify that the uncertainties for the data that includes the lower LHGRs are applicable to the higher LHGRs where LOCA and fuel melting analyses are performed.

Response

FRA-ANP (Framatome Advanced Nuclear Power) has been performing rod average burnup based LOCA analyses for well over a decade. [b, d, e]

The predicted minus measured centerline temperature differences at LHGRs  $\geq$  [e] and [e] kW/m are shown plotted versus burnup in Figures 14-10 and 14-11, respectively. The predicted minus measured centerline temperature differences that bound 95% of the data with a 95% confidence level are [d, e] and [d, e] for LHGRs  $\geq$  [e] and [e] kW/m, respectively. These uncertainties demonstrate that [b]. [b]

Figure 14-10: Predicted Minus Measured Centerline Temperature Differences vs.  
Burnup  
[e]

[b, c, d]

**Figure 14-11: Predicted Minus Measured Centerline Temperature Differences vs.  
Burnup  
[e]**

[b, c, d]

**Question 4**

Please provide LHGRs and design information for the EXTRAFORT test rod.

**Response**

The EXTRAFORT test rodlet was refabricated from a mother rod that was irradiated in a commercial 900 MW PWR reactor for five cycles to a rod average burnup of 57.2 GWd/tU. [b, c, d].

**Table 14-1: Design Information for the EXTRAFORT Mother Rod**

[b, c, d]



**Table 14-2: Thermal-Hydraulic Conditions for the EXTRAFORT Mother Rod**

[b, c, d]

**Table 14-3: EXTRAFORT Mother Rod Conditions History**

[b, c, d]

Table 14-3: EXTRAFORT Mother Rod Conditions History (Continued)

[b, c, d]

**Table 14-4: EXTRAFORT Mother Rod Power Shapes**

[b, c, d]

Table 14-4: EXTRAFORT Mother Rod Power Shapes (Continued)

[b, c, d]

**Table 14-5: Design Information for the EXTRAFORT Re-fabricated Test Rodlets**

[b, c, d]

**Table 14-6: Thermal-Hydraulic Conditions for the EXTRAFORT Re-fabricated Test Rodlets**

[b, c, d]

Table 14-7: Conditions History for the EXTRAFORT Re-fabricated Rod

[b, c, d]

**Question 5**

The comparison to IFA 432-1 inlet thermocouple only extends to a burnup of 9 GWd/MTU but the NUREG/CR-4717 report provides data up to a burnup of 27 GWd/MTU at the inlet thermocouple. Please provide the COPERNIC comparison up to the limit of the data or a justification why this comparison is not valid.

**Response**

The IFA 432-1 inlet thermocouple data presented in NUREG/CR-4717 extends up to a local burnup of 24.072 GWd/MTU. A comparison of the COPERNIC centerline temperature predictions with this data is presented in Figure 14-12.



Figure 14-12: Measured and Predicted Fuel Temperatures vs. Burnup

[d]

Question 6

Is Framatome a member of Halden? If so, Halden has refabricated two high (~ 59 GWd/MTU) burnup rods (one with a functional thermocouple) and placed them first in IFA-597.2 (HWR-442) and subsequently in IFA-597.3 (HWR-543) with measured centerline temperatures. Please compare COPERNIC code predictions to this data and include this data in the response to Question 3.1 above.

Response

The COPERNIC centerline fuel temperature predictions are compared with the IFA-597.2 (HWR-442) and IFA-597.3 (HWR-543) fuel temperature measurements in Figure 14-13. This rodlet attained a burnup of 61.5 GWd/tUO<sub>2</sub> or 69.8 GWd/tU.

**Figure 14-13: Fuel Centerline Temperature Measurements and Predictions vs.  
Burnup, IFA-597.2 and IFA-597.3**

[d]

**Figure 14-14: Not used**

[d]

Question 7

The athermal fission gas release model (Section 5.2.2) is dependent on open porosity but no values are provided for what is used for Framatome fuel. What values are used for open porosity? If more than one value is used, please provide the value for each fabrication process.

Response

The open porosity input to the COPERNIC code is the percentage of open porosity to the total pellet geometric volume. The open porosity percentage of the fuel supplied by FRA-ANP's present vendor is typically [b, d]. The [b, d] will be used until open porosity data obtained from the fuel vendor suggests a need to increase this value to [b, d] pellet fabrication open porosity measurements.

Question 8

The Section 5.2.3.5 explanation is not very clear about how the fission gas release model applies to varying conditions of power and temperature. It would help to have several examples for conditions of both increasing temperature and decreasing temperature. Also, examples of fast and slow rate of change in fuel temperature are warranted. It appears that the resolution thickness is not used in the final equations in COPERNIC for computing fission gas release. Is this interpretation correct?

Response

[b, c, d]

**Figure 14-15: FGR Transition Algorithm: Small Power Change**

[b, c, d]

Figure 14-16: FGR Transition Algorithm: Significant Power Increase

[b, c, d]

**Figure 14-17: FGR Transition Algorithm: Significant Power Decrease**

[b, c, d]



**Figure 14-18: Rapid Change in Fuel Temperature [d]**

[b, c, d]

**Figure 14-19: Slower Change In Fuel Temperature [d]**

[b, c, d]

Figure 14-20: Local Gas Concentration with Decreasing Temperatures ([d])

[b, c, d]

Question 9

A comparison of the COPERNIC upperbound fission gas release predictions to measured data (with > 7% measured release) from  $\text{UO}_2 - \text{Gd}_2\text{O}_3$  fuel rods with steady-state power operation (from Table 5-3) demonstrates that the code underpredicts 2 out of 6 rods (it is noted that one of the rods is only slightly underpredicted). A comparison of COPERNIC upperbound predictions to the transient measured data with > 5% release from  $\text{UO}_2 - \text{Gd}_2\text{O}_3$  rods (from Table 5-4) demonstrates the code underpredicts 5 out of 25 rods. This indicates that the code's upperbound fission gas release model for  $\text{UO}_2 - \text{Gd}_2\text{O}_3$  bounds much less than 95% of the data that are within the range of application for the rod pressure analysis. Also, the code does not appear to have been compared to the B&W segmented rodlets steady-state irradiated in ANO-1 and power ramped in the Studsvik R2 reactor. If not, why was this comparison not made and presented because these rods are representative of U. S. designs?

Response

[b]

It can be seen from Figures 5-15 and 5-16, however, that one steady-state and two transient  $\text{UO}_2 - \text{Gd}_2\text{O}_3$  fission gas release data points are under-predicted by the  $\text{UO}_2 - \text{Gd}_2\text{O}_3$  bounding fission gas release model (another steady-state data point is only very slightly under-predicted). [b, d].

[b, d]

The Mark-BEB rodlets have been run with the COPERNIC code and the best-estimate fission gas release predictions are tabulated below:

	<u>R1 Rodlet</u>	<u>R3 Rodlet</u>
FGR Measurements	9.4	11.3
COPERNIC Predictions	[b, d]	[b, d]

[b, d].

**Figure 14-21: Upper-bound Predicted vs. Measured Steady-state Fission Gas Release for  $\text{UO}_2\text{-Gd}_2\text{O}_3$  Fuel**

[b, d]

**Figure 14-22: Upper-bound Predicted vs. Measured Transient Fission Gas Release for  $\text{UO}_2$ , MOX and  $\text{UO}_2\text{-Gd}_2\text{O}_3$  Fuels**

[b, d]

Question 10

The standard deviation of the gaseous swelling model is on the order of the inferred gas porosity from the measured porosity distributions. In fact there are only 3 data points out of 14 that have inferred gaseous swelling greater than 0.6, i.e., significantly greater than the standard deviation. Of these 3 data points only one of these is predicted well by the gaseous swelling model while the other two data points are underpredicted by factors of 1.6 and 2.9. Therefore, the validity and the accuracy of the swelling model appears questionable. What is the impact of the gaseous swelling model on rod pressure, melting and strain predictions? Does the gaseous swelling model use local burnup or pellet average burnup? The COPERNIC steady-state gaseous swelling model (Equations 6-13 to 6-15) has been programmed into FRAPCON-3 with calculational results of 0.007 inches of displacement at a pellet average burnup of 62 GWd/MTU with a centerline temperature of 1200°C. Is this predicted displacement with this model reasonable for these conditions? If not, further discussions are necessary to understand the gaseous swelling model.

Response

Internal gas pressure, fuel melt, and cladding diametral strain predictions with the COPERNIC gaseous swelling model turned on and off are presented in Figures 14-23 through 14-25, respectively. These representative examples were generated with the typical Mark-BW17 Urania-Gadolinia cycle UO<sub>2</sub> rod cases described in Chapter 12. Note that the COPERNIC gaseous swelling model [b, d]. [b, d]

. Predicted diametral cladding strains that contain COPERNIC [b, d].

[b, d]

Although [b, d]

**Figure 14-23: Bounding Internal Gas Pressure With and Without COPERNIC Gaseous Swelling Model Effects  
Typical Mark-BW17 Urania-Gadolinia Cycle, UO<sub>2</sub> Rods**

[b, d]

**Figure 14-24: Fuel Melt With and Without COPERNIC Gaseous Swelling Model Effects  
Typical Mark-BW17 Urania-Gadolinia Cycle, UO<sub>2</sub> Rods**

[b, d]

**Figure 14-25: 1% Cladding Strain With and Without COPERNIC Gaseous Swelling  
Model Effects  
Typical Mark-BW17 Urania-Gadofinia Cycle, UO<sub>2</sub> Rods**

[b, d]



Figure 14-26: Measured and Predicted Cladding Diameter Variations

[b, d]

Figure 14-27: Measured and Predicted Cladding Diameter Variations

[b, d]

Question 11

Figure 6-8 (from September 1999 version) predicted versus measured densification data is significantly different from Figure 6-5 of the July 1998 version of COPERNIC; however, the densification and swelling models appear to be the same. Please explain why the data in the two figures are not the same.

Response

The densification and solid swelling models in the September 1999 and July 1998 versions are [b]. The gaseous swelling models in the two versions [b]. This [b] contributed to the predicted density [b] shown in Figures 6-8 (September 1999) and 6-5 (July 1998). Note that the measured and predicted axes in Figures 6-8 (September 1999) and 6-5 (July 1998) are interchanged.

**Question 12**

The fuel column growth data in Figure 6-9 (September 1999 version) appears to contain significantly less growth data than the same figure (Figure 6-6) in the July 1998 version of COPERNIC. Please discuss why there is less data in the current version of COPERNIC. Does the column growth data in Figure 6-11 include both ADU and AUC processed fuel or is it just AUC fuel?

**Response**

The fuel column growth data shown in Figure 6-6 (July 1998) was obtained from [b] irradiated in commercial PWRs, [d]. The fuel column growth data obtained for commercial PWRs only, which consists of the data from the initial [b] fuel rods plus an additional [b] fuel rods, [d]. The measured and predicted fuel column growth data from the commercial PWRs as well as [d] are all listed in Table 9-1 (September 1999). The measured and predicted fuel column growth data obtained from [d] are shown plotted in Figure 14-28. The fuel column growth data shown in Figure 6-11 includes both ADU and AUC processed fuel.

Figure 14-28: Measured and Predicted Fuel Column Growth (UO<sub>2</sub>) [d]

[b, d]

Question 13

Equation 7-1 for creep is a function of the shear stress component ( $\sigma_\theta - \sigma_r$ ). Please provide a derivation of how this shear stress is determined to be the only active determinant of creep from Hills or Von Mises equations because these are not the only shear stress or stress components in these equations.

Response

[c].

The shear stress along the slip plane ( $\tau_{ns}$ ) can be related to the principal stresses by the transformation of stresses which, expressed in tensor<sup>(9)</sup> notation, is

$$\tau_{ns} = a_{ni} a_{sj} \tau_{ij}$$

where  $a_{ni}$  and  $a_{sj}$  are the direction cosines.[c]

[c]

Von Mises<sup>(10)</sup> was, perhaps, the first to recognize that triaxial yielding of an isotropic material could be described by introducing a generalized stress defined as:

$$\sigma_\theta = \frac{1}{\sqrt{2}} \sqrt{(\sigma_{zz} - \sigma_{\theta\theta})^2 + (\sigma_{\theta\theta} - \sigma_{rr})^2 + (\sigma_{rr} - \sigma_{zz})^2}$$

Hill<sup>(11)</sup> extended the Von Mises formulation to anisotropic materials such as Zircaloy with the following generalized stress equation:

$$\sigma_g = \sqrt{\frac{R(\sigma_{rr} - \sigma_{\theta\theta})^2 + RP(\sigma_{\theta\theta} - \sigma_{zz})^2 + P(\sigma_{zz} - \sigma_{rr})^2}{P(R+1)}}$$

where R and P are the anisotropy constants which have been determined by testing<sup>(12)</sup> to be as follows for the current FRA-ANP Zircaloy-4 cladding:

$$[c] \quad [c]$$

Consider the following triaxial principal stress distribution<sup>(13)</sup> that may be considered typical for nuclear fuel rod cladding:

$$\sigma_{rr} = Q_1 - Q_2$$

$$\sigma_{\theta\theta} = Q_1 + Q_2$$

$$\sigma_{zz} = Q_1$$

where

$$Q_1 = \frac{r_s^2 P_s - r_b^2 P_b}{r_b^2 - r_s^2}$$

$$Q_2 = \frac{r_s^2 r_b^2 (P_s - P_b)}{r_m^2 (r_b^2 - r_s^2)}$$

and

$r_s$  = cladding inside radius

$r_b$  = cladding outside radius

$r_m = \frac{r_s + r_b}{2}$  = cladding mean radius

$P_s$  = internal pressure

$P_b$  = external pressure

[c]

**Question 14**

Will the FRAGEMA AFA 2G cladding that is fabricated in Europe be used in U. S. plants? Sections 7.1.2.2.1 and 7.1.2.3.1 refer to a number of cladding tube (AFA 2G) irradiation tests in the SILOE test reactor. Please provide further information on the manufacturing differences between the cladding from these tests and those manufactured commercially for U. S. plants, e.g., FCF Base Zr-4 and AFA 2G. Also, were the hoop stresses quoted in Table 7-1 positive or negative? (The creep model needs to be validated against the current U.S. fabricated FCF Zr-4 cladding, see next question).

**Response**

Approval of the COPERNIC code at this time is requested first for the advanced alloy M5 cladding only. A response for this Zr-4-based question will be provided at such time that approval for the COPERNIC code applications to Zr-4 cladding is requested.



**Question 15**

Section 7.1.2.3.2 and Figures 7-20, 21 and 22 all refer to creep data from fuel rods irradiated in the CAP test reactor. Pacific Northwest National Laboratory (PNNL) nor NRC is familiar with this test reactor. Please provide the test reactor or loop conditions that are pertinent to in-reactor creep such as coolant inlet-outlet temperatures, fast flux, system pressure, etc. Also, provide predicted versus measured creep for the FCF Zr-4 cladding used in the U.S. and the background information on this data.

**Response**

Approval of the COPERNIC code at this time is requested first for the advanced alloy M5 cladding only. A response for this Zr-4-based question will be provided at such time that approval for the COPERNIC code applications to Zr-4 cladding is requested.

**Question 16**

Section 7.1.2.3.3 notes that creep data from one rod was excluded from the uncertainty determination because it was next to gadolinia rods. Does this mean that the creep model uncertainty does not apply to fuel rods near gadolinia rods? Also, Figure 7-20 shows a considerable amount of measured-to-predicted data that are outside of the uncertainty bounds proposed. Please discuss why it is ok to discard this data from the uncertainty determination for creep and those data in Figure 7-20 that are not within the proposed bounding creep uncertainty. Please identify those analyses where over prediction of creep is conservative and those analyses where under prediction is conservative.

**Response**

Approval of the COPERNIC code at this time is requested first for the advanced alloy M5 cladding only. A response for this Zr-4-based question will be provided at such time that approval for the COPERNIC code applications to Zr-4 cladding is requested.

**Question 17**

Section 7.1.3.2.1 discusses the development of the M5 creep model from tube irradiations but no comparison to this data is provided, and the stress and temperature parameters of this data are also not provided. Please provide this data and comparisons to the M5 creep model. It is also stated that the secondary thermal creep rate is independent of alloy type, but no data is presented to corroborate this statement. Please provide this data.

**Response**

The advanced alloy M5 creep rate is modeled as [b, d].

**Table 14-8: Calibration Database for Creep Hardening Effects**  
[b]

Fuel rod	Test tube	Material	Cycle	Fast Fluence ( $\times 10^{25}$ n/m <sup>2</sup> )	Diametral Strain (%)	Secondary Thermal Creep Rate (%/s)
[b, d]						

Figure 14-29: Advanced Alloy M5 Creep Tests of Unirradiated Tubes at [b]

[b, d]

Figure 14-30: Advanced Alloy M5 Creep Tests of Unirradiated Tubes at [b]

[b, d]

Figure 14-31: Advanced Alloy M5 Secondary Thermal Creep Rate vs. Fluence  
[b]

[b, d]

**Figure 14-32: [b] Creep Strain vs. Fluence  
[b]**

[b, d]



Question 18

Does COPERNIC consider the effects of cladding growth (Section 7.3.2) in the diametral direction or is this implicit in the creep data? Also, the upperbound model underpredicts a significant amount of growth data in Figure 7-50. Please explain why this is acceptable. The alloy 5 growth model, Equation 7-27, is not linearly dependent but has a decreasing slope with fluence while the majority of Zircaloy growth data show a linear dependence with fluence. In addition, an initial examination of Figure 7-54 appears to show that a linear dependent model would provide as good or better prediction of the alloy 5 growth data compared to the model proposed. Please provide further information on why Equation 7-27 is more appropriate for predicting alloy 5 growth even though a linear model would be more conservative and provide as good a fit to the growth data.

Response

The effects of cladding growth (Section 7.3.2) in the diametral direction [b, d]. FRA-ANP [b, d]. [b, d]. Recent additional measured data<sup>(14)</sup> with rod average fluences up to  $1 \times 10^{22} \text{ n/cm}^2$ ,  $E > 1.0 \text{ MeV}$ , demonstrates [b, d].

Question 19

Section 8.1 discusses the COPERNIC corrosion model and comparisons to data. The coolant inlet temperatures are provided for some of the reactors from which corrosion data was taken but coolant outlet temperatures and LHGR are also important parameters. What were the outlet temperatures and average LHGR/cycle for both the Zr-4 and alloy 5 data (including the adjustment rod data) and identify high duty, medium duty and low duty plants (see 20 below)? Section 8.1.3.2 states that the alloy 5 data is based on the maximum average azimuthal oxide thickness over the span height. Please discuss how this is determined from actual measurements, e.g., is it an average over a given length and how many azimuthal orientations are measured?

Response

Approval of the COPERNIC code at this time is requested first for the advanced alloy M5 cladding only. A response for the Zr-4-based portion of this question will be provided at such time that approval for the COPERNIC code applications to Zr-4 cladding is requested.

The inlet and outlet temperatures and the average linear heat generation rate (LHGR) for each cycle are presented in Table 14-9 for the M5 data. FRA-ANP [b,e]. However, [b, e]. Average azimuthal oxide thicknesses are evaluated [b, d, e]. The maximum oxide thickness [b, e].

Table 14-9: Plant and Fuel Rod Data

Plant	CORE INLET TEMP. (°C)	CORE OUTLET TEMP. (°C)	Average LHGR / cycle (kW/m)	Plant Classification
			[b, e]	
[b, d, e]				

Plant Classification:  
[b, e]

**Question 20**

Also, oxide predictions and comparisons to data from Zr-4 are provided for all axial rod locations; however, NRC is most concerned with rod locations that experience maximum oxide thicknesses and corrosion from high duty plants. The axial locations with maximum oxide thicknesses are typically in the next to last span or the next to last two spans from the top of the assembly depending on the number of spacer grids per assembly. Please provide predicted minus measured versus both burnup and measured oxide thickness only for those axial spans with maximum measured oxide thickness for each rod and identify high duty, medium duty and low duty plants as well as defining the differences between the operating parameters of these different plants.

**Response**

Approval of the COPERNIC code at this time is requested first for the advanced alloy M5 cladding only. A response for this Zr-4-based question will be provided at such time that approval for the COPERNIC code applications to Zr-4 cladding is requested.

Question 21

From examination of Figure 8-11, the COPERNIC code appears to significantly underpredict a large amount of the measured oxide data from U. S. plants with Zr-4 cladding. Please provide predicted minus maximum measured oxide thickness only from rods from U. S. plants using both the COPERNIC and COROS02 corrosion models. Please provide predictions of this same U. S. data using the COPERNIC upper bound corrosion model. PNNL's comparison of the COROS02 and COPERNIC corrosion models at various temperatures for both Zr-4 and alloy 5 has demonstrated that COROS02 predicts the greater oxide thicknesses. Please discuss why this is acceptable.

Response

Approval of the COPERNIC code at this time is requested first for the advanced alloy M5 cladding only. A response for the Zr-4-based portion of the question will be provided at such time that approval for the COPERNIC code applications to Zr-4 cladding is requested.

The COROS02 and COPERNIC advanced alloy M5 models differ. The pre-transition phase of the COPERNIC M5 model uses a [e] function rather than [e] used in COROS02. This change provided [b] between oxide thickness measurements and predictions. Also, the initial COROS02 model was developed with [d] (see the response to Question 22), while the COPERNIC corrosion model was developed with the oxide thermal conductivity relationships described in Section 8.1.2.1.

Question 22

What is the basis for the oxide layer thermal conductivity functions provided at the bottom of page 8-3? It appears that the oxide thermal conductivity is determined based on the oxide surface temperature. Is this interpretation correct?

Response

Experimental data from a CEA (Commissariat à l'Energie Atomique - Atomic Energy Commission) program provided the basis for the COPERNIC oxide thermal conductivity relationships presented on page 8-3. The COPERNIC oxide thermal conductivities and the NFIR-III (Nuclear Fuel Industry Research Program) thermal conductivity<sup>(16)</sup> are plotted together for comparison in Figure 14-33. [b, d].

**Figure 14-33: Oxide Thermal Conductivity vs. Temperature and Oxide Layer Thickness**

[b, d]

**Question 23**

Please provide the average LHGR/cycle for the hydrogen pickup data provided in Figure 8-22. The applicability of using only 5 cycle data to estimate the hydrogen pickup fraction is questionable because there maybe other factors (such as heat flux) in the 3 and 4 cycle data that results in the 5 cycle data giving the lowest hydrogen pickup fractions.

**Response**

Approval of the COPERNIC code at this time is requested first for the advanced alloy M5 cladding only. A response for this Zr-4-based question will be provided at such time that approval for the COPERNIC code applications to Zr-4 cladding is requested.



Question 24

Please provide the background data for the fuel melting temperature relationship used by COPERNIC (Equations 10-11 and 12-2).

Response

[c] . Open and closed systems for heating the test samples have been used in fuel melt experiments. Closed systems<sup>(24,26)</sup> are generally preferred because the test sample is enclosed in a hermetically sealed crucible with a controlled atmosphere that restrains stoichiometry changes. Open systems<sup>(18-23,25)</sup> without controlled atmospheres, on the other hand, are notorious for causing stoichiometry changes that introduce errors in the measured melt temperatures. Melt temperature measurements have traditionally been performed either by post-cooling observations of microstructural changes or by the thermal arrest method where a marked change in the slope of the measured fuel temperature is observed. The most recent measurements have typically been performed with a closed system and the thermal arrest method because this approach is generally considered to produce more accurate measurements. The melt temperatures of unirradiated UO<sub>2</sub> determined by various investigators are listed below.

**Table 14-10: Unirradiated UO<sub>2</sub> Melt Temperature**

Reference	Year	Melting Point (°C)
Lambertson <sup>(18)</sup>	1953	2878
Wisniyi <sup>(19)</sup>	1957	2760
Ehlert <sup>(20)</sup>	1958	2860
Christensen <sup>(21)</sup>	1962	2790
Christensen <sup>(22)</sup>	1963	2800
Pashos <sup>(23)</sup>	1965	2800
Hausner <sup>(24)</sup>	1965	2805
Bannister <sup>(25)</sup>	1967	2860
Benz <sup>(26)</sup>	1970	2810
Rubin <sup>(27)</sup>	1970	2840
Tachibana <sup>(28)</sup>	1985	2845
Chotard <sup>(29)</sup>	1987	2852

[b, d].

Christensen's work<sup>(21,30)</sup> has traditionally been used for fuel melt because it is generally considered to be conservative. However, Christensen's measurements were performed in an open system and the stoichiometry of the test samples was not recorded. Furthermore, his initial data<sup>(21)</sup> did not report a decrease in melt temperature with burnup.

[b, c, d]

[b, c, d]

[b, d]

. Yamamouchi<sup>(31)</sup>, et al data.

A review of the available  $\text{UO}_2\text{-Gd}_2\text{O}_3$  fuel melt data<sup>(29,32-33)</sup> indicates that there is no significant difference between the  $\text{UO}_2$  and  $\text{UO}_2\text{-Gd}_2\text{O}_3$  fuel melt temperatures for gadolinia concentrations less than approximately 12 wt.%.

Table 14-11: Unirradiated (U,Gd) $\text{O}_2$  Melt Temperature

Gd <sub>2</sub> O <sub>3</sub> Content (wt.%)	Melting Point (°C)	Reference
0	2857	Chotard <sup>(29)</sup>
4	2881	
8	2861	
12	2867	
16	2865	
0	2844	Busch <sup>(32)</sup> Stoichiometric oxides
4	2851	
8	2858	
12	2836	
40	2791	
65	2585	
100	2444	
4	2855	Busch <sup>(32)</sup> substoichiometric oxides
8	2856	
12	2845	
40	2786	
65	2597	
0	2842	Watarumi <sup>(33)</sup> (homogeneous oxides)
0	2861	
6	2828	
6.6	2868	
8	2842	
10	2828	
13	2775	
19	2745	
25	2753	
31	2707	
37	2687	
6	2836	Watarumi <sup>(33)</sup> (heterogeneous oxides)
8	2836	
10	2829	

[d].

**Question 25**

Section 12.0 notes that COPERNIC is used for initialization of core thermal-hydraulic codes. Please list those calculated COPERNIC parameters used for initialization and the specific applications of the thermal-hydraulic codes.

**Response**

The COPERNIC parameters used for initialization of thermal-hydraulic codes (COBRA-IV, COBRA3C, LYNXT, etc.) are [d]. The specific thermal-hydraulic applications where fuel performance code initialization predictions are used include those related to the evaluation of locked rotor, ejected rod, etc. events.

Question 26

Section 12.1.1 (page 12-2) under discussion on Code Uncertainties it is noted that the code has an option that conservatively bounds the fissions gas release data and that this option is used to bound the fission gas release for the rod pressure predictions. However, there is a concern that this option will not bound the UO<sub>2</sub> - Gd<sub>2</sub>O<sub>3</sub> data within the fission gas release range that is important to the rod pressure analysis for UO<sub>2</sub> - Gd<sub>2</sub>O<sub>3</sub> rods (see Question 9 above) at the stated level of conservatism. Please discuss this issue further, particularly in relation to Question 9 above.

Response

[d]; see the response to Question 9.

Question 27

Section 12.1.1 (page 12-3) under the discussion on Transients it is noted that plant specific operating data may be used to establish simulated transients. Please explain further by what is meant by sufficient plant operating data and provide an example.

Response

The COPERNIC end-of-life (EOL) internal gas pressure analyses employ [d]. In addition, [d]. The Condition-I design transients discussed in section 12.1.1 account for [b, d]. All plants have the equipment and procedures necessary to gather the operational data required for core follow activities. The plant data gathered includes the time-dependent behavior of the reactor thermal power level, regulating rod and (where applicable) axial power shaping rod positions, RCS boron concentration, average moderator temperature, and axial power imbalance. In general, these data are collected approximately on an hourly basis. Most plants have the equipment necessary to electronically archive this data.

[e]. It would never be possible to eliminate the [e] [b, d] gas pressure analysis because [e]. Generally, it may only be possible, due [b, d], [e]. The [e] Condition I transient in the internal gas pressure analysis examples presented in Chapter 12 produced pressure [b, d] less than approximately [d].

The Condition-I design transients used in the COPERNIC internal gas pressure analyses are [b]. They are produced with [b, d]<sup>(34&35)</sup> (xenon distribution and control rod insertion) that would be [b, d]. [b, d] the typical Urania-Gadolinia cycle documented in Chapter 12 are shown in Figure 14-34. This example includes [b, d] with [b, d] and [e]. The [b] gas pressure difference [d]. This example demonstrates [d, e].

**Figure 14-34: Typical Mark-B Urania-Gadolinia Cycle Predictions [b]**

[b]

Question 28

There is a concern that the uncertainty factor provided in Equation 12-1 may be too small at the predicted operating temperatures (stored energy) calculated for LOCA initialization. Please discuss this issue further, particularly in relation to Question 3 above.

Response

[b, d, e].

**Question 29**

Are any of the example calculations provided in Section 12 for fuel cores with two 24-month cycles? It appears that there are no 24-month cycle results presented for the Mark BW-17 design. If so, please explain because it is anticipated that a large number of plants will be switching to 24-month cycles in the next few years.

**Response**

[b, d].



Question 30

The axial power distributions for the transients were found for the example licensing analyses, but the power distribution for the steady-state power operation were not found for the topical report. Please provide these axial power distributions. If there are more than 20 axial power profiles it would be helpful to condense the number down to 20 or less. Also, the steady-state power histories are only provided as plots versus burnup. Please provide these in tabular form to support the NRC audit calculation of these calculational examples?

Response

Forty-seven data sets of the normalized axial power distributions used for the Chapter 12 examples are listed in Table 14-12. The axial power distributions of each data set are provided in Table 14-13 through Table 14-59. The rod average burnups and linear heat generation rates are listed above each distribution presented.

Several different sets of axial power distributions are provided:

- [b, d, e]
- [b, d, e]
- [b, d, e]

[e] are not presented as separate sets because [e].

All of the steady-state axial power distributions used for the Chapter 12 examples are provided. If the reviewers need 20 or less distributions, it is left up to their discretion to select the appropriate distributions from those provided.

Table 14-12: Axial Power Distribution Data Sets

Typical Mark-B UO <sub>2</sub> Cycle, UO <sub>2</sub> Power Histories	
Table 14-13	[d]
Table 14-14	
Table 14-15	
Table 14-16	
Table 14-17	
Table 14-18	
Table 14-19	
Table 14-20	
Typical Mark-B UO <sub>2</sub> -Gd <sub>2</sub> O <sub>3</sub> Cycle, UO <sub>2</sub> Power Histories	
Table 14-21	[d]
Table 14-22	
Table 14-23	
Table 14-24	
Table 14-25	
Table 14-26	
Table 14-27	
Table 14-28	
Typical Mark-B UO <sub>2</sub> -Gd <sub>2</sub> O <sub>3</sub> Cycle, UO <sub>2</sub> -Gd <sub>2</sub> O <sub>3</sub> Power Histories	
Table 14-29	[d]
Table 14-30	
Table 14-31	
Table 14-32	
Table 14-33	
Table 14-34	
Table 14-35	
Typical Mark-BW UO <sub>2</sub> Cycle, UO <sub>2</sub> Power Histories	
Table 14-36	[d]
Table 14-37	
Table 14-38	
Table 14-39	
Table 14-40	
Table 14-41	
Table 14-42	
Table 14-43	
Typical Mark-BW UO <sub>2</sub> -Gd <sub>2</sub> O <sub>3</sub> Cycle, UO <sub>2</sub> Power Histories	
Table 14-44	[d]
Table 14-45	
Table 14-46	
Table 14-47	
Table 14-48	
Table 14-49	
Table 14-50	
Table 14-51	
Table 14-52	
Typical Mark-BW UO <sub>2</sub> -Gd <sub>2</sub> O <sub>3</sub> Cycle, UO <sub>2</sub> -Gd <sub>2</sub> O <sub>3</sub> Power Histories	
Table 14-53	[d]
Table 14-54	
Table 14-55	
Table 14-56	
Table 14-57	
Table 14-58	
Table 14-59	

Applications:

[d]

**Table 14-13: Typical Mark-B Uranium-Dioxide Cycle**  
[d]

[d]

**Table 14-13: Typical Mark-B Uranium-Dioxide Cycle**  
[d]

[d]

**Table 14-13: Typical Mark-B Uranium-Dioxide Cycle**  
[d]

[d]

**Table 14-13: Typical Mark-B Uranium-Dioxide Cycle**  
[d]

[d]

**Table 14-14: Typical Mark-B Uranium-Dioxide Cycle**  
[d]

[d]

**Table 14-15: Typical Mark-B Uranium-Dioxide Cycle**  
[d]

[d]



**Table 14-15: Typical Mark-B Uranium-Dioxide Cycle**  
[d]

[d]

Table 14-16: Typical Mark-B Uranium-Dioxide Cycle  
[d]

[d]

Table 14-16: Typical Mark-B Uranium-Dioxide Cycle  
[d]

[d]

Table 14-16: Typical Mark-B Uranium-Dioxide Cycle  
[d]

[d]

**Table 14-17: Typical Mark-B Uranium-Dioxide Cycle**  
[d]

[d]

**Table 14-17: Typical Mark-B Uranium-Dioxide Cycle**  
[d]

[d]

Table 14-17: Typical Mark-B Uranium-Dioxide Cycle  
[d]

[d]

**Table 14-18: Typical Mark-B Uranium-Dioxide Cycle**  
[d]

[d]



**Table 14-18: Typical Mark-B Uranium-Dioxide Cycle**  
[d]

[d]

**Table 14-18: Typical Mark-B Uranium-Dioxide Cycle**  
[d]

[d]

Table 14-18: Typical Mark-B Uranium-Dioxide Cycle  
[d]

[d]

**Table 14-19: Typical Mark-B Uranium-Dioxide Cycle**  
[d]

[d]

**Table 14-19: Typical Mark-B Uranium-Dioxide Cycle**  
[d]

[d]

**Table 14-19: Typical Mark-B Uranium-Dioxide Cycle**  
[d]

[d]

Table 14-19: Typical Mark-B Uranium-Dioxide Cycle  
[d]

[d]

**Table 14-19: Typical Mark-B Uranium-Dioxide Cycle**  
[d]

[d]



**Table 14-20: Typical Mark-B Uranium-Dioxide Cycle**  
[d]

[d]

Table 14-20: Typical Mark-B Uranium-Dioxide Cycle  
[d]

[d]

**Table 14-20: Typical Mark-B Uranium-Dioxide Cycle**  
[d]

[d]

**Table 14-20: Typical Mark-B Uranium-Dioxide Cycle**  
[d]

[d]

Table 14-20: Typical Mark-B Uranium-Dioxide Cycle  
[d]

[d]

**Table 14-21: Typical Mark-B Urania-Gadolinia Cycle**  
[d]

[d]

Table 14-21: Typical Mark-B Urania-Gadolinia Cycle  
[d]

[d]

**Table 14-21: Typical Mark-B Urania-Gadolinia Cycle**  
[d]

[d]



**Table 14-21: Typical Mark-B Urania-Gadolinia Cycle**  
[d]

[d]

Table 14-22: Typical Mark-B Urania-Gadolinia Cycle  
[d]

[d]

**Table 14-23: Typical Mark-B Urania-Gadolinia Cycle**  
[d]

[d]

**Table 14-23: Typical Mark-B Urania-Gadolinia Cycle**  
**[d]**

**[d]**

**Table 14-24: Typical Mark-B Urania-Gadolinia Cycle**  
[d]

[d]

**Table 14-24: Typical Mark-B Urania-Gadolinia Cycle**  
[d]

[d]

**Table 14-25: Typical Mark-B Urania-Gadolinia Cycle**  
[d]

[d]

**Table 14-25: Typical Mark-B Urania-Gadolinia Cycle**  
[d]

[d]



Table 14-25: Typical Mark-B Urania-Gadolinia Cycle  
[d]

[d]

**Table 14-26: Typical Mark-B Urania-Gadolinia Cycle**  
[d]

[d]

**Table 14-26: Typical Mark-B Urania-Gadolinia Cycle**  
[d]

[d]

**Table 14-26: Typical Mark-B Urania-Gadolinia Cycle**  
[d]

[d]

**Table 14-26: Typical Mark-B Urania-Gadolinia Cycle**  
[d]

[d]

Table 14-27: Typical Mark-B Urania-Gadolinia Cycle  
[d]

[d]

**Table 14-27: Typical Mark-B Urania-Gadolinia Cycle**  
[d]

[d]

**Table 14-27: Typical Mark-B Urania-Gadolinia Cycle**  
[d]

[d]



Table 14-27: Typical Mark-B Urania-Gadolinia Cycle  
[d]

[d]

**Table 14-28: Typical Mark-B Urania-Gadolinia Cycle**  
[d]

[d]

**Table 14-28: Typical Mark-B Urania-Gadolinia Cycle**  
[d]

[d]

**Table 14-28: Typical Mark-B Urania-Gadolinia Cycle**  
[d]

[d]

**Table 14-28: Typical Mark-B Urania-Gadolinia Cycle**  
[d]

[d]

**Table 14-29: Typical Mark-B Urania-Gadolinia Cycle**  
[d]

[d]

**Table 14-29: Typical Mark-B Urania-Gadolinia Cycle**  
[d]

[d]

**Table 14-29: Typical Mark-B Urania-Gadolinia Cycle**  
[d]

[d]



Table 14-29: Typical Mark-B Urania-Gadolinia Cycle  
[d]

[d]

**Table 14-30: Typical Mark-B Urania-Gadolinia Cycle**  
[d]

[d]

Table 14-31: Typical Mark-B Urania-Gadolinia Cycle  
[d]

[d]

**Table 14-31: Typical Mark-B Urania-Gadolinia Cycle**  
[d]

[d]

**Table 14-32: Typical Mark-B Urania-Gadolinia Cycle**  
[d]

[d]

**Table 14-32: Typical Mark-B Urania-Gadolinia Cycle**  
[d]

[d]

**Table 14-32: Typical Mark-B Urania-Gadolinia Cycle**  
[d]

[d]

**Table 14-33: Typical Mark-B Urania-Gadolinia Cycle**  
[d]

[d]



Table 14-33: Typical Mark-B Urania-Gadolinia Cycle  
[d]

[d]

Table 14-33: Typical Mark-B Urania-Gadolinia Cycle  
[d]

[d]

**Table 14-34: Typical Mark-B Urania-Gadolinia Cycle**  
[d]

[d]

**Table 14-34: Typical Mark-B Urania-Gadolinia Cycle**  
[d]

[d]

**Table 14-34: Typical Mark-B Urania-Gadolinia Cycle**  
[d]

[d]

**Table 14-34: Typical Mark-B Urania-Gadolinia Cycle**  
[d]

[d]

Table 14-35: Typical Mark-B Urania-Gadolinia Cycle  
[d]

[d]

**Table 14-35: Typical Mark-B Urania-Gadolinia Cycle**  
[d]

[d]



**Table 14-35: Typical Mark-B Urania-Gadolinia Cycle**  
[d]

[d]

**Table 14-35: Typical Mark-B Urania-Gadolinia Cycle**  
[d]

[d]

**Table 14-36: Typical Mark-BW17 Urania-Dioxide Cycle**  
[d]

[d]

**Table 14-36: Typical Mark-BW17 Urania-Dioxide Cycle**  
[d]

[d]

**Table 14-36: Typical Mark-BW17 Urania-Dioxide Cycle**  
[d]

[d]

Table 14-36: Typical Mark-BW17 Urania-Dioxide Cycle  
[d]

[d]

**Table 14-36: Typical Mark-BW17 Urania-Dioxide Cycle**  
[d]

[d]

Table 14-37: Typical Mark-BW17 Urania-Dioxide Cycle  
[d]

[d]



**Table 14-38: Typical Mark-BW17 Urania-Dioxide Cycle**  
[d]

[d]

**Table 14-38: Typical Mark-BW17 Urania-Dioxide Cycle**  
[d]

[d]

Table 14-39: Typical Mark-BW17 Urania-Dioxide Cycle  
[d]

[d]

**Table 14-39: Typical Mark-BW17 Urania-Dioxide Cycle**  
[d]

[d]

**Table 14-39: Typical Mark-BW17 Urania-Dioxide Cycle**  
[d]

[d]

**Table 14-40: Typical Mark-BW17 Urania-Dioxide Cycle**  
[d]

[d]

**Table 14-40: Typical Mark-BW17 Urania-Dioxide Cycle**  
[d]

[d]

**Table 14-40: Typical Mark-BW17 Urania-Dioxide Cycle**  
[d]

[d]



Table 14-41: Typical Mark-BW17 Urania-Dioxide Cycle  
[d]

[d]

**Table 14-41: Typical Mark-BW17 Urania-Dioxide Cycle**  
[d]

[d]

**Table 14-41: Typical Mark-BW17 Urania-Dioxide Cycle**  
[d]

[d]

**Table 14-41: Typical Mark-BW17 Urania-Dioxide Cycle**  
[d]

[d]

**Table 14-42: Typical Mark-BW17 Urania-Dioxide Cycle**  
[d]

[d]

**Table 14-42: Typical Mark-BW17 Urania-Dioxide Cycle**  
[d]

[d]

Table 14-42: Typical Mark-BW17 Urania-Dioxide Cycle  
[d]

[d]

**Table 14-42: Typical Mark-BW17 Urania-Dioxide Cycle**  
[d]

[d]



**Table 14-43: Typical Mark-BW17 Urania-Dioxide Cycle**  
[d]

[d]

Table 14-43: Typical Mark-BW17 Urania-Dioxide Cycle  
[d]

[d]

**Table 14-43: Typical Mark-BW17 Urania-Dioxide Cycle**  
[d]

[d]

**Table 14-43: Typical Mark-BW17 Urania-Dioxide Cycle**  
[d]

[d]

Table 14-44: Typical Mark-BW17 Urania-Gadolinia Cycle  
[d]

[d]

**Table 14-44: Typical Mark-BW17 Urania-Gadolinia Cycle**  
[d]

[d]

**Table 14-44: Typical Mark-BW17 Urania-Gadolinia Cycle**  
[d]

[d]

**Table 14-44: Typical Mark-BW17 Urania-Gadolinia Cycle**  
[d]

[d]



**Table 14-44: Typical Mark-BW17 Urania-Gadolinia Cycle**  
[d]

[d]

**Table 14-45: Typical Mark-BW17 Urania-Gadolinia Cycle**  
[d]

[d]

**Table 14-46: Typical Mark-BW17 Urania-Gadolinia Cycle**  
[d]

[d]

**Table 14-46: Typical Mark-BW17 Urania-Gadolinia Cycle**  
[d]

[d]

**Table 14-47: Typical Mark-BW17 Urania-Gadolinia Cycle**  
[d]

[d]

**Table 14-47: Typical Mark-BW17 Urania-Gadolinia Cycle**  
[d]

[d]

Table 14-48: Typical Mark-BW17 Urania-Gadolinia Cycle  
[d]

[d]

**Table 14-48: Typical Mark-BW17 Urania-Gadolinia Cycle**  
[d]

[d]



**Table 14-48: Typical Mark-BW17 Urania-Gadolinia Cycle**  
[d]

[d]

**Table 14-49: Typical Mark-BW17 Urania-Gadolinia Cycle**  
[d]

[d]

**Table 14-49: Typical Mark-BW17 Urania-Gadolinia Cycle**  
[d]

[d]

**Table 14-49: Typical Mark-BW17 Urania-Gadolinia Cycle**  
[d]

[d]

**Table 14-49: Typical Mark-BW17 Urania-Gadolinia Cycle**  
[d]

[d]

**Table 14-50: Typical Mark-BW17 Urania-Gadolinia Cycle**  
[d]

[d]

**Table 14-50: Typical Mark-BW17 Urania-Gadolinia Cycle**  
[d]

[d]

**Table 14-50: Typical Mark-BW17 Urania-Gadolinia Cycle**  
[d]

[d]



**Table 14-50: Typical Mark-BW17 Urania-Gadolinia Cycle**  
[d]

[d]

**Table 14-50: Typical Mark-BW17 Urania-Gadolinia Cycle**  
[d]

[d]

Table 14-51: Typical Mark-BW17 Urania-Gadolinia Cycle  
[d]

[d]

**Table 14-51: Typical Mark-BW17 Urania-Gadolinia Cycle**  
[d]

[d]

**Table 14-51: Typical Mark-BW17 Urania-Gadolinia Cycle**  
[d]

[d]

**Table 14-51: Typical Mark-BW17 Urania-Gadolinia Cycle**  
[d]

[d]

**Table 14-51: Typical Mark-BW17 Urania-Gadolinia Cycle  
63 GWd/tU, UO<sub>2</sub> Single Limiting Rod Analyses (Continued)**

**Table 14-52: Typical Mark-BW17 Urania-Gadolinia Cycle  
UO<sub>2</sub> Max Burnup Rod, Cladding Oxide**



**Table 14-52: Typical Mark-BW17 Urania-Gadolinia Cycle**  
[d]

[d]

**Table 14-52: Typical Mark-BW17 Urania-Gadolinia Cycle**  
[d]

[d]

Table 14-52: Typical Mark-BW17 Urania-Gadolinia Cycle  
[d]

[d]

**Table 14-52: Typical Mark-BW17 Urania-Gadolinia Cycle**  
[d]

[d]

**Table 14-53: Typical Mark-BW17 Urania-Gadolinia Cycle**  
[d]

[d]

Table 14-53: Typical Mark-BW17 Urania-Gadolinia Cycle  
[d]

[d]

Table 14-53: Typical Mark-BW17 Urania-Gadolinia Cycle  
[d]

[d]

**Table 14-53: Typical Mark-BW17 Urania-Gadolinia Cycle**  
[d]

[d]



Table 14-54: Typical Mark-BW17 Urania-Gadolinia Cycle  
[d]

[d]

**Table 14-55: Typical Mark-BW17 Urania-Gadolinia Cycle**  
[d]

[d]

**Table 14-55: Typical Mark-BW17 Urania-Gadolinia Cycle**  
[d]

[d]

**Table 14-56: Typical Mark-BW17 Urania-Gadolinia Cycle**  
[d]

[d]

Table 14-56: Typical Mark-BW17 Urania-Gadolinia Cycle  
[d]

[d]

**Table 14-56: Typical Mark-BW17 Urania-Gadolinia Cycle**  
[d]

[d]

Table 14-57: Typical Mark-BW17 Urania-Gadolinia Cycle  
[d]

[d]

**Table 14-57: Typical Mark-BW17 Urania-Gadolinia Cycle**  
[d]

[d]



**Table 14-57: Typical Mark-BW17 Urania-Gadolinia Cycle**  
[d]

[d]

**Table 14-58: Typical Mark-BW17 Urania-Gadolinia Cycle**  
[d]

[d]

Table 14-58: Typical Mark-BW17 Urania-Gadolinia Cycle  
[d]

[d]

**Table 14-58: Typical Mark-BW17 Urania-Gadolinia Cycle**  
[d]

[d]

**Table 14-58: Typical Mark-BW17 Urania-Gadolinia Cycle**  
[d]

[d]

**Table 14-59: Typical Mark-BW17 Urania-Gadolinia Cycle**  
[d]

[d]

Table 14-59: Typical Mark-BW17 Urania-Gadolinia Cycle  
[d]

[d]

**Table 14-59: Typical Mark-BW17 Urania-Gadolinia Cycle**  
[d]

[d]



**Table 14-59: Typical Mark-BW17 Urania-Gadolinia Cycle**  
[d]

[d]

Question 31

Section 12.4.1 states that the cladding strain analysis will be run with ..... and the gaseous swelling option turned off. Performing these analyses without gaseous swelling ..... produces more accurate predictions ..... at the very high local power levels that accompany these analyses. This appears to be contradictory to the comparisons to data in Figures 6-17, 6-18, and 6-19 that demonstrate that COPERNIC with gaseous swelling option turned on provides an adequate prediction of diametral strains. Please provide data that supports the conclusion that the exclusion of gaseous swelling in COPERNIC produces more accurate strain predictions.

Response

[e]

Ramp tests were recently performed to study the effects of pellet cladding mechanical interaction (PCMI) on cladding deformation<sup>(36)</sup>. Three rodlets, which were part of a segmented rod, were ramped to terminal power levels ranging from 39.5 to 41.5 kw/m. The ramp time to the terminal power levels was approximately 2-min. and the rods were held at the terminal power levels for 0 (zero hold time), 16-min. and 12-hrs. Although the terminal power level of these rods was well below fuel melt, it was sufficient to cause partial dish filling for the rodlets with hold times of 16-min. and 12-hrs. These power ramps were simulated with 2 and 3 dimensional finite element codes that don't contain gaseous swelling models. The overall computational results of the 2D finite element code agreed well with the data from the rodlets with terminal power level hold times of zero and 16-min. but the cladding diameter changes for the 12 hour hold time were underestimated because gaseous swelling was not included. The 3D finite element code, which is currently under development, tended to moderately overestimate the measured cladding diameter changes for these cases. [e].

**Question 32**

Section 12.5 states that COPERNIC will be used to generate cladding creep collapse initial conditions and example rod pressure results are provided in Figures 12-34 and 12-35. Are there any other initial conditions provided by COPERNIC for the creep collapse analysis, e.g., cladding temperatures? If so, please provide predictions of these initial conditions.

**Response**

The other initial conditions that are provided by COPERNIC for the creep collapse analysis include [e].

**Figure 14-35: Typical Mark-B Fuel Cycles  
Creep Collapse Analyses [d]**

[d]

**Figure 14-36: Typical Mark-BW17 Fuel Cycles  
Creep Collapse Analyses [d]**

[d]

**Figure 14-37: Typical Mark-B Fuel Cycles  
Creep Collapse Analyses [d]**

[d]

**Figure 14-38: Typical Mark-BW17 Fuel Cycles  
Creep Collapse Analyses [d]**

[d]

**Figure 14-39: Typical Mark-B Fuel Cycles  
Creep Collapse Analyses [d]**

[d]

**Figure 14-40: Typical Mark-BW17 Fuel Cycles  
Creep Collapse Analyses [d]**

[d]

**Figure 14-41: Typical Mark-B Fuel Cycles  
Creep Collapse Analyses [d]**

[d]

**Figure 14-42: Typical Mark-BW17 Fuel Cycles  
Creep Collapse Analyses [d]**

[d]

## References:

1. M. Kinoshita, et al., "High Burnup Rim Project (II) Irradiation and Examination to Investigate Rim Structured Fuel," Proceedings of the 2000 International Topical Meeting on LWR Fuel Performance, Park City Utah, April 10-13, 2000.
2. J. Nakamura, et al., "Thermal Diffusivity Measurements of a High-Burnup  $\text{UO}_2$  Pellet," Proceedings of the ANS International Topical Meeting on LWR Fuel Performance, Portland Oregon, March 2-6, 1997.
3. S. Yagnik, "Thermal Conductivity Recovery Phenomenon in Irradiated  $\text{UO}_2$  and (U,Gd)  $\text{O}_2$ ," Proceedings of the 2000 International Topical Meeting on LWR Fuel Performance, Park City Utah, April 10-13, 2000.
4. M. Lippens and L. Mertens, "High Burnup  $\text{UO}_2$  and (U,Gd) $\text{O}_2$  Specimens: Thermal Diffusivity Measurements and Post-Irradiation Characterization," Final Report, EPRI TR-106501, December 1996.
5. K. Une, et al., "Effects of Grain Size and PCI Restraint on the Rim Structure of  $\text{UO}_2$  Fuels," Proceedings of the 2000 International Topical Meeting on LWR Fuel Performance, Park City Utah, April 10-13, 2000.
6. [c]
7. Not used.
8. D.A. Wesley, et al., "Mark-BEB Ramp Testing Program," Proceedings of the 1994 International Topical Meeting on LWR Fuel Performance, West Palm Beach, FL, April 17-21, 1994.
9. I.H. Shames, "Mechanics of Deformable Solids," Prentice-Hall, Inc., 1965, p 21.
10. J.G. Merkle, "Engineering Approach to Multiaxial Plasticity," ORNL-4138, Oak Ridge National Laboratories.
11. R. Hill, "Yielding and Plastic Flow of Anisotropic Metals," Proceedings Ray Society, A193, 1948, pp 281-295.
12. A.F.J. Eckert, H.W. Wilson, and K.E. Yoon, "Program to Determine In-Reactor Performance of B&W Fuels - Cladding Creep Collapse", BAW-10084P-A, Rev. 3, October 1980.
13. A.P. Boresi, et. al., "Advanced Mechanics of Materials," John Wiley and Sons, 1978, pp 471-483.
14. J.T. Wilse and G.L. Garner, "Recent Results from the Fuel Performance Improvement Program at Framatome Cogema Fuels," Proceedings of the 2000 International Topical Meeting on LWR Fuel Performance, Park City Utah, April 10-13, 2000.
15. [c]
16. R. Van Nieuwenhove and E. Kolstad, "In-Pile Determination of Thermal Conductivity of Oxide Layer on LWR Cladding", EPRI TR-107718-P2, Final Report, October 1998.
17. [c]
18. W.A. Lambertson and M.H. Mueller, "Uranium Phase Equilibrium Systems: 1,  $\text{UO}_2 - \text{Al}_2\text{O}_3$ ", Journal of the American Ceramic Society, 36, p.329-331, 1953.
19. L.G. Wisniyi and S.W. Pijanowski, "The Thermal Stability of Uranium Dioxide", KAPL - 1702, UC-25, Metallurgy and Ceramics, November 1957.
20. T.C. Ehlert and J.L. Margrave, "Melting Point and Spectral Emissivity of Uranium Dioxide", Journal of the American Ceramic Society, 41, p. 330, 1958.



21. J.A. Christensen, "Irradiation Effects on Uranium Dioxide Melting", HW-69234, UC-25, Metals, Ceramics and Materials, Hanford Laboratories, March 1962.
22. J.A. Christensen, "Thermal Expansion and Change in Volume of Uranium Dioxide on Melting", Journal of the American Ceramic Society, 46, p. 607-608, December 1963.
23. T.J. Pashos, D.R. Dehalas, D.L. Keller and L.A. Neimark, "Irradiation Behavior of Ceramic Fuel", Proceedings of the Third United Nations International Conference on the Peaceful Uses of the Atomic Energy, Geneva 1964, Vol.II, p. 472-484, United Nations, Geneva, 1965.
24. H. Hausner, "Determination of the Melting Point of Uranium Dioxide", Journal of Nuclear Materials, 15, 179-183, 1965.
25. M.J. Bannister, "Melting Temperatures in the System Uranium-Uranium Dioxide", Journal of Nuclear Materials, 24, p. 221-251, 1970.
26. R. Benz, G. Balog, and B.H. Baca, "U - UO<sub>2</sub> - UN<sub>2</sub> Phase Diagram", High Temperature Science, 2, p. 221-251, 1970.
27. B.F. Rubin, "Summary of (U,Pu)O<sub>2</sub> Properties and Fabrication Methods", GEAP 13582, AEC Research and Development Report, November 1970.
28. T. Tachibana, T. Ohmori, S. Yamamouchi and T. Itaki, "Determination of Melting Point of Mixed-Oxide Fuel Irradiated in Fast Breeder Reactor", Journal of Nuclear Science and Technology, 22, p. 155-157, February 1985.
29. A. Chotard, P. Melin, M. Bruet and B. François, "Out of Pile Physical Properties and in Pile Thermal Conductivity of (U,Gd)O<sub>2</sub>", Properties of Materials for Water Reactor Fuel Elements and Method of Measurement, IAEA, Vienna, 13-16 October 1986, IWGFPT/26, p. 77-87, 1987.
30. J.A. Christensen, R.J. Allio and A. Bianchera, "Melting Point of Irradiated Uranium Dioxide", Trans. Am. Nucl. Soc., 7, p. 390-391, 1964.
31. S. Yamamouchi, T. Tachibana, K. Tsukui and M. Oguma, "Melting Temperature of Irradiated UO<sub>2</sub>-2% Gd<sub>2</sub>O<sub>3</sub> Pellets up to Burnup of about 30 GWd/tU", Journal of Nuclear Science and Technology, 25, p. 528, 1988.
32. R.A. Bush, "Properties of the Urania-Gadolinia System (Part 1)", EPRI NP-7561-D, project X 101-3, Final report, January 1992.
33. K. Watarumi, "Determination of Physical Properties of (U,Gd)O<sub>2</sub> Compounds", Nuclear Fuel Industries Ltd., NF-DK-1286, July 5, 1991.
34. BAW-10122A, Rev. 1, "Normal Operating Controls," G. E. Hanson, May 1984.
35. BAW-10163P-A, "Core Operating Limit Methodology for Westinghouse Designed PWRs," B. J. Delano, et al., June 1989.
36. S. Bourreau, et al, "Ramp testing of PWR fuel and multi-dimensional finite element modeling of PCMI," paper presented at the ANS 2000 International Topical Meeting on LWR Fuel Performance, Park City, Utah, April 10, 2000.



UNITED STATES  
NUCLEAR REGULATORY COMMISSION  
WASHINGTON, D.C. 20555-0001

May 14, 2001

Mr. T. A. Coleman, Vice President  
Government Relations  
Framatome ANP  
3315 Old Forest Road  
P. O. Box 10935  
Lynchburg, Virginia 24506-0935

SUBJECT: REQUEST FOR ADDITIONAL INFORMATION - CHAPTER 13 OF  
FRAMATOME TOPICAL REPORT BAW-10231P (TAC NO. MA9783)

Dear Mr. Coleman:

By letter dated July 31, 2000, Framatome requested a review of Topical Report BAW-10231P, "COPERNIC Fuel Rod Design Code." The staff has determined that additional information for Chapter 13, MOX Applications, is required in order to complete our review.

The enclosed questions have been discussed with your staff. As discussed with your staff, by June 30, 2001, please respond to the uranium-related questions and provide a schedule for responding to the MOX-related questions. If you have any questions concerning our review, please contact me at (301) 415-1321.

Sincerely,

A handwritten signature in black ink, appearing to read "Stewart Bailey", is written over the typed name.

Stewart Bailey, Project Manager, Section 2  
Project Directorate III  
Division of Licensing Project Management  
Office of Nuclear Reactor Regulation

Project No. 693

Enclosure: Request for Additional Information

cc w/enc: See next page

Mr. T. A. Coleman

Project No. 693

cc:

Mr. James Mallay  
Director, Regulatory Affairs  
Framatome ANP  
2101 Horn Rapids Road  
Richland, WA 99352

Mr. F. McPhatter, Manager  
Framatome ANP  
3315 Old Forest Road  
P.O. Box 10935  
Lynchburg, VA 24506-0935

Mr. R. Schomaker  
Framatome ANP  
3315 Old Forest Road  
P.O. Box 10935  
Lynchburg, VA 24506-0935

Mr. Michael Schoppman  
Framatome ANP  
1911 N. Ft Myer Drive  
Rosslyn, VA 22209

## REQUEST FOR ADDITIONAL INFORMATION

### TOPICAL REPORT BAW-10231P, CHAPTER 13

#### "COPERNIC FUEL ROD DESIGN CODE"

#### MOX APPLICATIONS

The questions provided below address COPERNIC evaluations related to normal operation. A second round of questions related to mixed oxide (MOX) fuel application to transient and accident analyses will be issued separately.

1. It is recognized that weapons grade plutonium will be used for MOX for commercial application in the U.S. However, the isotopic plutonium ratios are significantly different between reactor grade (reprocessed LWR fuel) plutonium and weapons grade plutonium. Please provide the plutonium ratios for reactor grade and weapons grade plutonium and; also, the tabular values of pellet radial power profiles to be used for weapons grade plutonium and how these values were determined. If the reactor grade and weapons grade MOX radial profiles are proposed to be similar, provide the calculational results for both MOX types that demonstrate this conclusion.
2. Please provide the specifications (including nominal values) of oxygen-to-metal (O/M) ratio,  $\text{PuO}_2$  particle size, and grain size specified for the U.S. commercial application.
3. For the experimental thermal MOX data, what were the O/M ratios used for code verification?
4. For the MOX fission gas release data, please provide the nominal and range of  $\text{PuO}_2$  particle size for the different experimental rods used for code verification?
5. The conductivity equation for unirradiated MOX (Eq. 4-44) defines the term,  $y$ , as Pu content in weight-percent, but it appears that this may be weight fraction. Please verify which unit is intended. If the Pu content is in weight fraction, the correction for Pu conductivity is small for 100 wt%  $\text{PuO}_2$ , which appears to be too low (see questions 6 and 8 below).
6. The Halden Reactor Project correction for unirradiated MOX is an 8 percent reduction in the uranium thermal conductivity (at all temperatures) when the Pu concentration is equal to or below 12 wt%. This is significantly higher than the value used in COPERNIC. Also, the COPERNIC model for uranium and MOX pellet thermal conductivity at high burnups and nominal stoichiometry ( $x = 0.02$ ) is significantly higher in the range from 500 to 1500 K than similar burnup-dependent models, such as those proposed by ORNL/Kurchatov (Popov, 2000), Halden (Wiesenack, 2000, HPR-589) and Baron (Baron 1998). Please justify the higher thermal conductivity values used by COPERNIC for unirradiated and high burnup MOX (see question 8 below).

7. Recent high-temperature data on unirradiated uranium fuel pellet thermal conductivity (Ronchi et al., 1999) has indicated that the conductivity in the range from 2000 to 3000 K is significantly lower than the COPENIC equations for uranium and, by implication, for LWR MOX also. Most of the current conductivity models (including COPENIC) are based on very old data at high temperature from which there was considerable scatter. The more recent data appears to have less scatter and better experimental techniques to minimize the scatter due to heat loss and other effects. Please justify the higher estimates of COPENIC conductivity in this high temperature range because the discrepancy affects the LHGR margin to center fuel melting.
8. The integral MOX experiments provided, where centerline temperatures are measured, to verify the COPENIC integral thermal predictions of MOX fuel rods are limited to very low burnup levels, i.e., less than 5 GWd/MTU. Please provide COPENIC predictions of at least three of the following Halden MOX instrumented assemblies, IFA-597.4/5/6, IFA-606, IFA-610, and IFA-648.1, that achieved burnups of approximately 24 GWd/MTM to 57 GWd/MTM, or suggest other Halden MOX instrumented assemblies. Please justify the reasons for eliminating some of the data and/or assemblies for COPENIC comparisons and the reasons for selecting others (this should be discussed with the NRC reviewer prior to issuing a response to the request for additional information). Also, rod pressures due to fission gas release were measured for two experimental Halden MOX fuel rods in IFA-597.4/5/6. COPENIC predictions of rod pressure are also needed, where appropriate.
9. What are the gas production values (xenon, krypton and helium) used in COPENIC for MOX. Justify their application to weapons grade Pu. Also, how are the release fractions for helium determined in the rod pressure analysis, LOCA analyses, and other analyses where it is important?
10. Has Framatome (or other parties) examined the interface between MOX fuel and the cladding at high burnups to determine if there are any chemical reactions (such as Zr-oxide formation or other reactions) between the fuel and cladding?

#### REFERENCES

- Baron, D., 1998. "About the Modeling of the Fuel Thermal Conductivity Degradation at High Burnup. Accounting for Recovery Processes with Temperature" paper 2.5 in *Proceedings of the NEA Seminar on Thermal Performance of High-Burnup LWR Fuel*, Cadarache, France, 3-6 March 1998.
- Popov, S.G., et al., 2000. *Thermophysical Properties of MOX and UO<sub>2</sub> Fuels including the Effects of Irradiation*, ORNL/TM-2000/351, Oak Ridge National Laboratory, Oak Ridge, TN.
- Ronchi, C., M. Shiendlin, M. Musella, and G.J. Hyland, 1999. "Thermal Conductivity of Uranium Dioxide up to 2900 K from Simultaneous Measurement of the Heat Capacity and Thermal Diffusivity," *Journal of Applied Physics*, Vol. 85 no. 2, pages 776 to 789.

W. Wiesenack and T. Tverberg, 2000. "Thermal Performance of High Burnup Fuel - In-Pile Temperature Data And Analysis," in *Proceedings of the ANS International Topical Meeting on Light Water Reactor Fuel Performance, Park City, Utah, April 2000*, pages 730 to 737.  
(As-modified for MOX by HWR-589)



July 27, 2001  
NRC:01:033

Document Control Desk  
ATTN: Chief, Planning, Program and Management Support Branch  
U.S. Nuclear Regulatory Commission  
Washington, D.C. 20555-0001

**Partial Response to RAI**

- Ref.: 1. Letter, Stewart Bailey (NRC) to T. A. Coleman, (Framatome Cogema Fuels), "Request for Additional Information - Framatome Topical Report BAW-10231P (TAC NO. MA6792)," August 11, 2000.
- Ref.: 2. Letter, T. A. Coleman (Framatome ANP) to U.S. Nuclear Regulatory Commission, GR0-021.doc, February 5, 2001.
- Ref.: 3. Letter, Stewart Bailey (NRC) to T. A. Coleman (Framatome ANP), "Request for Additional Information - Chapter 13 of Framatome Topical Report BAW-10231P (TAC NO. MA9783)," May 14, 2001.

Reference 1 provided a request for additional information (RAI) on Framatome Cogema Fuels (FCF) topical report BAW-10231P, "COPERNIC Fuel Rod Design Code." That RAI addressed the UO<sub>2</sub> applications of the code. Reference 2 contained the Framatome ANP response to the RAI.

Reference 3 is the RAI associated with the MOX applications for COPERNIC. However, two of the questions in the RAI (numbers 6 and 7) refer to UO<sub>2</sub> applications. The responses to these two questions are enclosed. Framatome plans to apply the UO<sub>2</sub> portion of the COPERNIC topical report within the next few months. Therefore, receipt of the SER by August 31, 2001 constitutes a critical need in our schedule.

In a telephone conference with the NRC held on May 23, 2001, Framatome ANP agreed to revise some of the figures that had been included in the response to question 2 of the initial RAI. The revised figures are enclosed. Since the topical report was printed double-sided, the enclosed change pages typically have revisions on one side only.

Power level hold time for LOCA initialization is discussed in Chapter 12, "Application Methodology," of BAW-10231P. In order to clarify the manner in which the hold time is determined, Framatome ANP has developed a method for linking the hold time to the requirements in the plant-specific technical specifications. A description of this method is

**Framatome ANP Richland, Inc.**

2101 Horn Rapids Road  
Richland, WA 99352

Tel: (509) 375-8100  
Fax: (509) 375-8402

enclosed as a clarification to facilitate the NRC's review and should be included in your evaluation of BAW-10231P.

In accordance with the provisions of 10 CFR 2.790(b), Framatome ANP requests that these responses be considered proprietary and withheld from public disclosure. Attachment 1 is an affidavit supporting this request. Attachment 2 is the proprietary version of the RAI responses, revised figures, and unsolicited response. Attachment 3 is the non-proprietary version. After the SER is received, Framatome ANP will incorporate all the enclosed material into either the body or an appendix of the approved version of BAW-10231P.

Very truly yours,



James F. Mallay, Director  
Regulatory Affairs

cel

Enclosures

cc: S. N. Bailey, NRC  
R. Caruso, NRC  
J. S. Wernell, NRC  
S. L. Wu, NRC  
C. E. Beyer, PNNL  
M. S. Schoppman  
20A13 File/Records Management



## AFFIDAVIT

STATE OF WASHINGTON   )  
                                  ) ss.  
COUNTY OF BENTON     )

1.     My name is James F. Mallay. I am Director, Regulatory Affairs, for Framatome ANP ("FRA-ANP"), and as such I am authorized to execute this Affidavit.

2.     I am familiar with the criteria applied by FRA-ANP to determine whether certain FRA-ANP Information is proprietary. I am familiar with the policies established by FRA-ANP to ensure the proper application of these criteria.

3.     I am familiar with the FRA-ANP information included in two of the attachments (responses to RAI and change pages) to letter NRC:01:033, dated July 27, 2001 from James F. Mallay to (NRC). These two attachments are referred to herein as "Documents." Information contained in these Documents has been classified by FRA-ANP as proprietary in accordance with the policies established by FRA-ANP for the control and protection of proprietary and confidential information.

4.     These Documents contain information of a proprietary and confidential nature and is of the type customarily held in confidence by FRA-ANP and not made available to the public. Based on my experience, I am aware that other companies regard information of the kind contained in these Documents as proprietary and confidential.

5.     These Documents have been made available to the U.S. Nuclear Regulatory Commission in confidence with the request that the information contained in these Documents be withheld from public disclosure.

6. The following criteria are customarily applied by FRA-ANP to determine whether information should be classified as proprietary:

- (a) The information reveals details of FRA-ANP's research and development plans and programs or their results.
- (b) Use of the information by a competitor would permit the competitor to significantly reduce its expenditures, in time or resources, to design, produce, or market a similar product or service.
- (c) The information includes test data or analytical techniques concerning a process, methodology, or component, the application of which results in a competitive advantage for FRA-ANP.
- (d) The information reveals certain distinguishing aspects of a process, methodology, or component, the exclusive use of which provides a competitive advantage for FRA-ANP in product optimization or marketability.
- (e) The information is vital to a competitive advantage held by FRA-ANP, would be helpful to competitors to FRA-ANP, and would likely cause substantial harm to the competitive position of FRA-ANP.

7. In accordance with FRA-ANP's policies governing the protection and control of information, proprietary information contained in these Documents has been made available, on a limited basis, to others outside FRA-ANP only as required and under suitable agreement providing for nondisclosure and limited use of the information.

8. FRA-ANP policy requires that proprietary information be kept in a secured file or area and distributed on a need-to-know basis.

9. The foregoing statements are true and correct to the best of my knowledge,  
information, and belief.

James P. Kelly

SUBSCRIBED before me this 26<sup>th</sup>  
day of July, 2001.

Valerie W. Smith

Valerie W. Smith  
NOTARY PUBLIC, STATE OF WASHINGTON  
MY COMMISSION EXPIRES: 10/10/04



6. The Halden Reactor Project correction for unirradiated MOX is an 8 percent reduction in the uranium thermal conductivity (at all temperatures) when the Pu concentration is equal to or below 12 wt%. This is significantly higher than the value used in COPENIC. Also, the COPENIC model for uranium and MOX pellet thermal conductivity at high burnups and nominal stoichiometry ( $x = 0.02$ ) is significantly higher in the range from 500 to 1500 K than similar burnup-dependent models, such as those proposed by ORNL/Kurchatov (Popov, 2000), Halden (Wiesenack, 2000, HPR-589) and Baron (Baron 1998). Please justify the higher thermal conductivity values used by COPENIC for unirradiated and high burnup MOX (see question 8 below).

The COPENIC  $\text{UO}_2$  fuel thermal conductivity relationship [b, c]

The COPENIC thermal conductivity relationship [b, c]

the Baron<sup>(6)</sup> relationship which has been shown to conservatively over-predict measured fuel temperatures<sup>(7)</sup>.

The integrals of the above thermal conductivities are shown in Figures 1, 2 and 3 for MOX and  $\text{UO}_2$ . [b, c]

**APPENDIX A**

[b, c]

## REFERENCES

- [1] P.G. Lucuta, H.J. Matzke, I.J. Hastings, "A Pragmatic Approach to Modeling Thermal Conductivity of Irradiated UO<sub>2</sub> Fuel: Review and Recommendations," J. Nucl. Mater., Vol. 232, pp. 166-180(1996).
- [2] W. Wiesenack, "Assessment of UO<sub>2</sub> Conductivity Degradation Based on In-pile Temperature Data," Proceedings of the International Topical Meeting on Light Water Reactor Fuel Performance, Portland, U.S.A., pp. 507-511 (1997).
- [3] S. Yagnik, "Thermal Conductivity Recovery Phenomena in Irradiated UO<sub>2</sub> and (U, Gd)O<sub>2</sub>, Proceedings of the International Topical Meeting on Light Water Reactor Fuel Performance, Park City, Utah U.S.A., pp. 634-645 (2000).
- [4] C. Duriez, J.P. Alessandri, T. Gervais, Y. Philipponneau, "Thermal Conductivity of Hypostoichiometric Low Pu Content (U,Pu)O<sub>2-x</sub> Mixed Oxide" J.Nucl. Mater., Vol. 277 pp. 143-158 (2000)
- [5] S.G. Popov, J.J Carbajo, V.K. Ivanov, G.L. Yoder, "Thermophysical Properties of MOX and UO<sub>2</sub> Fuels Including the Effects of Irradiation" Report ORNL/TM-2000/351
- [6] D. Baron, "About the Modeling of the Fuel Thermal Conductivity Degradation at High Burnup, Accounting for Recovery Processes with Temperature," Paper 2.5 in proceedings of the NEA Seminar on Thermal Performance of High-Burnup LWR Fuel, Cadarache, France, 3-6 March 1998
- [7] D. D. Lanning, C. E. Beyer, "Assessment of Recent Data and Correlations for Fuel Pellet Thermal Conductivity," Presented at the 2001 Enlarged Halden Program Group Meeting, Lillehammer, Norway 11-16 March 2001. Published in Halden Report HRP-356
- [8] D. D. Lanning, C. E. Beyer, M. E. Cunningham, "FRAPCON-3 Fuel rod temperature Predictions with fuel conductivity degradation caused by fission products and gadolinia additions," Proceedings of the International Topical Meeting on Light Water Reactor Fuel Performance, Park City, Utah U.S.A., pp. 244-258 (2000).

**Table 1: FRAMATOME-ANP database for the validation of the MOX fuel thermal conductivity relationship of COPENIC**

[b, c, d]

**Figure 1 – MOX Thermal Conductivity Integrals**

[b, c]

**Figure 2 – UO<sub>2</sub> Thermal Conductivity Integrals**

[b, c]

**Figure 3 – UO<sub>2</sub> Thermal Conductivity Integrals**

[b, c]



7. Recent high-temperature data on unirradiated uranium fuel pellet thermal conductivity (Ronchi et al., 1999) has indicated that the conductivity in the range from 2000 to 3000 K is significantly lower than the COPERNIC equations for uranium and, by implication, for LWR MOX also. Most of the current conductivity models (including COPERNIC) are based on very old data at high temperature from which there was considerable scatter. The more recent data appears to have less scatter and better experimental techniques to minimize the scatter due to heat loss and other effects. Please justify the higher estimates of COPERNIC conductivity in this high temperature range because the discrepancy affects the LHGR margin to center fuel melting.

[b, c, e]

**Figure 14-3: COPERNIC and NFIR-III Thermal Conductivity Comparison  
60 GWd/tU Burnup - [c]**

[b, c, d]

**Figure 14-4: COPERNIC and JAERI Thermal Conductivity Comparison - Sample No.2  
63 GWd/tU Burnup, 83-89% Density Range, [c]**

[b, c, d]

**Figure 14-5: COPERNIC and JAERI Thermal Conductivity Comparison - Sample No.3  
63 GWd/tU Burnup, 92-96% Density Range, [c]**

[b, c, d]

**Figure 14-6: Rim Effect at 60 GWd/tU  
IFA 562**

[b, c, d]

Question 6

Is Framatome a member of Halden? If so, Halden has refabricated two high (~ 59 GWd/MTU) burnup rods (one with a functional thermocouple) and placed them first in IFA-597.2 (HWR-442) and subsequently in IFA-597.3 (HWR-543) with measured centerline temperatures. Please compare COPERNIC code predictions to this data and include this data in the response to Question 3.1 above.

Response

The COPERNIC centerline fuel temperature predictions are compared with the IFA-597.2 (HWR-442) and IFA-597.3 (HWR-543) fuel temperature measurements in Figure 14-13. This rodlet attained a burnup of 61.5 GWd/tUO<sub>2</sub> or 69.8 GWd/tU.

**Figure 14-13: Fuel Centerline Temperature Measurements and Predictions vs.  
Burnup, IFA-597.2 and IFA-597.3**

[d]

**Figure 14-14: Not used**

[d]

Question 28

There is a concern that the uncertainty factor provided in Equation 12-1 may be too small at the predicted operating temperatures (stored energy) calculated for LOCA initialization. Please discuss this issue further, particularly in relation to Question 3 above.

Response

[b, d, e].

**Question 29**

Are any of the example calculations provided in Section 12 for fuel cores with two 24-month cycles? It appears that there are no 24-month cycle results presented for the Mark BW-17 design. If so, please explain because it is anticipated that a large number of plants will be switching to 24-month cycles in the next few years.

**Response**

[b, d].

#### Clarification of Power Level Hold Time for LOCA Initialization

Section 12 (Application Methodology) of BAW-10231P describes the methodology that will be used to predict the initialization conditions of fuel rods for reload safety evaluations. Section 12.2.1 specifies the methodology that will be used to generate the LOCA initialization predictions. The fuel rod is simulated to operate with a specified limiting rod power history and is then ramped to the LOCA  $F_Q$  limit at the time in life when the LOCA transient originates. The topical states [b, c]

Plant technical specifications place limits on key controlled measurable parameters such as control rod insertion, axial power imbalance, and thermal power level to ensure that the initial conditions for accidents are maintained during operation. The limits define boundaries of core operation where power peaking factors could equal the LOCA  $F_Q$  limit (or the maximum allowable peaking limit for another accident if it is more limiting than the LOCA). Should one of the control parameters reach or exceed its limit, required actions and completion times are specified by the technical specifications. The required actions and completion times ensure that power peaking factors are restored within their limits promptly. These technical specification limits, together with their corresponding actions and completion times, limit the amount of time that the fuel could operate with power peaking factors in excess of the specified acceptable fuel design limits.

Allowable completion times for these tech spec required actions typically fall in the range of 15 minutes to 4 hours. Plants that operate with fixed incore detector systems have the additional option of generating an incore flux map at regular intervals (typically 2 hours) to provide a direct check on the power peaking factors; this provides assurance that both the  $F_Q$  and  $F_{\Delta H}$  peaking factors are verified to remain within their technical specification limits.

Based upon the protection provided by the technical specifications, the amount of time that the fuel could operate at LOCA transient initialization conditions is typically limited to a range of 15 minutes to 4 hours, depending upon the individual plant tech spec requirements. [b, c]

The primary protection for the LOCA  $F_Q$  peaking factor is afforded by the axial power imbalance (or axial flux difference) limits, [b, c]





February 5, 2002  
NRC:02:010

Document Control Desk  
ATTN: Chief, Planning, Program and Management Support Branch  
U.S. Nuclear Regulatory Commission  
Washington, D.C. 20555-0001

**Response to Informal Request on BAW-10231P, "COPERNIC Fuel Rod Design Code"**

- Ref.: 1. Letter, Stewart Bailey (NRC) to T. A. Coleman (Framatome ANP), "Request for Additional Information – Framatome Topical Report BAW-10231P (TAC NO. MA6792), August 1, 2000.
- Ref.: 2. Letter, Letter, T. A. Coleman (Framatome ANP) to U. S. Nuclear Regulatory Commission, GR0-021.doc, February 5, 2001.
- Ref.: 3. Letter, Stewart Bailey (NRC) to T. A. Coleman (Framatome ANP), "Request for Additional Information – Chapter 13 of Framatome Topical Report BAW-10231P (TAC NO. MA9783), May 14, 2001.
- Ref.: 4. Letter, James F. Mallay (Framatome ANP) to Document Control Desk (NRC), "Partial Response to RAI," NRC:01:033, July 27, 2001.

On several occasions the NRC has asked Framatome ANP to provide additional information to assist in the NRC's review of BAW-10231P, "COPERNIC Fuel Rod Design Code." Reference 1 transmitted a request for additional information (RAI) on the UO<sub>2</sub> applications of this report. Reference 2 contained Framatome's response to that RAI. Reference 3 provided an RAI that addressed primarily the MOX applications for COPERNIC. However, two of the questions in that RAI referred to UO<sub>2</sub> applications. Reference 4 contained our response to those two questions.

In addition to information provided in References 2 and 4, Framatome ANP provided an informal response to an NRC question concerning time in life for LOCA initialization. Attached to this letter is a formal, referenceable response to that question.

**Framatome ANP, Inc.**

2101 Horn Rapids Road  
Richland, WA 99352


Tel: (509) 375-8100  
Fax: (509) 375-8402

Document Control Desk  
February 5, 2002

NRC:02:010  
Page 2

Based on discussions with the NRC, Framatome understands that this letter and attachment will provide an adequate basis for completing the SER for the application of BAW-10231P to  $UO_2$ .

Very truly yours,

  
James F. Mallay, Director  
Regulatory Affairs

/lmk

Attachment

cc: J. S. Cushing  
D. G. Holland  
Project 693

## ATTACHMENT

### Supplement to RAI #25 on BAW-10231P

#### Question:

Figures 12-21, -22, -23, -24, -25, and, -26 in BAW-10231P show a trend of increasing volumetric average fuel temperatures with burnups for LOCA initial conditions. This raises a concern that the LOCA PCT may not be limiting in BOL. FCF needs to address the trend of increasing fuel temperatures with burnups to allay this concern. Please evaluate the LOCA PCT results for these figures as compared to the PCT limit of 2200 degree F.

#### Response:

The NRC-approved BWNT LOCA EM (BAW-10192P-A) and RSG LOCA EM (BAW-10168P-A) are the calculational frameworks used to demonstrate compliance to the five criteria of 10CFR50.46 for B&W-designed plants and Westinghouse- and CE-designed plants, respectively. The detailed methods used to show compliance are prescribed in 10 CFR 50 Appendix K. Relative to fuel temperature trends, Appendix K Section I.A.1 gives the requirements for the initial stored energy in the fuel. It states:

"The steady-state temperature distribution and stored energy in the fuel before the hypothetical accident shall be calculated for the burn-up that yields the highest calculated cladding temperature (or, optionally, the highest calculated stored energy). To accomplish this, the thermal conductivity of the  $\text{UO}_2$  shall be evaluated as a function of burn-up and temperature, taking into consideration differences in initial density, and the thermal conductance of the gap between the  $\text{UO}_2$  and the cladding shall be evaluated as a function of the burn-up taking into consideration fuel densification and expansion, the composition and pressure of the gases within the fuel rod, the initial cold gap dimension with its tolerances, and cladding creep."

An NRC-approved steady-state fuel code like TACO3 (BAW-10162) or COPENIC simply provides a set of inputs (namely fuel temperatures, hot and cold fuel pin dimensions, pin gas pressure, and pin gas composition) that are derived from the parameters listed in the Appendix K requirements. These inputs are then used in the analyses that show compliance to 10 CFR 50.46 for the limits of fuel operation covering currently approved burnups for Mark-B and Mark-BW fuel types.

LBLOCA analyses performed for the B&W-designed plants with BAW-10192P-A typically complete five analyses at BOL, five analyses at a limiting MOL burnup (typically at 40, but ranging from 20 to 55 GWd/mtU) and at least one analysis at the EOL condition based on inputs from the TACO3 code. The time-in-life conditions at which the potential limiting PCT analyses are performed are strongly influenced by the fuel stored energy and pin pressure predicted by the steady-state fuel code. After the COPENIC code is approved, it can be used to generate steady-state LOCA initialization inputs at several times in life to

provide fuel pin parameters that will determine how the PCT varies with burnup. This method is used to define an allowed linear heat rate limit versus burnup curve that will maintain the calculated PCTs below the 2200 F limit for the entire fuel pin burnup range.

The LBLOCA analyses performed with BAW-10168P-A for the Westinghouse or CE plants define a  $K_{burnup}$  curve that is used to restrict the total peaking as a function of time in life to ensure that the PCT predicted by analyses performed near the beginning of life remains limiting. The  $K_{burnup}$  curve is set based on LBLOCA analyses performed at limiting fuel pin burnups that cover the licensed fuel pin burnup range. This burnup curve may need to be redefined when the specific NRC-approved steady-state fuel code used for the fuel reload licensing contract is changed (i.e. TACO3 to COPENIC).

**Change Pages**

**Summary of Pages Replaced**

<b>Document</b>	<b>Section</b>	<b>Page(s)</b>	<b>Reason</b>
Topical Report	Table of Contents	v & vi	Correct misspelling of Neodymium
Topical Report	Table of Contents	xix	Replaced to reflect addition of MOX section
Topical Report	4.3.3.1	4-16	Changed "weight %" to "weight fraction"
Topical Report	4.5.4	4-20	Correct misspelling of Neodymium
Topical Report	Figures 4-14 thru 4-27	4-49 thru 4-62	Correct misspelling of Neodymium in Figure titles
Topical Report	14	14-5, 14-6, 14-22, 14-23, 14-67	Incorporate revisions specified in NRC:01:033 (Partial Response to RAI) dated July 27,2001
NRC:03:027, "Final Responses to RAIs on Chapter 13 of BAW-10231P", dated 4/18/03	Attachment 2	1	Changed wording to "in Figures 1 through 4B"
NRC:03:027	Attachment 2	6	Changed Figure 4 to Figures 4A and 4B to reflect separate data for each rod

\* Note: Pages summarized in the above Table that were contained in the Topical Report are the old pages from BAW-10231, Revision 0. The new replacement pages are contained in BAW-10231, Revision 1.



4.6.2. Validation of Mixed Oxide Fuels .....	4-27
4.6.2.1. MOX .....	4-27
4.6.2.2. $UO_2$ - $Gd_2O_3$ .....	4-27
4.6.3. Uncertainties .....	4-28
4.6.3.1. FRAMATOME Database .....	4-28
4.6.3.2. US/NRC Halden Database .....	4-28
4.6.3.3. HALDEN PROJECT Database .....	4-28
4.6.3.4. Summary .....	4-29
REFERENCES .....	4-31
FIGURES .....	4-35
FIGURE 4-1 ROUGHNESS FACTOR VERSUS DIMENSIONLESS GAP FOR DIFFERENT DIMENSIONLESS TEMPERATURE JUMP LENGTHS .....	4-36
FIGURE 4-2 COMPARISON OF MEASURED AND PREDICTED GASEOUS CONDUCTANCES .....	4-37
FIGURE 4-3 COMPARISON OF MEASURED AND PREDICTED GASEOUS CONDUCTANCES [b.] .....	4-38
FIGURE 4-4 COMPARISON OF MEASURED AND PREDICTED GASEOUS CONDUCTANCES [b.] .....	4-39
FIGURE 4-5 COMPARISON OF MEASURED AND PREDICTED GASEOUS CONDUCTANCES [b.] .....	4-40
FIGURE 4-6 COMPARISON OF MEASURED AND PREDICTED GASEOUS CONDUCTANCES [b.] .....	4-41
FIGURE 4-7 COMPARISON OF MEASURED AND PREDICTED GASEOUS CONDUCTANCES [b.] .....	4-42
FIGURE 4-8 COMPARISON OF MEASURED AND PREDICTED GASEOUS CONDUCTANCES [b.] .....	4-43
FIGURE 4-9 COMPARISON OF MEASURED AND PREDICTED GAP CONDUCTANCES [b.] .....	4-44
FIGURE 4-10 COMPARISON OF MEASURED AND PREDICTED GAP CONDUCTANCES [b.] .....	4-45
FIGURE 4-11 MEASURED AND PREDICTED GAP CONDUCTANCES vs PRESSURE [b.] .....	4-46
FIGURE 4-12 MEASURED AND PREDICTED GAP CONDUCTANCES vs PRESSURE [b.] .....	4-47
FIGURE 4-13 HEAT TRANSFER GAP MULTIPLIER X VS RADIAL MECHANICAL HOT GAP .....	4-48
FIGURE 4-14 COMPARISON OF MEASURED (NEODYNIUM) AND PREDICTED RADIAL POWER PROFILES [b.] .....	4-49
FIGURE 4-15 COMPARISON OF MEASURED (NEODYNIUM) AND PREDICTED RADIAL POWER PROFILES [b.] .....	4-50
FIGURE 4-16 COMPARISON OF MEASURED (NEODYNIUM) AND PREDICTED RADIAL POWER PROFILES [b.] .....	4-51
FIGURE 4-17 COMPARISON OF MEASURED (NEODYNIUM) AND PREDICTED RADIAL POWER PROFILES [b.] .....	4-52
FIGURE 4-18 COMPARISON OF MEASURED (NEODYNIUM) AND PREDICTED RADIAL POWER PROFILES [b.] .....	4-53
FIGURE 4-19 COMPARISON OF MEASURED (NEODYNIUM) AND PREDICTED RADIAL POWER PROFILES [b.] .....	4-54
FIGURE 4-20 COMPARISON OF MEASURED (NEODYNIUM) AND PREDICTED RADIAL POWER PROFILES [b.] .....	4-55
FIGURE 4-21 COMPARISON OF MEASURED (NEODYNIUM) AND PREDICTED RADIAL POWER PROFILES [b.] .....	4-56
FIGURE 4-22 COMPARISON OF MEASURED (NEODYNIUM) AND PREDICTED RADIAL POWER PROFILES [b.] .....	4-57



FIGURE 4-23	COMPARISON OF MEASURED (NEODYNIUM) AND PREDICTED RADIAL POWER PROFILES [b.] .....	4-58
FIGURE 4-24	COMPARISON OF MEASURED (NEODYNIUM) AND PREDICTED RADIAL POWER PROFILES [b.] .....	4-59
FIGURE 4-25	COMPARISON OF MEASURED (NEODYNIUM) AND PREDICTED RADIAL POWER PROFILES [b.] .....	4-60
FIGURE 4-26	COMPARISON OF MEASURED (NEODYNIUM) AND PREDICTED RADIAL POWER PROFILES [b.] .....	4-61
FIGURE 4-27	COMPARISON OF MEASURED (NEODYNIUM) AND PREDICTED RADIAL POWER PROFILES - MOX [b.] .....	4-62
FIGURE 4-28	MEASURED AND PREDICTED FUEL TEMPERATURES VS BURNUP [b.] .....	4-63
FIGURE 4-29	MEASURED AND PREDICTED FUEL TEMPERATURES VS BURNUP [b.] .....	4-64
FIGURE 4-30	MEASURED AND PREDICTED FUEL TEMPERATURES VS BURNUP [b.] .....	4-65
FIGURE 4-31	MEASURED AND PREDICTED FUEL TEMPERATURES VS BURNUP [b.] .....	4-66
FIGURE 4-32	MEASURED AND PREDICTED FUEL TEMPERATURES VS BURNUP [b.] .....	4-67
FIGURE 4-33	MEASURED AND PREDICTED FUEL TEMPERATURES VS TIME [b.] .....	4-68
FIGURE 4-34	[c.] .....	4-69
FIGURE 4-35	MEASURED AND PREDICTED FUEL TEMPERATURES VS BURNUP (IFA 431-1, INLET) .....	4-70
FIGURE 4-36	MEASURED AND PREDICTED FUEL TEMPERATURES VS BURNUP (IFA 431-1, OUTLET) .....	4-71
FIGURE 4-37	MEASURED AND PREDICTED FUEL TEMPERATURES VS BURNUP (IFA 431-2, INLET) .....	4-72
FIGURE 4-38	MEASURED AND PREDICTED FUEL TEMPERATURES VS BURNUP (IFA 431-2, OUTLET) .....	4-73
FIGURE 4-39	MEASURED AND PREDICTED FUEL TEMPERATURES VS BURNUP (IFA 431-3, INLET) .....	4-74
FIGURE 4-40	MEASURED AND PREDICTED FUEL TEMPERATURES VS BURNUP (IFA 431-3, OUTLET) .....	4-75
FIGURE 4-41	MEASURED AND PREDICTED FUEL TEMPERATURES VS BURNUP (IFA 431-5, INLET) .....	4-76
FIGURE 4-42	MEASURED AND PREDICTED FUEL TEMPERATURES VS BURNUP (IFA 431-5, OUTLET) .....	4-77
FIGURE 4-43	MEASURED AND PREDICTED FUEL TEMPERATURES VS BURNUP (IFA 431-6, INLET) .....	4-78
FIGURE 4-44	MEASURED AND PREDICTED FUEL TEMPERATURES VS BURNUP (IFA 431-6, OUTLET) .....	4-79
FIGURE 4-45	MEASURED AND PREDICTED FUEL TEMPERATURES VS BURNUP (IFA 432-1, INLET) .....	4-80
FIGURE 4-46	MEASURED AND PREDICTED FUEL TEMPERATURES VS BURNUP (IFA 432-1, OUTLET) .....	4-81
FIGURE 4-47	MEASURED AND PREDICTED FUEL TEMPERATURES VS BURNUP (IFA 432-2, INLET) .....	4-82
FIGURE 4-48	MEASURED AND PREDICTED FUEL TEMPERATURES VS BURNUP (IFA 432-3, INLET) .....	4-83
FIGURE 4-49	MEASURED AND PREDICTED FUEL TEMPERATURES VS BURNUP (IFA 432-3, OUTLET) .....	4-84
FIGURE 4-50	MEASURED AND PREDICTED FUEL TEMPERATURES VS BURNUP (IFA 432-5, INLET) .....	4-85
FIGURE 4-51	MEASURED AND PREDICTED FUEL TEMPERATURES VS BURNUP (IFA 432-6, INLET) .....	4-86
FIGURE 4-52	MEASURED AND PREDICTED FUEL TEMPERATURES VS BURNUP	





## **APPENDIX A - Correspondence with the NRC, Including Requests for Additional Information and Responses**

1. Letter from FCF (T.A. Coleman) to U.S. NRC, September 16, 1999.
2. Letter from FCF (T.A. Coleman) to U.S. NRC, December 2, 1999.
3. Letter from U.S. NRC (Stewart Bailey) to FCF (T.A. Coleman), August 11, 2000.
4. Letter from FCF (T.A. Coleman) to U.S. NRC, September 29, 2000.
5. Letter from FRAMATOME ANP (T.A. Coleman) to U.S. NRC, February 5, 2001.
6. Letter from U.S. NRC (Stewart Bailey) to FRAMATOME ANP (T.A. Coleman), May 14, 2001.
7. Letter from FRAMATOME ANP (J.F. Mallay) to U.S. NRC, February 5, 2002.



where

[b., e.],

[b., e.],

[b., e.],

[b., e.], and

[b., e.].

#### 4.3.2.2. Porosity and RIM Model

The correction for porosity is a function of temperature as follows (Ref. 4-12):

$$\lambda_{\text{POR}}^{\text{Bu}} = \lambda_{100}^{\text{Bu}} \cdot (1 - \alpha \cdot \text{POR}) \quad \alpha = 2.58 - 5.8 \cdot 10^{-4} \cdot T_c \quad \text{Eq. 4-40}$$

where

$T_c$  : temperature (°C), and

POR : porosity fraction.

Fuel rims have been observed on fuel pellet peripheries when the local rim burnup exceeds a value of approximately [e.] or when the average pellet burnup exceeds a value of approximately [e.]. The rim porosity has also been observed [e.]. The following rim model was selected based upon these observations:

$$[b., e.] \quad \text{Eq. 4-41}$$

where

$B_S$  : [b., e.],

$B_A$  : average pellet burnup,

$C_3$  : [b., e.], and

$C_4$  : [b., e.].

and

$$[b., d.] \quad \text{Eq. 4-42}$$



where

POR : porosity fraction,

r : [b., e.]

r<sub>S</sub> : [b., e.], and

C<sub>S</sub> : [b., e.].

[b., e.]

Eq. 4-43

#### 4.3.3. Adaptation to Mixed Fuels

The COPERNIC UO<sub>2</sub> thermal conductivity relationship has been adapted to mixed oxide and gadolinia fuels with the following modifications.

##### 4.3.3.1. MOX

[b., d.]

Eq. 4-44

where

x = 2.00 - O/M,

F(y) = [b., d.],

F(y) = [b., d.],

O/M : oxygen to metal ratio, and

y : Pu content (weight%).

##### 4.3.3.2. UO<sub>2</sub>-Gd<sub>2</sub>O<sub>3</sub>

The ratio of the thermal conductivity of gadolinia bearing fuel to UO<sub>2</sub> fuel [ $\lambda(z,T) = \lambda(\text{UGd})\text{UO}_2 / \lambda(\text{UO}_2)$ ] is:

[b., d.]

Eq. 4-45



#### 4.5. Fuel Pellet Radial Power Profiles

##### 4.5.1. Phenomenon

The thermal power produced within the fuel corresponds to the volumetric distribution of fissions. The latter depends on the initial isotopic distribution within the fuel and the irradiation conditions (temperature, power, environment, ...). These conditions establish the radial distribution for both the neutron flux and the resulting isotopic composition. The primary phenomena involved are:

- attenuation of the neutron flux towards the pellet center due to self-shielding and capture,
- fissile atom depletion within the pellet,
- the progressive enrichment of a fine Pu peripheral layer through captures in U238,
- burnout of a burnable absorber like gadolinium.

##### 4.5.2. Model

The radial power distributions within the pellet were determined separately with the APOLLO2 neutronic transport code (Ref. 4-15). These predictions produced tabulated data which were incorporated in COPERNIC.

Sensitivity studies were run to define the calculational basis for  $\text{UO}_2$  fuel. These are:

- an infinite medium cell layout,
- a uniform temperature for all isotopes (except U238),
- a radial temperature profile for U238, and
- a self-shielding calculation at BOL.

The radial mesh must be sufficiently fine towards the pellet outer edge to correctly represent the peripheral rim effect. Better accuracy at high burnups is obtained with 20 rings.

##### 4.5.3. Available Options

###### 4.5.3.1. Generic Tables for $\text{UO}_2$

The generic tables for  $\text{UO}_2$  were established for:

[d., c.]

#### 4.5.3.2. Tables for MOX

MOX generic tables were established for:

[d., e.]

#### 4.5.3.3. Tables for $\text{UO}_2\text{-Gd}_2\text{O}_3$

[d., e.]

#### 4.5.4. Experimental Validation

The radial burnup distributions obtained with the APOLLO2 tables were validated with radial Neodymium profiles which were obtained with Electron Probe Micro Analyses (EPMA). The rods used are given in Table 4-3.

The validation of the generic  $\text{UO}_2$  tables was performed with a number of samples from PWR rods that had two initial enrichments and a variety of burnups (Figures 4-14 to 4-26). Good agreement between measurements and predictions is observed in these figures.

The measured to predicted comparison for the MOX generic tables was performed [e.]. No allowance is made for the scatter in the radial power due to the presence of Pu-rich spots and the fuel is assumed to be homogeneous in the calculations. Therefore, the measured to predicted comparison has a wide scatter; however, the temperature benchmark results for MOX fuel are satisfactory as shown later in the last section describing the global experimental validation. Note that the periphery effect for MOX is much smaller than  $\text{UO}_2$  at a comparable burnup (Figure 4-27).

#### 4.5.5. Range of Application

- $\text{UO}_2$  generic tables:
  - U235 enrichment [d., e.]
  - Burnup [d., e.]
- MOX generic tables:
  - Pu content [d., e.]
  - Burnup [d., e.]
- $\text{UO}_2\text{-Gd}_2\text{O}_3$  specific tables:
  - $\text{Gd}_2\text{O}_3$  content [d., e.]
  - User specified input



## FIGURE 4-14 COMPARISON OF MEASURED (NEODYNIUM) AND PREDICTED RADIAL POWER PROFILES [b.]

[b.]



COFERMIO

FCF Non Proprietary

Chapter 4

PAGE 4-50

**FIGURE 4-15 COMPARISON OF MEASURED (NEODYNIUM) AND  
PREDICTED RADIAL POWER PROFILES [b.]**

[b.]



## FIGURE 4-16 COMPARISON OF MEASURED (NEODYNIUM) AND PREDICTED RADIAL POWER PROFILES [b.]

[b.]





**FIGURE 4-17 COMPARISON OF MEASURED (NEODYNIUM) AND  
PREDICTED RADIAL POWER PROFILES [b.]**

[b.]



## FIGURE 4-18 COMPARISON OF MEASURED (NEODYNIUM) AND PREDICTED RADIAL POWER PROFILES [b.]

[b.]



COPIED

FCF Non Proprietary

Chapter 4

PAGE 4-54

**FIGURE 4-19 COMPARISON OF MEASURED (NEODYNIUM) AND  
PREDICTED RADIAL POWER PROFILES [b.]**

[b.]



## FIGURE 4-20 COMPARISON OF MEASURED (NEODYNIUM) AND PREDICTED RADIAL POWER PROFILES [b.]

[b.]



COFERMIO

FCF Non Proprietary

Chapter 4

PAGE 4-56

**FIGURE 4-21 COMPARISON OF MEASURED (NEODYNIUM) AND  
PREDICTED RADIAL POWER PROFILES [b.]**

[b.]



**FIGURE 4-22 COMPARISON OF MEASURED (NEODYNIUM) AND  
PREDICTED RADIAL POWER PROFILES [b.]**

[b.]



**FIGURE 4-23 COMPARISON OF MEASURED (NEODYNIUM) AND  
PREDICTED RADIAL POWER PROFILES [b.]**

[b.]



**FIGURE 4-24 COMPARISON OF MEASURED (NEODYNIUM) AND  
PREDICTED RADIAL POWER PROFILES [b.]**

[b.]





COPERNIC

FCF Non Proprietary

Chapter 4

PAGE 4-60

**FIGURE 4-25 COMPARISON OF MEASURED (NEODYNIUM) AND  
PREDICTED RADIAL POWER PROFILES [b.]**

[b.]



## FIGURE 4-26 COMPARISON OF MEASURED (NEODYNIUM) AND PREDICTED RADIAL POWER PROFILES [b.]

[b.]



**FIGURE 4-27 COMPARISON OF MEASURED (NEODYNIUM) AND  
PREDICTED RADIAL POWER PROFILES - MOX [b.]**

[b.]

**Figure 14-3: COPERNIC and NFIR-III Thermal Conductivity Comparison  
100% Theoretically Dense Fuel  
60 GWd/tU Burnup**

[b, c, d]

**Figure 14-4: COPERNIC and JAERI Thermal Conductivity Comparison  
Sample No.2  
100% Theoretically Dense Fuel  
63 GWd/tU Burnup, 83-89% Initial Density Range**

[b, c, d]

**Figure 14-5: COPERNIC and JAERI Thermal Conductivity Comparison  
Sample No.3  
100% Theoretically Dense Fuel  
63 GWd/tU Burnup, 92-96% Initial Density Range**

[b, c, d]

**Figure 14-6: Rim Effect at 60 GWd/tU  
IFA 562**

[b, c, d]

Figure 14-12: Measured and Predicted Fuel Temperatures vs. Burnup

[d]

**Question 6**

Is Framatome a member of Halden? If so, Halden has refabricated two high (~ 59 GWd/MTU) burnup rods (one with a functional thermocouple) and placed them first in IFA-597.2 (HWR-442) and subsequently in IFA-597.3 (HWR-543) with measured centerline temperatures. Please compare COPERNIC code predictions to this data and include this data in the response to Question 3.1 above.

**Response**

The COPERNIC centerline fuel temperature predictions are compared with the IFA-597.2 (HWR-442) and IFA-597.3 (HWR-543) fuel temperature measurements in Figures 14-13 and 14-14, respectively. This rodlet attained a burnup of 61.5 GWd/tUO<sub>2</sub> or 69.8 GWd/tU.

**Figure 14-13: Fuel Centerline Temperature Measurements and Predictions vs.  
Burnup, IFA-597.2**

[d]

**Figure 14-14: Fuel Centerline Temperature Measurements and Predictions vs.  
Burnup, IFA-597.3**

[d]



**Question 7**

The athermal fission gas release model (Section 5.2.2) is dependent on open porosity but no values are provided for what is used for Framatome fuel. What values are used for open porosity? If more than one value is used, please provide the value for each fabrication process.

**Response**

The open porosity input to the COPERNIC code is the percentage of open porosity to the total pellet geometric volume. The open porosity percentage of the fuel supplied by FRA-ANP's present vendor is typically [b, d]. The [b, d] will be used until open porosity data obtained from the fuel vendor suggests a need to increase this value to [b, d] pellet fabrication open porosity measurements.

Question 28

There is a concern that the uncertainty factor provided in Equation 12-1 may be too small at the predicted operating temperatures (stored energy) calculated for LOCA initialization. Please discuss this issue further, particularly in relation to Question 3 above.

Response

Based upon the analysis performed for Question 3 above, it is recommended to [b, d]. This [b, d] was determined to be [e] in the Question 3 analysis. The recommended replacement equations that were derived based upon [b, d], therefore, are:

Equation 12-1 replacement

[d, e]

Equation 12-3 replacement

[d, e]

where

T	=	COPERNIC best-estimate temperature (°C),
T <sub>95/95</sub>	=	temperature (°C) that bounds 95% of the data with a 95% confidence,
T <sub>L</sub>	=	limiting melt temperature (°C), and
Bu	=	pellet burnup (GWd/tU).

**Question 29**

Are any of the example calculations provided in Section 12 for fuel cores with two 24-month cycles? It appears that there are no 24-month cycle results presented for the Mark BW-17 design. If so, please explain because it is anticipated that a large number of plants will be switching to 24-month cycles in the next few years.

**Response**

[b, d].

**RESPONSE TO OUTSTANDING REQUESTS FOR ADDITIONAL INFORMATION****TOPICAL REPORT BAW-10231P, CHAPTER 13****"COPERNIC MOX APPLICATIONS"**

Below are responses to the outstanding 1<sup>st</sup>- and 2<sup>nd</sup>-Round questions received on the COPERNIC MOX Addendum.

**Round 1, Question 8:**

The integral MOX experiments provided, where centerline temperatures are measured, to verify the COPERNIC integral thermal predictions of MOX fuel rods are limited to very low burnup levels, i.e., less than 5 GWd/MTU. Please provide COPERNIC predictions of at least three of the following Halden MOX instrumented assemblies, IFA-597.4/5/6, IFA-606, IFA-610, and IFA-648.1, that achieved burnups of approximately 24 GWd/MTM to 57 GWd/MTM, or suggest other Halden MOX instrumented assemblies. Please justify the reasons for eliminating some of the data and/or assemblies for COPERNIC comparisons and the reasons for selecting others (this should be discussed with the NRC reviewer prior to issuing a response to the request for additional information). Also, rod pressures due to fission gas release were measured for two experimental Halden MOX fuel rods in IFA-597.4/5/6. COPERNIC predictions of rod pressure are also needed, where appropriate.

**Response:**

Framatome ANP considers the lower-burnup experiment IFA-597.4/5/6 to be atypical of MIMAS fuel performance. The follow-on experiment IFA-597.7 showed very high fission gas release at the beginning of the irradiation, as indicated in Halden Status Report HR1110. This level is unusual and not consistent with other experiments.

Therefore, Framatome ANP selected the experiments IFA-606, IFA-610.2, IFA-610.4, and IFA-648.1, which are more representative of MIMAS fuel, to demonstrate the adequacy of the COPERNIC thermal predictions. Measured versus predicted central temperatures for these four experiments are provided in Figures 1 through 4.

The fission gas release for IFA-606, rodlet 3, which yielded the highest release fraction, was predicted<sup>1</sup> to be 15.9% compared to the measured value of 12.2%.

It is concluded that COPERNIC provides very good agreement with the measured data.

**Figure 4**

**IFA648.1 Measured and Predicted Peak Teamperatures**

**[d]**